Recent Advances in Microporous Materials Membrane for Hydrogen Separation against Light Gases

Nicholaus Prasetya[1,3,*], I Gede Wenten[2] and Bradley P. Ladewig[3,*]

[1] Institute of Functional Interface (IFG), Karlsruhe Institute of Technology, Hermann-von-Helmholtz-Platz 1, 76344, Eggenstein-Leopoldshafen, Germany

[2] Department of Chemical Engineering, Institut Teknologi Bandung, Jalan Ganesha 10, Bandung 40132, Indonesia

[3] Paul Wurth Chair, Faculty of Science, Technology and Medicine, University of Luxembourg, 2, Avenue de l'Université, L-4365 Esch-sur-Alzette, Luxembourg

Corresponding author: nicholaus.prasetya@partner.kit.edu, nicholaus.prasetya@uni.lu bradley.ladewig@uni.lu

Abstract

With the pressing concern of the climate change, hydrogen will undoubtedly play an essential role in the future to accelerate the way out from fossil fuel-based economy. In this case, the role of membrane-based separation cannot be neglected since, compared with other conventional process, membrane-based process is more effective and consumes less energy. Regarding this, metal-based membranes, particularly palladium, are usually employed for hydrogen separation because of its high selectivity. However, with the advancement of various microporous materials, they could challenge the *status quo* of the metal-based membranes since they could offer both high hydrogen permeability and selectivity while also relatively cheaper to be produced. In this article, the advancement of five main microporous material membranes, namely silica-based membranes, zeolite membranes, carbon-based membranes, metal organic frameworks/covalent organic frameworks (MOF/COF) membranes and microporous polymeric membranes are extensively discussed. Their performances for hydrogen separation are then summarized to give further insights regarding the pathway that should be taken to direct the research direction in the future.

1. Introduction

With the pressing concern of global climate change, hydrogen will undoubtedly play an essential role as the main source of clean energy carrier in the future. Within the context of hydrogen economy, the main advantages of using hydrogen are primarily to reduce the concentration of the greenhouse gases in the atmosphere and also to eliminate the dependency fossil fuels-based economy that continuously aggravates the environmental issues [1,2]. It is then expected that such energy transition will significantly contribute in mitigating the climate change issues, particularly if the hydrogen can be fully produced from renewable resources and by utilizing clean energy.

Despite its potential as a rich energy source and its abundance, the hydrogen does not come naturally as a gas and is always in combination with other elements. Therefore, there are a number of common ways to produce hydrogen such as by hydrocarbon reforming [2]. Up to now, hydrogen production from steam methane reforming (SMR) combined with water gas shift (WGS) reaction can still be considered as the most economically viable and therefore cannot be neglected from the perspective of

hydrogen economy, although it still depends on the fossil fuels [2,3]. In the case, the syngas containing H_2 and CO is firstly produced and the CO will be further converted into CO_2 through WGS reaction. The separation of H_2 from the CO_2 and unconverted CH_4 in this case becomes crucial so the H_2 can be further used for power generation [4,5].

Hydrogen can also be obtained by recovering the purge gases from various industries such as from the ammonia plant, iron and steel industry in the form of coke oven gas or off-gas from refineries [6–8]. In the case of ammonia plant, for example, the hydrogen is firstly produced mostly through natural gas reforming to synthesize ammonia which is mainly further used in fertilizer industries. About 96% of the ammonia is still currently produced through the conventional energy-intensive Haber-Bosch process and therefore contributes to around 1.4-1.8% of the global CO_2 emission while also utilizing around 2% of the global energy production [9,10]. Considering the vast amount of the hydrogen required to produce ammonia, it is then also released in a significant amount from an ammonia plant. It is estimated that a stream of up to 180-240 Nm^3 per ton of ammonia has to be purged containing large quantities of hydrogen (up to 67% of H_2, 25% of N_2 and a mixture of other gases) [11]. The hydrogen in this stream is has a huge potential to be recovered as an energy carrier once it can be effectively and efficiently separated from the rest of the stream components. Another example can also be seen in the post-combustion gaseous stream from the production of carbon black consisting of approximately 60.5% N_2, 17.9% CO, 16.4% H_2 and 5.3% CO_2 [12]. Once this flue gas is further used for power generation by converting to CO_2, water and heat, the remaining flue gas still consists of low concentration of hydrogen that could potentially be recovered from the nitrogen as the major component.

Another scenario can also be seen in the future regarding the planning to transport the hydrogen. Taking into account that transporting hydrogen through the pipeline is the lowest-cost alternative, there is a possibility to utilize the existing network of the natural gas pipeline to co-transport hydrogen with natural gas [13]. Depending upon the gas grid infrastructure, hydrogen might be blended with the concentration between 5-20% [14]. If such a scenario can be fully implemented in the future, one of the main challenges is then to find a reliable technology that can effectively and efficiently purify the hydrogen from methane at the desired locations.

Up to now, the separation process of hydrogen from these light gases can be carried out by employing several techniques such as through liquid absorption, pressure swing adsorption (PSA) or cryogenic separation [7,15–17]. However, because of a number of disadvantages associated with these processes, particularly the relatively high-energy demand, membrane technology could be a better alternative to make the hydrogen separation process more energy-efficient and attractive in the future [15].

The use of membrane for hydrogen purification is indeed not a new technology. Various polymers have then been investigated to be used as a membrane material for hydrogen separation from various gases. In 2008, these studies have then been nicely summarized by Robeson by indicating the existence of the upper bound encountered in polymeric membranes for hydrogen separation [18]. Based on this study, it can be clearly seen that there exists a permeability-selectivity trade-off encountered in polymeric membranes. A polymeric membrane with high hydrogen permeability such as PTMSP usually exhibits a low hydrogen selectivity and vice versa.

Considering the trade-off issue encountered in the polymeric membranes, the use of dense metallic membranes is also very attractive and therefore have also been investigated as a promising membrane material for hydrogen separation. In this case, palladium (Pd) and its alloys are probably the most common metallic membrane material investigated for hydrogen purification. The use of palladium to separate hydrogen has then been reported as early as 1866 [19], which has become the foundation of various studies and discussions about this material and its alternative in the 1950-1960 [20–22]. In general, palladium is a promising membrane material for hydrogen separation since it can offer almost an infinite selectivity towards hydrogen and thus a pure hydrogen flow at the downstream side can be obtained. Despite their high effectiveness, these metallic membranes suffer from a number of disadvantages. Firstly, palladium is a rare earth metal. This causes the production cost of a palladium membrane to be more expensive than a polymeric membrane. In order to reduce the production cost of a palladium-based membrane, it has to be fabricated instead as a thin layer on a porous substrate. Secondly, a palladium membrane can also suffer from the hydrogen embrittlement when operated below 300^{o}C which could lead to the mechanical deformation of the membrane [23,24]. Therefore, palladium must be alloyed, either to form a binary alloy or a ternary alloy, with other metals to address the embrittlement problem and also to improve its chemical resistance [23,25].

Addressing the above issues, a number of researches have then been directed to investigate other promising materials for hydrogen purification, particularly microporous materials. In this case, the employment of microporous materials has gained an increased interest because they could offer high productivity and selectivity and thus surpassing the upper bound limit. As can be seen in the Figure 1, there is an increasing trend in the publications related to various microporous materials for hydrogen separation. Such a possibility is particularly driven by the possibility to rationally tailor the pore structure of these materials for selectively permeating hydrogen while rejecting other impurities. For example, as can also be seen in the Figure 1, there is an increasing trend from around 2010 in research and development in the field of metal organic frameworks, covalent organic frameworks and microporous polymeric membranes (polymer of intrinsic microporosity and thermally-rearranged polymer) whose architecture can be rationally designed by selecting appropriate building blocks. This review then intends to highlight the recent advances of these promising materials in the field of hydrogen separation, which could then be used as a guidance to choose the next membrane materials for hydrogen purification.

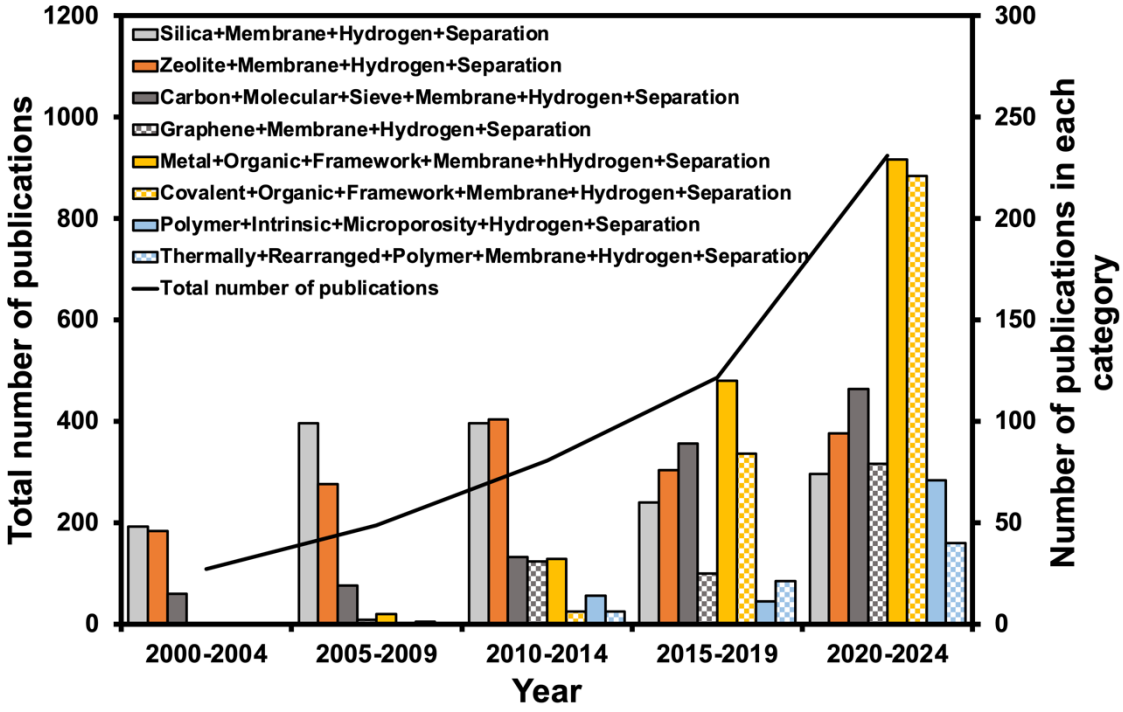

Figure 1. Number of publications of microporous materials membrane for hydrogen separation based on Scopus

2. Gas transport in the microporous materials

The gas transport occurring through a membrane can usually be described through solution-diffusion mechanism as illustrated in the Figure 2(A). In this case, the gas permeation occurs through three steps: (i) adsorption and dissolution of the gas into the membrane matrix, (ii) diffusion of the gas across the membrane matrix and (iii) desorption at the downstream side. The selectivity is therefore determined both by the solubility and diffusivity of the gas molecules in the membrane material. The gas transport of the membranes fabricated from polymeric materials can usually be described by this phenomenon. However, in a microporous material with a more complex and porous structure, the gas transport mechanisms could also be governed by a combination of different mechanisms [26,27].

There are at least three phenomenon that could also occur during when the gas molecules are transported across the membrane. In the ultra- or micropores region, the gas molecular sieving can occur, as illustrated in the Figure 2(B). In this case, the membrane selectivity is governed by the ability of a certain gas molecule to pass through the pores. When the pores in a microporous membrane become larger and falls within the range of 0.3 to 1 nm, the gas transport can now be governed by surface diffusion, as illustrated in the Figure 2(C). Lastly, the Knudsen flow can also govern the gas transport process across a microporous membrane, as illustrated in the Figure 2(D), when the pore size in the membrane falls in range between 1 to 50 nm. This occurs when the mean free path of a gas molecule is much larger than the pore diameter. All of these gas transport could then occur simultaneously in a microporous membrane. For instance, when a microporous membrane contains some large pores or defective parts, the gas transport occurring through these defective sites might be governed by both surface and Knudsen diffusion, while the rest might be molecularly sieved by the non-defective

sites of the membrane. Moreover, the ability for a certain gas molecule before being transported across the membrane could also be affected by the adsorption of the molecule on the membrane, which in the case of microporous polymeric membranes corresponds to the material's solubility.

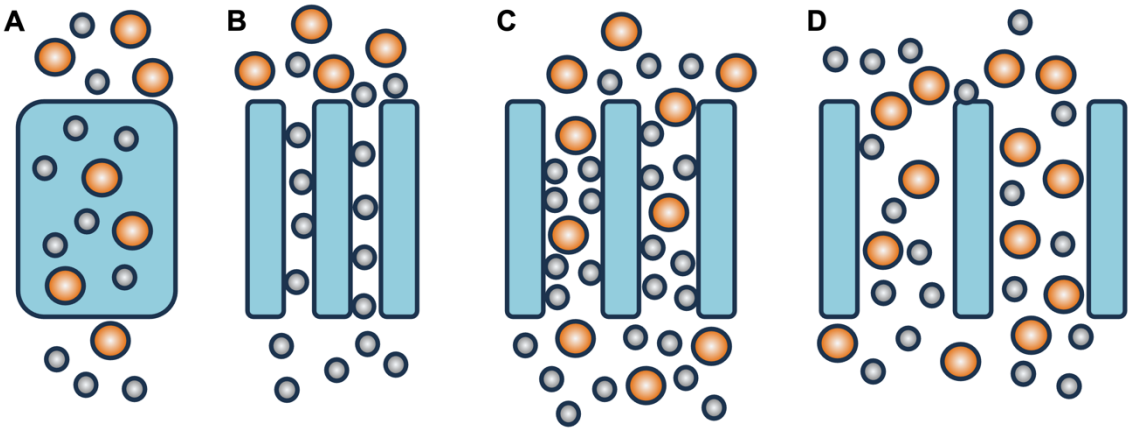

Figure 2. A schematic of the possible gas transport phenomenon through a microporous membrane: solution-diffusion (A), molecular sieving (B), surface diffusion (C) and Knudsen diffusion (D)

3. Microporous membrane materials for hydrogen separation

3.1 Silica-based membranes

The use of silica-based membrane for hydrogen purification has been studied as early as 1989 where the decomposition of tetraethoxysilane (TEOS) was used as a silica precursor and an inorganic porous glass was used as the support [28]. From this early study, it was found that the H_2/N_2 selectivity of the silica membrane is about twice higher than the selectivity of the porous support. In silica-based membranes, the separation is governed based on the molecular sieving phenomenon. This is in contrast to the separation of their support layer which is normally governed by the Knudsen diffusion. Therefore, a defect-free silica-based membrane could exhibit a very high hydrogen permselectivity towards light gases.

In general, as illustrated in the Figure 3, a microporous silica-based membrane can be fabricated either by a sol-gel [29–51] or chemical vapor deposition (CVD) method [52–82]. In a sol-gel technique, a porous substrate is usually firstly dipped in a silica colloidal precursor containing silica nanoparticles. This is then followed by drying and sintering the coated substrate to obtain a porous silica structure [83]. This process can be repeated several times to obtain a defect-free silica membrane. Three approaches, namely (i) silica polymers, (ii) particulate-sol and (iii) templating, can then be used to fabricate a silica membrane based on the sol-gel method and various factors might affect the membranes properties and their hydrogen separation performance [84].

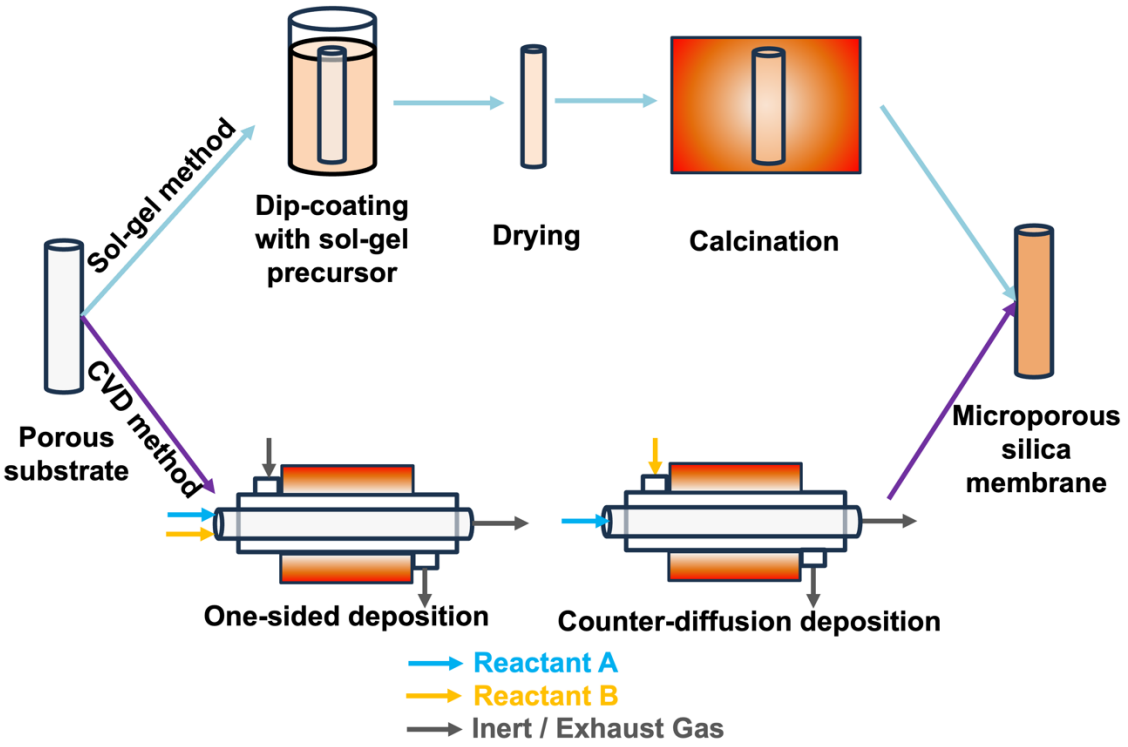

Figure 3. A schematic diagram of the microporous silica membrane preparation

A study comparing TEOS and three different silica precursors, namely 1,1,3,3-tetraethoxy-1,3-dimethyldisiloxane (TEDMDS), bis(triethoxysilyl)ethane (BTESE) and hexaethoxy disiloxane (HEDS) has revealed that the TEOS-derived silica membrane gives the best H_2/N_2 selectivity around 340 with the lowest H_2 permeance around 3 x 10^{-7} mol m^2 s^{-1} Pa^{-1} since it results in the membrane with the smallest pore size [44–46]. Meanwhile the order of the pore size of the rest is HEDS < BTESE < TEDMDS-derived silica membrane. All the silica membranes fabricated using these precursors have exhibited low H_2/N_2 selectivity in the range of 7-20 because of their looser pore structure with the TEDMDS-derived silica membrane shows the lowest H_2 permeance around 1 x 10^{-6} 10^{-7} mol m^2 s^{-1} Pa^{-1} because of the presence of the impermeable pendant groups in its network. Another investigation has also indicated that there is a difference between the silica membrane prepared from acid-catalyzed polymeric silica sol and base-catalyzed colloidal silica sol [35]. The former leads to the formation of low-branched silica particles leading to interpenetration and denser thin film while the latter results in highly branched silica particles that cannot interpenetrate because of the steric hindrance. As a result, the latter pathway produces better and applicable silica membrane since the former produces an almost non-permeable silica membrane. For the silica polymers pathway, carefully controlling the clusters condensation rate during the silica network polymerization is essential to obtain a defect-free silica membrane [85]. In the case of templating method, for example, the selection of the correct templating agent is crucial to obtain a silica membrane with narrow pore distribution. It has been observed that the use of methacryloxypropyltrimethoxysilane (MOTMS) as a templating agent can increase the micropore volume and narrow down the pore distribution of the membrane and thus resulting in almost 40 times increase of hydrogen permeance than the membrane fabricated without MOTMS [33].

One of the main challenges related to the sol-gel process is the required time for the calcination since this may take up to 12 h including the ramping up to the target temperature and the holding time [86]. In this respect, a 1 hour calcination step with the ramping up step of more than 100°C s^{-1} has not just managed to reduce the calcination time but also to produce a good silica membrane with H_2 permeance and selectivity against N_2 around 1 x 10^{-7} mol m^2 s^{-1} Pa^{-1} and 40, respectively [42]. Another study has also shown the possibility to use a hot plate at 550°C for calcination [41]. With just one hour calcination time, a silica membrane with H_2 permeance around 1 x 10^{-7} mol m^2 s^{-1} Pa^{-1} and selectivity against CO_2, N_2 and CH_4 around 17, 250 and 250, respectively, can be obtained. However, contamination from the environments must be fully avoided to obtain a defect-free membrane.

Differing from the sol-gel method, a CVD technique relies on the reaction of the silica precursor in the gas phase occurring around the pores of the substrate in order to modify them [87]. Such a reaction can then be accelerated by various factors including the presence of the catalyst in the precursor such as tetraisoporpyl titanate [60] and the presence of opposing reactants such as water vapor that also contributes in reducing the fabrication temperature [70]. Meanwhile, the quality of the silica membrane produced with CVD method is often influenced by various reaction parameters such as the flow direction of the reactants, reaction temperature and time and the presence of other components. In this case, a defect-free silica membrane can usually be obtained by prolonging the reaction time leading to lower hydrogen permeance and higher hydrogen permselectivity as the pore of the substrates become smaller [53,54,56,57]. In order to obtain a homogeneous silica membrane, it has also been observed that flowing the two reactants on different sides of the porous substrate (outer and inner sides) yields a more uniform silica membrane with better hydrogen permselectivity [59]. This is because the formation of a uniform silica film within the substrate pores will be more promoted rather than being accumulated on the surface of the substrate that can lead to film cracking as the thickness increases. Meanwhile, to obtain a thinner silica membrane to increase the hydrogen permeance, introducing a barrier on the pore surface of the porous substrate such as by introducing temporary carbon layer [64] or by firstly coating a silica sol-gel layer on the barrier will limit the active region of the CVD and thus helping to assist in obtaining a thinner silica membrane.

Moreover, choosing the correct silica precursor is also crucial to obtain a silica membrane with excellent hydrogen separation performance. For example, the use of TEOS as silica precursor might result in a silica membrane with higher hydrogen permeance than the one fabricated from $SiCl_4$ when using Vycor glass as the support [62]. This is because TEOS diffuses slower than $SiCl_4$ into the support pores because of its molecular size and thus considerable pore blocking might be resulted when $SiCl_4$ is used as the precursor. In this case, one study has investigated the use of three different silica precursors, namely tetramethoxysilane (TMOS), phenyltrimethoxysilane (PhTMS) and 3-aminopropylmethyldiethoxysilane (APMDES) and the membranes were fabricated using the CVD method [52]. It was observed that the H_2/N_2 selectivity follows the order of TMOS-deposited (1265) > PhTMS-deposited (633) > APMDES-deposited (100) silica membrane. This is caused by the fact that TMOS-deposited silica membrane has the smallest pore size distribution than the others and thus has shown an excellent H_2 selectivity, even though this also means that it has the slowest H_2 permeance

compared to the rest of the membranes. In addition, the selection of the support material is also crucial to obtain a silica membrane that can combine excellent hydrogen permeance and selectivity. For example, comparative studies employing Vycor glass and alumina as a support have indicated that the H_2/CO_2 and H_2/CH_4 selectivity of the former is about 4-5 times higher than the latter (up to more than 10000) [53,54]. This is because the SiO_2/Vycor glass membrane has more constricted pores than the SiO_2/alumina and thus more effective in hindering the adsorption of gases with kinetic diameter of more than 0.3 nm. However, this must also be compensated by the slower hydrogen permeance, which was found about one order of magnitude lower. Another study using alumina as the support has also shown that by firstly coating the alumina substrate with boehmite sol as an intermediate layer can produce an ultrathin silica membrane with thickness less than 50 nm and increase its hydrothermal stability [55,69]. Moreover, both the hydrogen permeance and the H_2/CO_2 and H_2/CH_4 of this silica membrane has also been improved from its uncoated counterpart for about 60% to be around 1.6 x 10^{-7} mol m^2 s^{-1} Pa^{-1} and about 2-3 times to be around 590 and 940, respectively [55]. This is because the intermediate layer coated on the support gives a finer microstructure and a membrane with fewer defects can be obtained. The advantages of using of boehmite as the intermediate layer can then be further enhanced by applying differential pressure when the silica membrane is fabricated using a counter diffusion approach since it can more effectively deposit the film in the pores of this intermediate layer [81]. As a result, the H_2/CO_2 and H_2/CH_4 selectivity of this membrane can reach as ahigh as 1200 and 24000, respectively. In another study, coating the alumina substrate with an intermediate layer from silica is also possible. In this case, a looser silica membrane from phenyltriethoxysilane before the deposition of the selective silica layer made from TEOS is also found to be very effective to significantly enhance the hydrogen permeance up to around 3.6 x 10^{-6} mol m^2 s^{-1} Pa^{-1} while maintaining satisfactory H_2/CH_4 selectivity around 30 [79].

A silica-based membrane for hydrogen separation can also be modified by embedding the membrane with various metals or metal oxides such as cobalt [30,31,38,42], nickel [32,37], niobium [47], palladium [50] and zirconia [40] to improve its separation performance and structural stability. The incorporation of metal or metal oxides inside the silica membrane is expected to improve its hydrothermal stability by increasing its resistance against densification when operated at high temperature. This could then result in an excellent H_2/CO_2 selectivity around 1500 even when the membrane was operated at 600°C and 600 kPa [30]. In addition, in comparison to the non-doped silica membrane, the hydrogen permeation activation energy of the metal-doped silica membrane is also lower and thus indicating the significant reduction of the dense structure in the metal-doped silica membranes [31,32]. Despite its proven efficacy, the metal-loading inside the membrane must also be optimized. For instance, in a zirconia-doped silica membrane, increasing the zirconia content in the silica sol from 10% to 50% results in a silica membrane with lower hydrogen permeance and selectivity [40]. The hydrogen permeation activation energy also increases from 3.4 kJ mol^{-1} to 44 kJ mol^{-1} and thus indicating the densification of the SiO_2-ZrO_2 network structure. The silica membrane with the lowest zirconia content also performs better after hydrothermal treatment giving H_2/N_2 selectivity around 190 compared to around 15 found in the silica membrane with the highest zirconia content. Similarly, if a silica membrane is doped with more than 50% niobium, structural densification occurs leading to low H_2

permeance and H_2/CO_2 selectivity around 3 x 10^{-9} mol m^2 s^{-1} Pa^{-1} and 15, respectively, after a hydrothermal treatment [47]. When the content of the niobium is less than 50%, after hydrothermal treatment, the H_2 permeance and H_2/CO_2 selectivity of the membrane can still be maintained around 3.1 x 10^{-8} mol m^2 s^{-1} Pa^{-1} and 207, respectively. Moreover, high metal doping might also lead to structural instability of the silica membranes [32].

There are also other non-conventional approaches to introduce metal into the silica membrane. A silica membrane can be binary doped such as with palladium-cobalt [29] and palladium-niobium [49]. A synergistic effect can be seen in the case of Pd-Nb BTESE-derived silica membrane, as illustrated in the Figure 4 (A, B and C), where the niobium contributes in creating a denser silica membrane structure to improve the membrane selectivity while the Pd contributes in enhancing the H_2 permeance through preferential adsorption [49]. As a result, the H_2 permeance and H_2/CO_2 selectivity of the Pd-Nb silica membrane can reach up to 1.1 x 10^{-7} mol m^{-2} s^{-1} Pa^{-1} and 107, respectively, which is significantly higher than bare BTESE-derived silica membrane. The introduction of the metal can also be carried out after the fabrication of the silica membrane as studied in the impregnation of palladium nanoparticles in the silica membrane through vacuum method as can be seen in the Figure 4 (D, E and F) [39]. In this case, the Pd nanoparticle might contribute in plugging the membrane defects. As a result, the H_2 permeation is more activated in the Pd-impregnated silica membrane as indicated by higher activation energy at 6.32 kJ mol^{-1} in comparison to 4.22 kJ mol^{-1} observed in the non-modified one because of its denser structure. Consequently, this results in lower H_2 permeance of the Pd-impregnated silica membrane that is found to be around 2.3 x 10^{-8} mol m^{-2} s^{-1} Pa^{-1} than the non-impregnated counterpart that falls around 3.4 x 10^{-8} mol m^{-2} s^{-1} Pa^{-1}. However, the H_2/N_2 selectivity of the former is about 4 times higher than the latter and reaches 115.

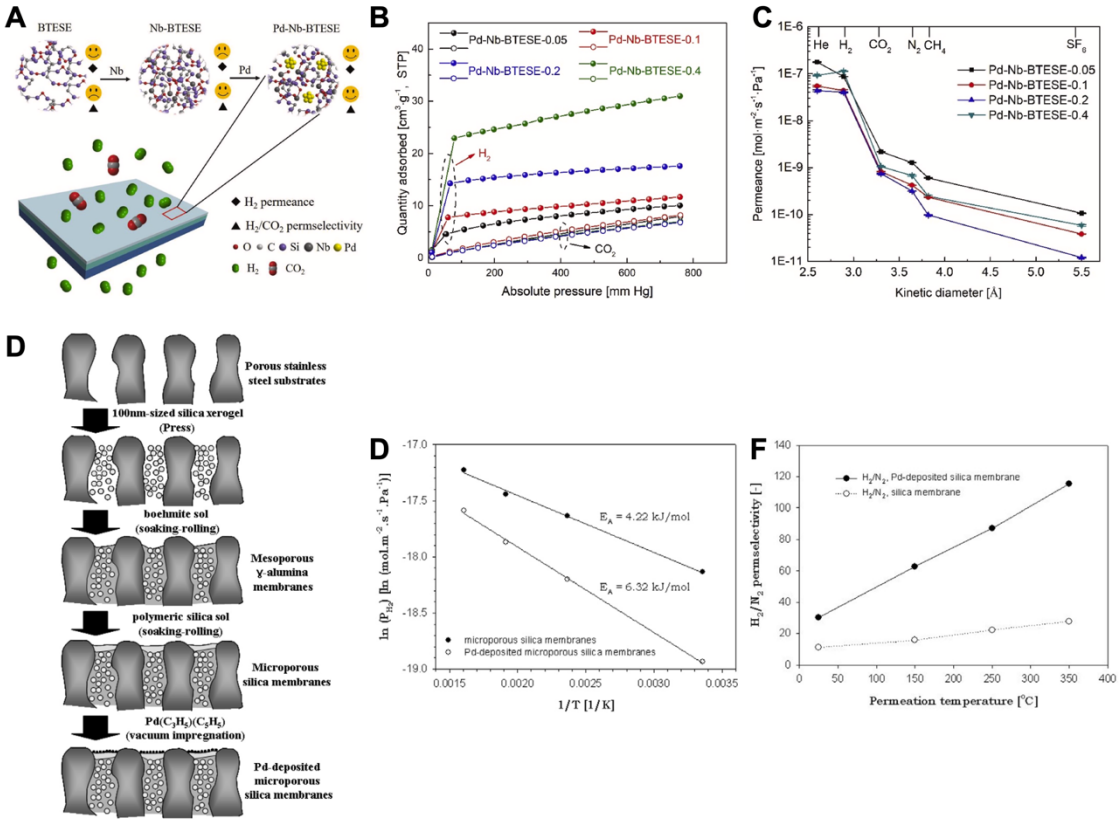

Figure 4. Illustration of the synergistic effect of the Pd-Nb-BTESE silica membrane (A) and the impact of Pd-Nb loading on hydrogen adsorption (B) and gas separation performance (C). Illustration of the palladium-impregnated silica membrane through vacuum-assisted method (D) and its impact on the hydrogen permeation activation energy (E) and H2/N2 selectivity (F). Reproduced with permission from [49] (A,B and C) and [39] (D, E and F). Copyright 2020 and 2008, respectively, Elsevier.

Operating the silica membrane at higher temperature could be more beneficial for hydrogen separation [34,38,39,57,72]. This has been exemplified by a study showing that the H_2/N_2 selectivity of the silica membrane can be improved from around 20 to be around 102 by increasing the temperature from 423 to 873 K [34]. In another study, the H_2/CO_2 of a cobalt-silica membrane can also be improved from 45 to 160 by elevating the operating temperature from 100°C to 250°C. In these cases, the hydrogen permeance of a silica membrane can be significantly increased as the temperature is elevated while the permeance of other light gases barely changes or even slightly decreases [34,72].

3.2 Zeolite membranes

In the perspective of the hydrogen separation, employing zeolite membranes is actually quite promising since it can offer a number of advantages such as well-defined pore size and better physical and chemical properties. They can also be operated at high temperature like a silica membrane since they are inorganic materials. As illustrated in the Figure 5, a number of zeolite membranes fabricated from different zeolites such as AlPO-18 [88], CHA [89], DDR [90–96], DD3R [97], FAU [98–101], LTA [102–111], Si-CHA [112,113], silicalite 1 [114,115], silicalite 2 MEL [116], MFI [117–123], NaA [124–127], SAPO 17 [128], SAPO 34 [129–138], SSZ 13 [113,137,139–145], STT [146,147], titanosilicate AM-3 [148,149], titanosilicate-umbite [150,151] and ZSM 5 [152–156] have been investigated for this purpose. They can be fabricated through two main

routes, namely *in-situ* crystallization by hydrothermal reaction, microwave-assisted or ionothermal reaction [99,100,102–105,107,108,117,119,123,132] or seeding followed by secondary growing [90,109–113,115,116,124–127,129–131,134,136,140,143–145]. Moreover, a stronger attachment between the zeolite and the support layer can also be achieved through substrate functionalization such as with 1,4-diisocyanate [106], 3-aminopropyltriethoxysilane [100,104,105,127], 3-chloropropyltrimethoxysilane [102], polyethyleneimine [126] and polydopamine [101,103]. By doing this, both the physical and covalent bond of the zeolite and the support layer can be greatly improved.

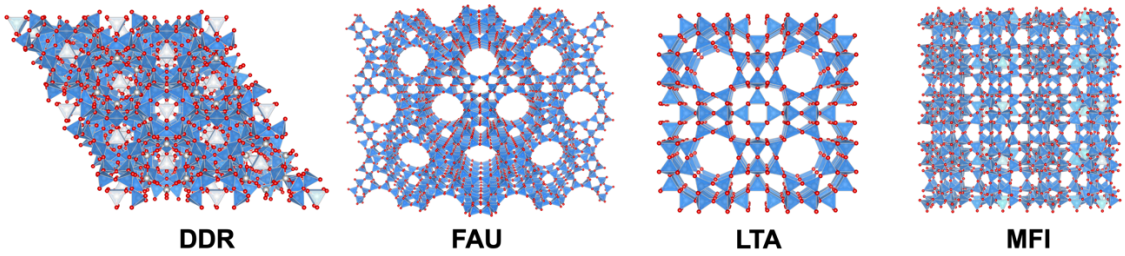

Figure 5. Some examples of zeolites used as a membrane material for hydrogen separation

In addition to a conventional single-layer membrane, a zeolite membrane can also be fabricated as a multi-layer membrane such as in the case of FAU-LTA [157], ZSM-5-silicalite-1 [152] and multi-layer LTA [105]. In this case, functionalization with 3-aminopropyltriethoxysilane at the zeolite interlayer seems necessary to act as a protective barrier for the existing layer when it undergoes the next synthesis step [157]. One of the main functions of this strategy is then to heal the defects existing in the first layer such as observed in the case of triple-layer LTA zeolite membrane, as illustrated in the Figure 4 (A and B), where the H_2 separation factor from CO_2, N_2 and CH_4 can be increased from 7; 5.8 and 4.9, respectively, observed in the single layer LTA zeolite membrane to be 12.5; 8.6 and 6.5, respectively in the triple-layer LTA zeolite membrane [105]. The application of this multi-layer approach can then also be widened by using other materials as the intermediate layer such as palladium [158]. Apart from its role to separate the hydrogen from nitrogen, the zeolite layer also contributes to protect the palladium layer against cracking in the event of drastic operating temperature changes. As a result, the H_2/N_2 separation performance of the zeolite-palladium composite membrane can be stably maintained at around 300 when the operating temperature is periodically cycled between 350^{o}C and 500^{o}C. Meanwhile, almost 300% drop in H_2/N_2 selectivity is observed in the pure palladium membrane during this cycling.

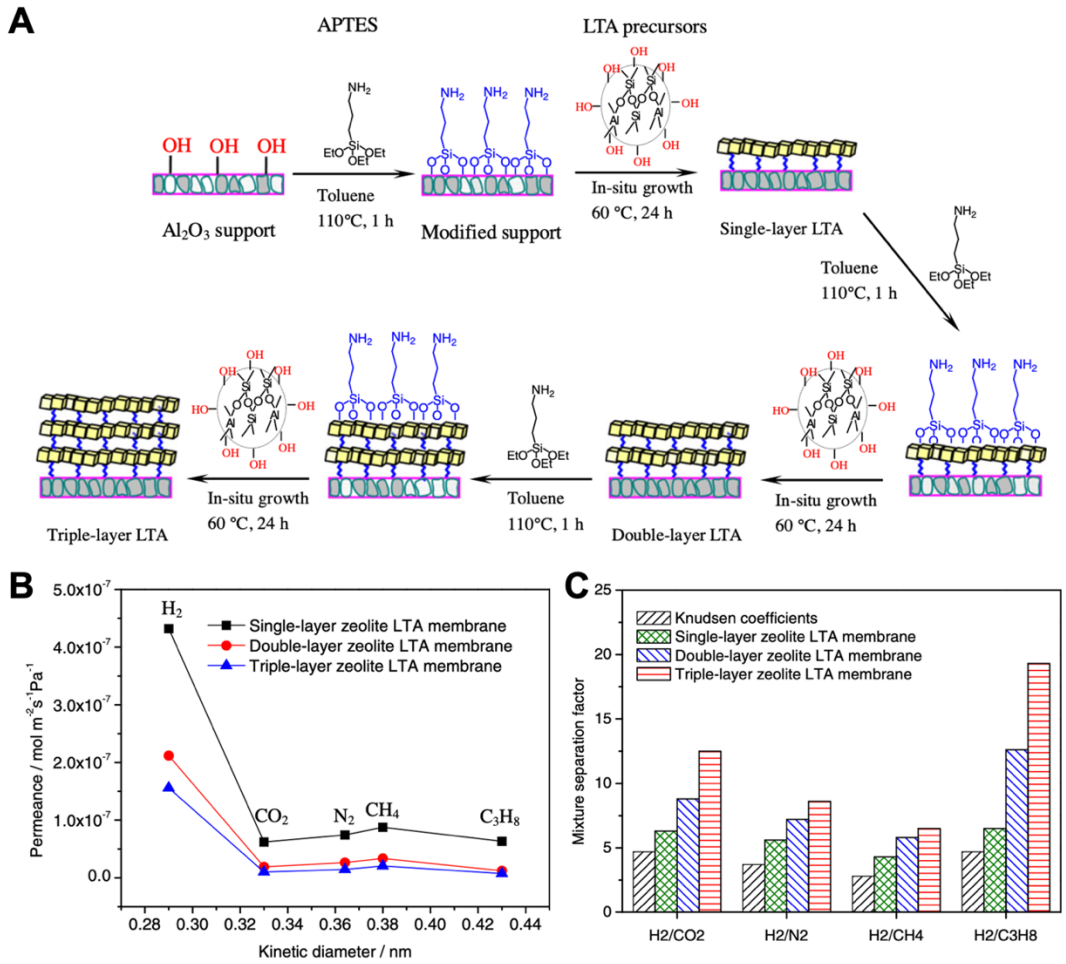

Figure 6. An illustration to fabricate a multi-layer LTA zeolite membrane functionalized with APTES at the interlayer (A) and the comparative gas separation performance of the resulting zeolite membranes with different layers (B and C). Reproduced with permission from [105]. Copyright 2012 Elsevier.

Despite all of these numerous investigations, it should also be noted that not all of the investigated zeolite membranes have shown promising performance for hydrogen separation since the employment of a zeolite with pore aperture around 0.3 nm is required to only allow the hydrogen permeation whose kinetic diameter is around 0.289 nm. Therefore, zeolite membranes such as FAU with pore size around 0.7 nm [98] or silicalite 2 MEL with pore size around 0.55 nm [116] might not be suitable for this purpose because their hydrogen molecular sieving capability will be limited.

It does not mean, however, that zeolite with larger pore size should be completely excluded to be applied for hydrogen separation purpose. One strategy to utilize this particular zeolite is to do a modification or a post-treatment process to reduce its pore size in order to enhance the hydrogen separation performance by using silica. For example, the zeolitic pore of the MFI [117–122] and ZSM 5 [129,152] can be reduced by using methyldiethoxysilane (MDES) which is decomposed at high temperature to produce amorphous SiO_2. In another study, tetraethylorthosilicate (TEOS) can also be used as a silica precursor to modify the pore of a DDR zeolite membrane [93]. The effectiveness of this deposition process can also be improved by increasing the number of acidic sites in the zeolite such as through ion exchange process [121].

This modification process can then significantly improve the hydrogen separation performance of a zeolite membrane. For example, in the case of MFI zeolite membrane, the H_2 selectivity against CO_2, N_2 and CH_4 can be improved significantly from Knudsen selectivity value to be around 141, 63, 180, respectively with only about 25% loss on the hydrogen permeance [122]. In another case, although the untreated ZSM 5 shows almost no H_2/CO_2 separation, the H_2/CO_2 selectivity can be increased to be around 47 after the modification. However, this must be compensated with lower H_2 permeance that decreases about one order of magnitude to be around 1 x 10^{-7} mol m^{-2} s^{-1} Pa^{-1} [129]. A similar result is also obtained with the DDR membrane. After modification, up to one order of magnitude lower H_2 permeance is observed to be around 2 x 10^{-8} mol m^{-2} s^{-1} Pa^{-1} but the H_2/CO_2 selectivity can be significantly improved from 2.6 to be around 33 [93].

However, it should be noted that this strategy cannot be generally applied towards all types of zeolite membrane since it must be ensured that the modifier fits into the zeolite pore and the membrane has a relatively good quality with low inter-crystalline defects [117]. In the case where the modifier cannot go inside the zeolitic pore, however, there is still a chance that such a modification can bring a beneficial impact by modifying the non-zeolitic pores or healing the membrane defective sites. This has been investigated to modify the SAPO 34 membrane [129]. In this case, the modifier does not modify the SAPO 34 pore but rather modifies the non-zeolitic pore because of the difficulty of the MDES to go into the SAPO 34 pores After the modification, the H_2/CH_4 selectivity can be increased to 59 from 39 without any significant loss on the H_2 permeance since the H_2 mostly goes through the zeolitic pore. In another study using DDR zeolite membrane, the membrane is modified using tetramethoxysilane to heal the defective sites [96]. As a result, compared to the unmodified membrane, the H_2 permeance of the modified membrane falls to 1.36 x 10^{-7} mol m^{-2} s^{-1} Pa^{-1}, which is around one order of magnitude lower, but its H_2/CH_4 selectivity can be significantly improved from around 3 to be around 45.

Another strategy to use zeolite with relatively large pore size is, as has also been briefly mentioned above, to fabricate it as a composite zeolite membrane to exploit the synergistic effect originated from its constituents. For example, in the case of FAU-LTA composite zeolite membrane, the pore aperture of FAU is around 0.74 nm [157]. Despite this, its combination with the LTA can create a new composite membrane with higher hydrogen selectivity (10.6; 8.6 and 7.1 against CO_2, N_2 and CH_4, respectively) than the membrane fabricated solely from the FAU (8; 7.2 and 5.6 against CO_2, N_2 and CH_4, respectively) which could be contributed from the synergistic effects between the two zeolites and their interlayer structure.

In addition to the pore size adjustment, the hydrogen separation performance of a zeolite membrane can also be improved when it is operated at higher temperature [118,119,129,137,152]. For example, at 150°C, the H_2/CO_2 separation of a ZSM-5/silicalite-1 bilayer membrane is found to be around 14 which then increases to be around 24 as the temperature is elevated to 450°C because of the reduced adsorption affinity of the zeolite to CO_2 [152]. A similar trend has also been observed for MFI zeolite membrane where the H_2/CO_2 separation factor can be increased about three times to be around 21 where it is operated at 300°C rather than at 150°C [118]. However, one cannot neglect the fact that a contrasting situation might also be observed as reported

in a number of cases. For example, the H_2/CH_4 selectivity of a modified SAPO 34 zeolite membrane decreases from around 59 at 25°C to be around 28 at 250°C [129]. In another study, a Ti-silicate zeolite membrane has also shown a decrease in H_2/N_2 selectivity from around 47 at 40°C to be around 31 at 150°C [150]. Si-CHA zeolite membrane has also shown a decreasing trend in the H_2/CH_4 selectivity from 85 to be around 77 as the operating temperature increases from 25°C to 150°C that is mainly caused by lower H_2 permeance at higher temperature [112]. Therefore, evaluating this trend case by case is particularly crucial since this behavior depends strongly upon a number of factors such as the effect of the adsorption of the permeating gases and the permeation activation energies through the zeolite membranes, whose differences might also be more strengthened when each gas permeates through different pores in the zeolite membrane [112,150].

Some zeolite membranes such as AIPO-18 [88], DD3R [97], SAPO-34 [138] and Si-CHA [112] have also shown a negative hydrogen separation performance trend with increasing operating pressure. For instance, when the operating pressure drop increases from 0.2 MPa to 1 MPa, the H2 permeance in the AIPO-18 membrane recues almost half to be around 0.6 x 10^{-7} mol m^{-2} s^{-1} Pa^{-1} and its H_2/CH_4 selectivity drops from around 25 to 19 [88]. In another study employing Si-CHA, the H_2/CH_4 selectivity drops from 85 to be around 50 as the pressure drops increases from 0.2 MPa to 1 MPa [112]. Such cases might be attributed because of the hydrogen coverage in the zeolite does not linearly increase with increasing pressure because of the weak hydrogen adsorption resulting in the hydrogen permeance reduction and thus renders the membrane for being ineffective to inhibit the permeation of other light gases [88,97].

3.3 Carbon-based membranes

In the area of carbon-based membranes, there are two material classes that could be promising for hydrogen purification, namely carbon molecular sieve (CMS) membrane and graphene-based membranes. Both materials are very attractive to be applied for this purpose since they can exhibit a sharp molecular sieving ability to produce a highly selective membrane.

Carbon molecular sieve (CMS) membranes

CMS membrane is a carbon-based membrane that is produced through pyrolysis of polymeric precursors. Because of this reason, it can be easily inferred that one of the most important aspects in producing a high-quality CMS membrane for hydrogen separation is the selection of the polymers. Various polymers have then been investigated as a precursor for CMS membranes, either as a self-standing or a supported CSM membrane, applied for hydrogen separation including cellulose or regenerated cellulose [159–164], cross-linked polyester [165], Kapton [166], lignin-based or lignin-derived polymers [167–169], Matrimid [170,171], novolac polymer (phenol-formaldehyde) [172–176], phenolphthalein-based cardo poly (arylene ether ketone) [177], polyamides [178], polybenzimidazole [179,180], polydopamine [181], polyetherimide [182–184], polyfurfuryl alcohol [185–189], polyhedral oligomeric silsesquioxanes (POSS) [190], poly(phthalazinone ether sulfone ketone) [191], polyimide [184,192–200], polyimide/azide [201], polymer of intrinsic microporosity (PIMs) [202], polypyrrolone [203], poly(siloxane imide) [204], Tröger's base polymer [205–207], wood tar [208] or a blend of polymers such as poly(2,6-dimethyl-1,4-phenyleneoxide) (PPO)–

polyvinylpyrrolidone (PVP) [209], poly styrene sulfonic acid-Tröger's base polymer [206], polyimide-polyvinylpyrrolidone [210], PBI-Matrimid [180,211], PBI-P84 [180,211] and PBI-Torlon [180,211].

Considering the huge possibilities of the precursors, selecting the correct precursor for a CMS membrane becomes crucial. For example, in a systematic study involving four different polyimides with different groups (aromatic, phenyl ether, $(CH_3)_2$ and $(CF_3)_2$) results in four different polyimides with four different chain structures: rod-like (PPD-PMDA), curved (ODA-PMDA), helical (BAPP-PMDA) and helical with higher fractional free volume (BDAF-PMDA), respectively [198]. As expected, a CMS membrane with highest H_2 permeability around 1673 Barrer is obtained from the helical-chain BDAF-PMDA while the rod-like PPD-PMDA shows the lowest H_2 permeability around 366 Barrer. This is because the pendant groups in the helical-chain polyimide contributes in sterically hindering the orderliness of the graphite-like sheets packing leading to a more open micropore structure after the pyrolysis. However, the H_2/N_2 selectivity of the former is only found to be around 12. Meanwhile, the PPD-PMDA-derived CMS membrane shows H_2/N_2 selectivity around 73 and thus exhibiting a more enhanced molecular sieving for hydrogen separation.

Once an appropriate polymer has been chosen, the pyrolysis process of these precursors can be conducted in the absence of oxygen and the temperature is usually set to be around 400-1000°C, which has to be optimized since this will affect the *sp3*/*sp2* ratio in the CMS membranes. In this case, a CMS membrane with high quantity of *sp3* type of defects usually exhibits high hydrogen permeance and thus controlling the conversion of the *sp3* to *sp2* hybridized carbon is crucial to obtain a CMS membrane with excellent molecular sieving property [160,192]. In this case, increasing the pyrolysis temperature of the precursor can usually bring a positive impact to increase the number of ultramicropores and also the *sp2* hybridized carbon resulting in the enhanced hydrogen molecular sieving of the CMS membranes but optimization is also necessary in order to avoid the shrinkage of the pores resulting in a defective CMS membrane [160,169–171,177,178,202,205,208,209]. For instance, when using aromatic polyamide as the carbon precursor for the CMS membrane, increasing the pyrolysis temperature from 550°C to 925°C results in a significant increase of H_2/CO_2 selectivity more than 150 times to be around 366, although the H_2 permeability also decreases from around 687.4 to 9.1 Barrer. This could be attributed to the generation of ultra-microporous regions in the CMS membrane that might exclusively allow hydrogen to be adsorbed and passed through the membrane resulting as indicated by the enhancement of both the diffusive and sorption selectivity, as illustrated in the Figure 7 (A and B) [178]. A similar situation is also observed when employing PIM as the carbon precursor [202]. By increasing the pyrolysis temperature from 600°C to 800°C the H_2/N_2 and H_2/CH_4 selectivity increases from around 28 and 40, respectively, to be around 128 and 363, respectively, without significant reduction of the H_2 permeability which can be maintained around 2177 Barrer [202]. In another study, by increasing the carbonization temperature of phenolphthalein-based cardo poly (arylene ether ketone) from 700 to 900°C, the interlayer spacing of the graphitic-like crystallite in the CMS also decreases resulting in an increase of the H_2/CH_4 selectivity from 311 to 1859, even though this has to be compromised with the reduction of the hydrogen permeance from around 4.6×10^{-7} to be around 2×10^{-7} mol m^{-2} s^{-1} Pa^{-1} [177]. In another investigation using cellulose hollow

fiber as precursor, increasing the pyrolysis temperature from 500°C to 850°C also brings down the *sp3*/*sp2* ratio of the CMS membrane from 0.73 to 0.36 resulting in a decrease of H_2 permeance from 466.8 GPU to 148.2 GPU but significantly enhancing the H_2/CO_2 selectivity from 11.1 to 83.9 [160]. In addition to the appropriate pyrolysis temperature selection, the dwelling time at this particular temperature could also crucially affect the performance of the resulting CMS membrane. For example, as investigated using cellophane as the precursor, by prolonging the dwelling time at the final pyrolysis temperature to 240 minutes, more ultramicroporous regions in the CMS membrane can be generated [164]. As a result, the H_2 permeability only slightly decreases from 148 to 109 Barrer but the H_2/CO_2 and H_2/N_2 selectivity can be more than doubled to be around 22 and 1086, respectively.

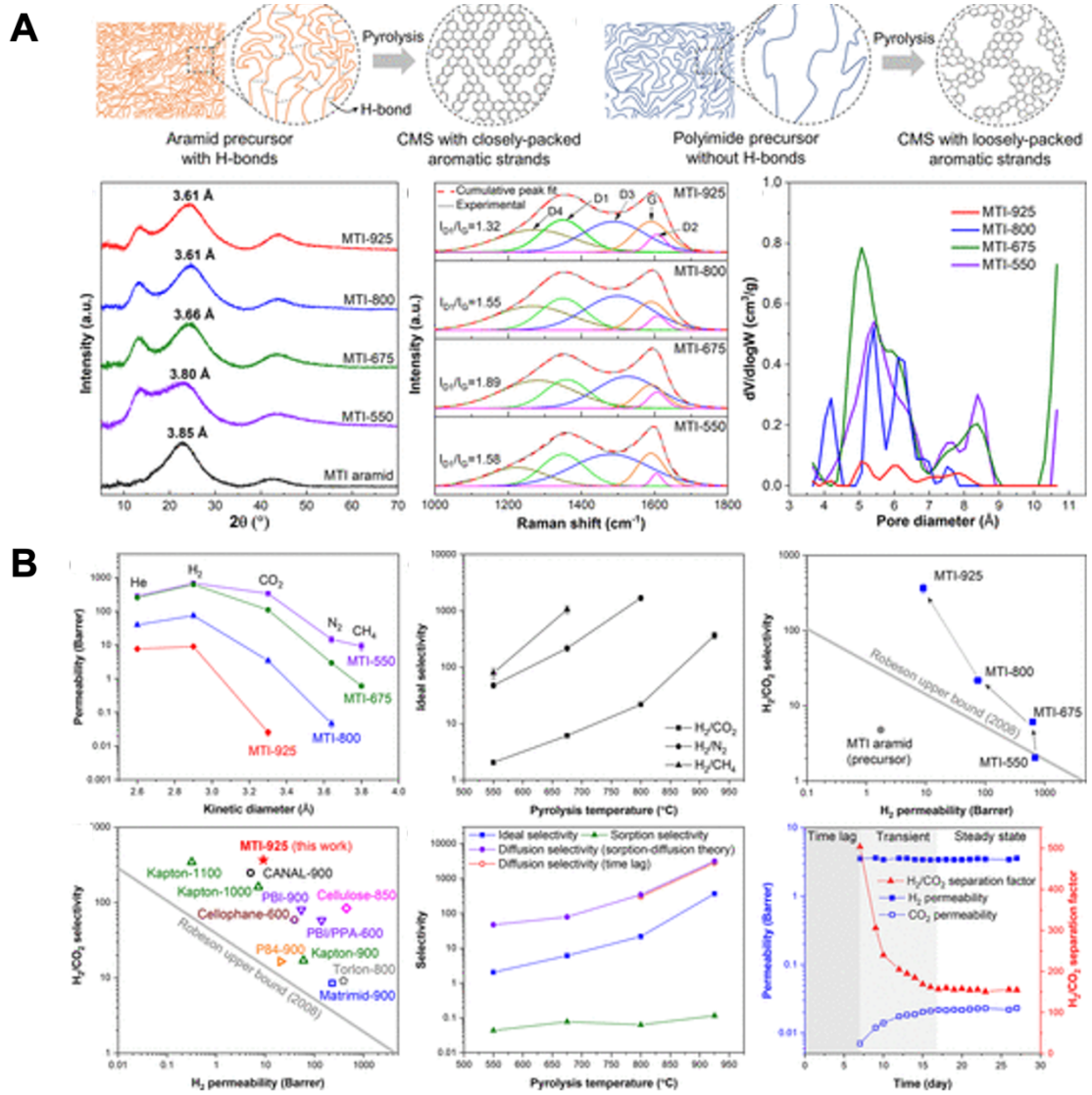

Figure 7. The illustration and the trend of the ultra-microporous generation through pyrolysis at different temperatures of an aromatic polyamide as a precursor of CMS membrane (A) and the hydrogen separation performance of the resulting CMS membranes pyrolyzed at different temperatures (B). Reproduced with permission from [178]. Copyright 2022, American Chemical Society.

The hydrogen separation performance of the CMS membranes can then be improved by employing various strategies. This can be done, for example, by adding various metals

such as aluminum [174], copper [161], iron [167] ytterbium [179] and zinc [197] to the precursor. For instance, in addition to lowering the pyrolysis temperature, the use of iron as an additive to the precursor also contributes in maintaining the neck structure of the CMS membrane to improve the hydrogen selectivity [167]. At the same pyrolysis temperature, the hydrogen permeance of the iron-added CMS is not markedly different from the non-added one (132 vs 124 x 10^{-9} mol m^{-2} s^{-1} Pa^{-1}, respectively) but the H_2/CH_4 and H_2/N_2 selectivity in the iron-added CMS membrane can be significantly improved from its non-added counterpart from 54 and 32, respectively, to be 584 and 293, respectively [167]. Similarly, when using zinc as the additive, the H_2 permeability and the H_2/CH_4 selectivity of the resulting CMS membrane constructed from polyimide can be significantly increased from 5852 to 6768 Barrer and from 84.3 to 370, respectively, since the presence of Zn^{2+} ion might help in molecularly sieve the larger gas molecules and barely affect the hydrogen permeation [197]. In another investigation using ytterbium as the dopant, compared with the pristine CMS membrane, the H_2 permeability of the metal-doped polybenzimidazole-derived CMS membrane can be increased from 519 to 1556 Barrer while its H_2 selectivity against CO_2, N_2 and CH_4 can be almost doubled to be around 12, 411 and 1532, respectively [179]. In this case, the ytterbium can establish a coordination bonding with the imidazole precursor resulting in tightened interchain packing of the precursor. As a result, after carbonization, more ultramicropores regions can be formed which are responsible to enhance the hydrogen molecular sieving.

In addition to metal doping, the CMS precursor can also be mixed with other materials such as glycerol [162], micro-nanocrystalline cellulose [212], propylene glycol [162], TiO_2 [186] and zeolite [186,213–215]. The beneficial aspect of having this composite is the possibility of the additive to tailor the porous structure of the resulting CMS membranes and rendering them to be more suitable for hydrogen separation [212,215][162]. For instance, by using around 1 wt% of propylene glycol as the additive, the H_2/CH_4 selectivity of the cellulose-derived CMS membrane can be increased to 3498 from 684 observed in the CMS membrane fabricated without additive [162]. This performance does not have to be compromised with low hydrogen permeability since it can be maintained around 500 Barrer. In another study using zeolite as an additive at 7.5 wt%, the H_2 permeability in the 10X zeolite-doped CMS membrane can be improved to 1709 Barrer with H_2/N_2 and H_2/CH_4 selectivity of 105 and 551, respectively [213].

Alternatively, the hydrogen separation performance of a CMS membrane can also be improved through post-modification strategy. This has been investigated, for example, by post-modifying the pore of the polyimide (PI) and polyetherimide (PEI)-derived CMS membranes with a carbon layer formed from the carbonization of poly(*p*-phenylene oxide) (PPO) a [184]. Compared with the pristine CMS membranes, the H_2 permeability of the post-modified CMS membranes can be increased almost 3 times to be around 1450 and 812 Barrer for PPO/PI and PPO/PEI, respectively. More remarkably, the H_2/N_2 and H_2/CH_4 selectivity for both CMS membranes can also be significantly improved from the range of 9-17 to be around 172 and 18-24 to be around 136 for PPO/PI and PPO/PEI, respectively. This has been attributed to the formation of the carbon layer from PPO that can simultaneously improve the hydrogen molecular sieving by reducing the pore size of the PI- and PEI-derived CMS membranes and also enhance their gas sorption.

Since the gas transport through the CMS membranes are also an activated process, the hydrogen selectivity of this material can also be affected by the operating temperature. In this case, operating the membrane at higher temperature might result in an increase in hydrogen selectivity [159,160,192,205] even though a number of studies have also observed the contrasting trend [161,172,177,195]. Higher operating temperature usually leads to the faster diffusion of the hydrogen. Meanwhile, the impact of the sorption of other gases also becomes lower resulting in an increase of hydrogen selectivity [160]. However, when the hydrogen permeation across the CMS membranes is less affected by the change of the temperature compared with other gases, as usually indicated through the permeation activation energy, the reverse situation might occur, namely lower selectivity at high temperature [161,172]. It has also been reported that higher operating pressure might help to increase the CMS membrane hydrogen selectivity [205]. An increase of around 20% in H_2/CO_2 and H_2/N_2 selectivity and 50% in H_2/CH_4 selectivity has been reported as the operating pressure is increased from 2 to 4 bar since the H_2 permeability barely changes compared to other gases [205].

One of the most crucial issues encountered in the CMS membrane is the aging phenomenon which is caused by sorption of oxygen and water molecules [160,167,204,215]. For instance, it has been observed that after 400 days storing in ambient condition, almost half of the hydrogen permeance is lost [167]. In another study, 50 days of storage leads to the reduction of H_2 permeance and H_2/CO_2 selectivity about 40% and 10%, respectively [160]. Regarding this phenomenon, it seems likely that, when the aging is reversible, the membrane performance might be partially brought back through heat treatment [160]. For instance, it has been observed that up to 74% of the H_2 permeability can be recovered after heat-treating the aged CMS membrane [215]. However, it can also happen that the physisorption or chemisorption occurring in the CMS membrane is already irreversible and thus heat treating the CMS membrane does not help to gain back its initial performance [161,167]. Therefore, in order to make the CMS membrane performance more stable and predictable, a high temperature treatment in the air atmosphere might then be carried out to fasten the aging. It has been observed that this process can half the aging time of a CMS membrane from 28 days to 14 days before the hydrogen permeability stabilizes [204].

Graphene-based membranes

Graphene is a 2D nanomaterial of a carbon allotrope where the carbon atoms are arranged in a hexagonal lattice. Although a perfect graphene membrane is impermeable to any gases, its defective counterparts could be used in a gas separation process. In the field of hydrogen purification, this has been demonstrated by using graphene with exceptionally high hydrogen permeance (in the order of 10^{-2} mol m^{-2} s^{-1} Pa^{-1}) with satisfactory H_2/CO_2 selectivity around 8 when its thickness can be controlled within the atomic scale [216,217]. The graphene membrane can also be modified using ozone to simultaneously control its defective sites to improve the hydrogen permeance and selectivity up to around 300% and 150%, respectively [218]. The pores in the graphene material can also be artificially fabricated such as by employing focused ion beam, which can then be further modified by depositing nickel microislands responsible to enhance the CO_2 adsorptive property and thus hindering its permeation [219]. As a result, a graphene membrane with H_2 permeance H_2/CO_2 selectivity around 20000 GPU and 26, respectively, can be obtained. However, most studies are more directed towards the use

of its derivatives, namely graphene oxide (GO) and reduced graphene oxide (rGO). Differing from graphene, GO is not a completely 2D material and therefore can be non-uniformly stacked to become permeable to small gases, as long as the energy barrier of gas permeation can be surpassed [220].

A defect-free GO membrane for hydrogen separation can be prepared through different methods such as vacuum filtration [221–234], spin coating [220,224,235] and spray-evaporation [236]. Regardless of the chosen method, the GO membrane fabrication is usually initiated by preparing a GO suspension. In order to obtain a good GO membrane, the steps involved in this phase, such as centrifugation and dilution, need to be optimized [221]. Once a good GO suspension is obtained, the next crucial step is to obtain a smooth GO membrane with less wrinkle sites and excellent interlayer stacking resulting in an optimum *d* spacing between the GO nanosheets that is sufficient to molecularly sieve hydrogen from other light gases. In this step, modifying the substrate with Silicalite-1 to improve the interfacial adhesion of the GO membrane [234], synthesizing the GO with Brodie instead of Hummer method [229], having a large GO nanosheets, which can be obtained through repeated freeze-thaw method [224] or pre-cross-link the GO nanosheets with cations [232], ethylenediamine [225] or cysteamine [231] have been proven to be helpful to control the *d* spacing of the GO membrane so it can perform well for hydrogen purification. In the case of spin-coating, directly spin-coating a GO solution on a polyethersulfone substrate, rather than firstly contacting the substrate to the air-liquid interface of the GO suspension, can produce a GO membrane with interlocked layer structure exhibiting molecular sieving ability [220]. In another study, spinning polyethyleneimine (PEI) as an intermediate layer between GO nanosheets, as can be seen in the Figure 8 (C and D), might also help to reduce the electrostatic repulsive force between two GO nanosheets and thus resulting in a more homogeneous interlayer GO stacking [235]. When compared with the normal GO membrane prepared without PEI as the intermediate layer, the H_2/CO_2 selectivity of the latter is about 6 times higher reaching about 30 with H_2 permeance 1200 Barrer. Meanwhile, in the case of self-standing GO membrane, Even though most of the GO membranes for hydrogen separation are fabricated on a porous support, using a slow filtration rate during the collection of the GO nanosheets is crucial to produce a good GO membrane exhibiting a molecular sieving capability since faster filtration leads to a more haphazard arrangement of the GO stacks and thus producing a looser membrane [237].

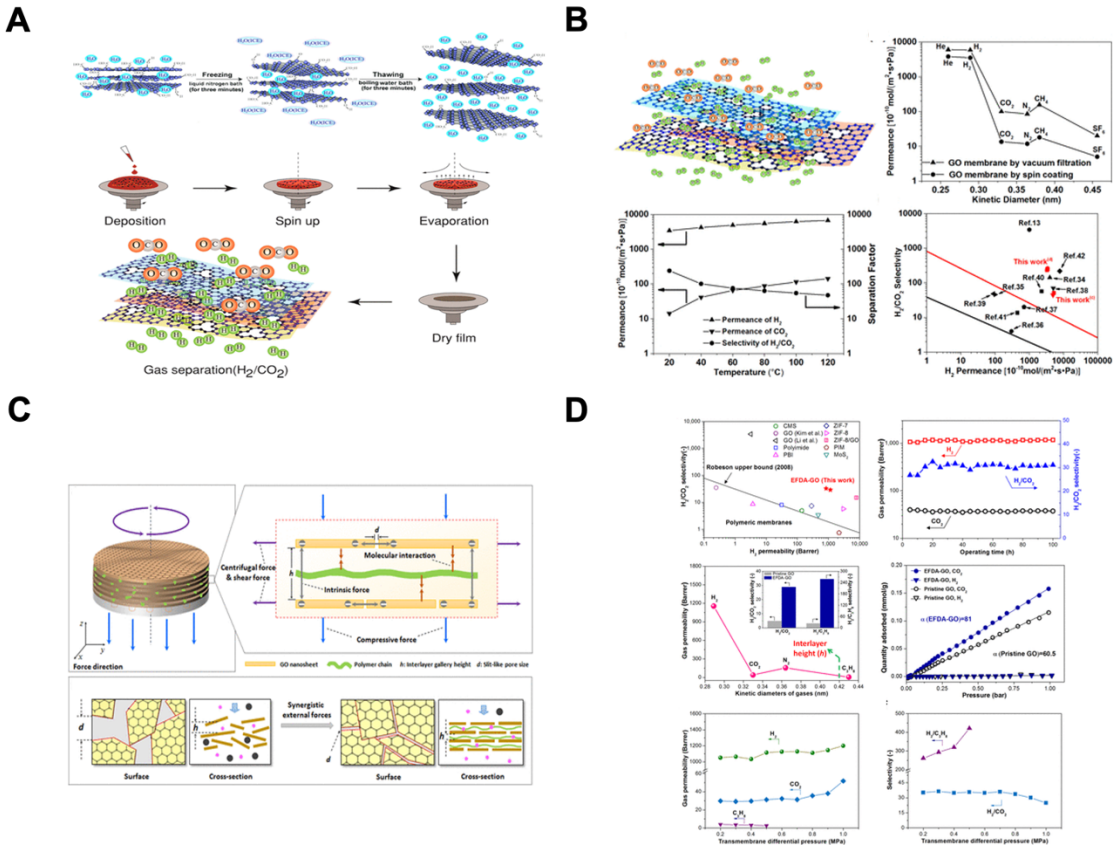

Figure 8. Illustration of the strategy to fabricate a GO membrane with freeze-thaw approach (A) and PEI as an intermediate layer (C) and their corresponding hydrogen separation performance shown in (B) and (D), respectively. Reprinted with permission from [224] and [235], respectively. Copyright 2016, American Chemical Society

The hydrogen separation performance of a GO membrane can then be influenced by a number of factors but the gas pathways in a GO membrane is considered to be mainly influenced by the interlayer spacing of the GO sheets and the structural defects [220]. The interlayer spacing of a GO membrane can then be reduced by reducing it into an rGO membrane [238]. However, this strategy barely positively impacts the hydrogen separation performance of the modified membrane [222]. Therefore, controlling the structural defects of a GO membrane might be a more effective way to obtain a GO membrane with excellent hydrogen separation performance. In this case, it has been observed that the hydrogen permeance in a GO membrane decreases exponentially as the membrane thickness increases [221]. It is then hypothesized that the hydrogen and other small gases permeate through the structural defects of the GO membrane with molecular sieving ability. Therefore, by optimizing the membrane thickness down to 9 nm, a GO membrane with H_2/CO_2 and H_2/N_2 selectivity of around 3400 and 900, respectively, can be obtained [221].

Moreover, the hydrophilicity of the GO membrane and the presence of various functional groups in the GO membrane can also influence the hydrogen separation performance. It has been observed that a GO membrane might show a CO_2-philic transport property in its pristine state where CO_2 is the fastest gas transported across the membrane [220]. However, this condition can be reversed by thermally annealing and operating the membrane at elevated temperature to open up the GO pore and renders it to be less CO_2-philic and thus resulting in H_2/CO_2 selectivity around 40.

However, it should also worth to note that, even though the hydrogen permeance of a GO membrane can be enhanced at high temperature, operating the GO membrane at elevated temperature might also result in the reduction of its initial selectivity [220,226,228,230,233]. For example, when operated at 120°C, although the hydrogen permeance increases up to three times compared to the room temperature operation, the H_2/CO_2 selectivity of a GO membrane has been observed to get lower from around 240 to 47 [224]. In another study, the H_2/N_2 selectivity of a surfactant-modified GO operated at 100°C also reduces to be around 10 from 30 when operated at room temperature [228]. This might then be caused by various factors including the faster diffusion process of the gas transport at high temperature and also because the GO membrane becomes more porous [220,228].

3.4 Metal organic frameworks (MOF)- and covalent organic framework (COF)-based membranes

Metal organic frameworks (MOF)

In the last two decades there is a growing interest in the research and development in the field of metal organic frameworks (MOFs) as a promising next generation of porous materials that can be used for various purposes such as water purification [239], sensor [240] and also gas separation [241]. As the name indicates, MOF is constructed from metal clusters which are connected by organic linkers. In addition to its high surface area and porosity, one of the main selling points of MOFs is their tailorable architecture, which means that one can rationally design a MOF for a specific purpose and this possibility is principally endless.

Various MOFs, as illustrated in the Figure 9, have then been investigated to be achieve this objective such as CAU-1 [242], CAU-10-H [243], CAU-10-PDC [244], CuBTC [245–254], MIL-53(Al) [255], MIL-53(Al)-NH_2 [256,257], MOF-74(Mg) [258], MOF-74(Ni) [259], UiO-66 [260,261], UiO-66-NH_2 [262], ZIF-7 [263–266], ZIF-8 [253,263,266–268,268–294], ZIF-9 [295,296], ZIF-67 [296–298], ZIF-78 [299], ZIF-90 [300–302], ZIF-95 [303–305] and ZIF-100 [306]. As in the case of the zeolite membrane, there are two main routes that can be used to fabricate a MOF membrane for hydrogen separation, namely *in-situ* crystallization [243,250,252,263,266,270,272,276,295] and seeding followed by crystal growing [244,249,253,256,259,261,262,264,273–275,281,282,299,304]. However, in the case of MOF membranes, there are more rooms to be explored since this material offers a different chemistry than zeolite. One of the strategies that are often explored is by separately preparing the metal and ligand solution which can then brought in contact through different methods. For example, a substrate can be firstly covered by metal hydroxide nanostrand, metal oxide or metal sol to be later converted into MOF once exposed to the ligand precursor either in the solution or in a vapor-assisted mode as exemplified in the case of CuBTC [247,254] and ZIF-8 [279,289,293]. Another strategy is by employing a layer by layer assembly method where the substrate is exposed consecutively to the metal and ligand precursor [251,269,271,297]. Counter-diffusion is also another method to produce a MOF membrane where the metal and ligand precursor are located on the different side of the substrate so the substrate acts as a porous barrier between the two precursors. This method has been used to produce ZIF-8 membrane [267,284]. A rather rapid MOF membrane can also be fabricated through an evaporation-induced crystallization [245], electrospray deposition [265] or crystallization using sustained precursor method [290] which can significantly reduce

the production time of the MOF membranes. Moreover, MOF membranes can also be produced with a certain orientation to improve its hydrogen molecular sieving effect. This is exemplified in the case of ZIF-95 where the presence of MOF seeds and MOF building block on a porous substrate can be converted into *c*-oriented dense membrane through vapor-assisted process [305].

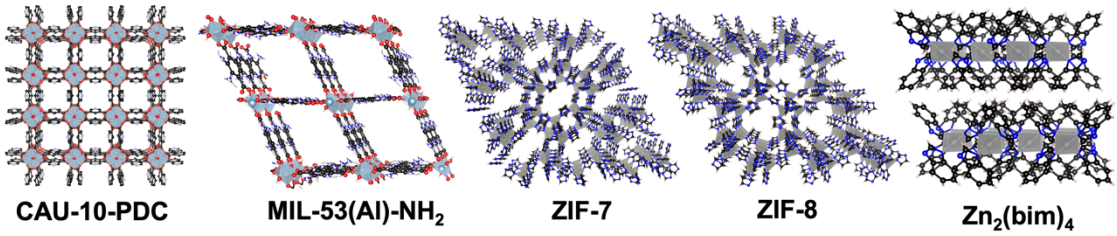

Figure 9. Some examples of MOFs used as a membrane material for hydrogen separation

The substrate for the MOF membranes can also be firstly modified before the MOF is grown on its surface. In the case of inorganic substrates, they can be firstly coated or modified by various methods such as immersing in the ligand solution [268], oxidization [252], coating with various molecules such as 3-aminopropytriethoxysilane [282,295,300,303], 3-aminopropytriethoxysilane-TiO_2 [285], chitosan [249], cobalt nanosheets [298], gelatin containing metal hydroxide nanostrands [275], layered double hydroxide (LDH) [277], LDH-ZnO [272], metal gels [287], poly(methyl methacrylate) (PMMA) which is followed by hydrolysis process [250], polydopamine [306], polydopamine-modified carbon nanotube [286] and ZnO [270,276,278,280,291,296]. Meanwhile, in the case of a polymeric substrate, hydrolysis [246], ammoniation [248,257] or coating with other materials with similar property as the MOF, such as metal phenolic networks [288], metal ions [246] or ZnO array [266], can also be an option to increase the MOF attachment to the support.

In the first development of a MOF membrane for hydrogen separation, a number of researches have been devoted to CuBTC since this MOF is relatively simple to be prepared. However, considering its relatively big pore aperture, the separation factor might not be too satisfactory. Addressing this issue, ZIF family MOF, such as ZIF-7, ZIF-8, ZIF-9, ZIF-95 and ZIF-100 might offer a more promising separation performance since their pore aperture usually lies around 0.3 nm. Using a microfluidic approach, a ZIF-7 membrane has exhibited H_2 permeance around 22 x 10^{-10} mol m^{-2} s^{-1} Pa^{-1} and H_2 selectivity against N_2 and CH_4 around 35 and 34, respectively, [263]. In another investigation, a ZIF-7 membrane with higher H_2 permeance about 4.5 x 10^{-8} mol m^{-2} s^{-1} Pa^{-1} can be obtained with H_2 selectivity against CO_2, N_2 and CH_4 around 13.6; 18 and 14, respectively [264]. In the case of ZIF-8, up to around 23 and 78 in H_2/N_2 and H_2/CH_4 selectivity, respectively, with H_2 permeance 1.4 x 10^{-8} mol m^{-2} s^{-1} Pa^{-1} has been reported [272]. Even though the ZIF-8 framework is reported to be flexible and its pore aperture is a little bit bigger than ZIF-7, such a high hydrogen selectivity could be associated with the reduction of the ZIF-8 grain size and the suppression of the ZIF-8 framework flexibility when it is grown in the confined environment of ZnO nanocrystals. Using the same idea of a confined growing of ZIF-8, an ultrathin ZIF-8 membrane with thickness around 550 nm can also be produced using a counter-diffusion approach employing polydopamine-wrapped single-walled carbon nanotube as the interlayer [267]. The resulting membrane shows H_2 permeance around 6.3 x 10^{-7} mol m^{-2} s^{-1} Pa^{-1} and H_2

selectivity against CO_2, N_2 and CH_4 around 43, 20 and 38, respectively. A good separation performance has also been exhibited by ZIF-9 membrane that has H_2 permeance and H_2/CO_2 separation factor around 1.1 x 10^{-7} mol m^{-2} s^{-1} Pa^{-1} and 22, respectively [295]. Using a secondary growing strategy by utilizing the ZIF-95 nanosheet geometry as the seed, a defect-free ZIF-95 membrane can also be grown on an alumina substrate showing a promising H_2 separation performance [304]. The H_2 permeance of the membrane is reported to be around 1.7 x 10^{-7} mol m^{-2} s^{-1} Pa^{-1} and its H_2 selectivity against CO_2, N_2 and CH_4 is found to be around 42, 37 and 40, respectively. When the orientation of the ZIF-95 can be controlled, a slightly better performance with H2 permeance around 7.9 x 10^{-7} mol m^{-2} s^{-1} Pa^{-1} and H_2/CH_4 selectivity around 54 can also be obtained [305]. In the case of ZIF-100, it has been found that the H_2/CO_2 selectivity of this MOF membrane can reach 70 with H_2 permeance around 5.8 x 10^{-8} mol m^{-2} s^{-1} Pa^{-1} [306]. Even though its pore aperture is slightly larger than the kinetic diameter of CO_2, its high separation performance is attributed to the strong CO_2 adsorption within the framework resulting in the retardation of CO_2permeation.

In order to further improve the hydrogen separation performance, the MOF membranes can also be post-modified such as through functionalization. For instance, a ZIF-67 membrane can be post-modified by introducing ethylenediamine into its pores [298]. Even though the H_2 permeance decreases more than twice to be around 6.5 x 10^{-7} mol m^{-2} s^{-1} Pa^{-1}, the H_2/CO_2 selectivity can be significantly improved from around 17 to 30. Using the same molecule, the pore of MOF-74(Mg) has also been successfully modified to improve its H_2/CO_2 separation from around 11 to be 28 while maintaining H_2 permeance around 1.2 x 10^{-7} mol m^{-2} s^{-1} Pa^{-1} [258]. In addition to the pore narrowing effect, the presence of the amine group from ethylenediamine in a MOF with big pore aperture such as MOF-74(Mg) can also hinder the CO_2 passage through the adsorption effect. Post-modification can also be carried out by exploiting the functional group in the MOF such as with the aldehyde group of ZIF-90 which can be functionalized through imine condensation with ethanolamine [301] or with organosilica [302]. Compared with the non-modified membrane, the H_2 permeance of the ethanolamine-functionalized ZIF-90 only drops around 16% to be around 2 x 10^{-7} mol m^{-2} s^{-1} Pa^{-1} but the H_2 selectivity against CO_2, N_2 and CH_4 significantly improves to be around 15, 16 and 19, respectively. A more significant improvement, however, is obtained for the organosilica-modified ZIF-90, as illustrated in the Figure 10 (A), which shows H_2 selectivity against CO_2 and CH_4 to be around 20 and 71, respectively. Post-modification can also be carried out with rapid thermal treatment as exemplified in ZIF-8 [294]. By thermally treating the ZIF-8 at 360°C for less than 10s, the lattice flexibility of the ZIF-8 can be significantly reduced and thus resulting in a ZIF-8 membrane with H_2/N_2 and H_2/CH_4 selectivity of more 200, which is more than 10-fold improvement than the pristine ZIF-8 membrane and also significantly higher than most of the ZIF-8 polycrystalline membranes.

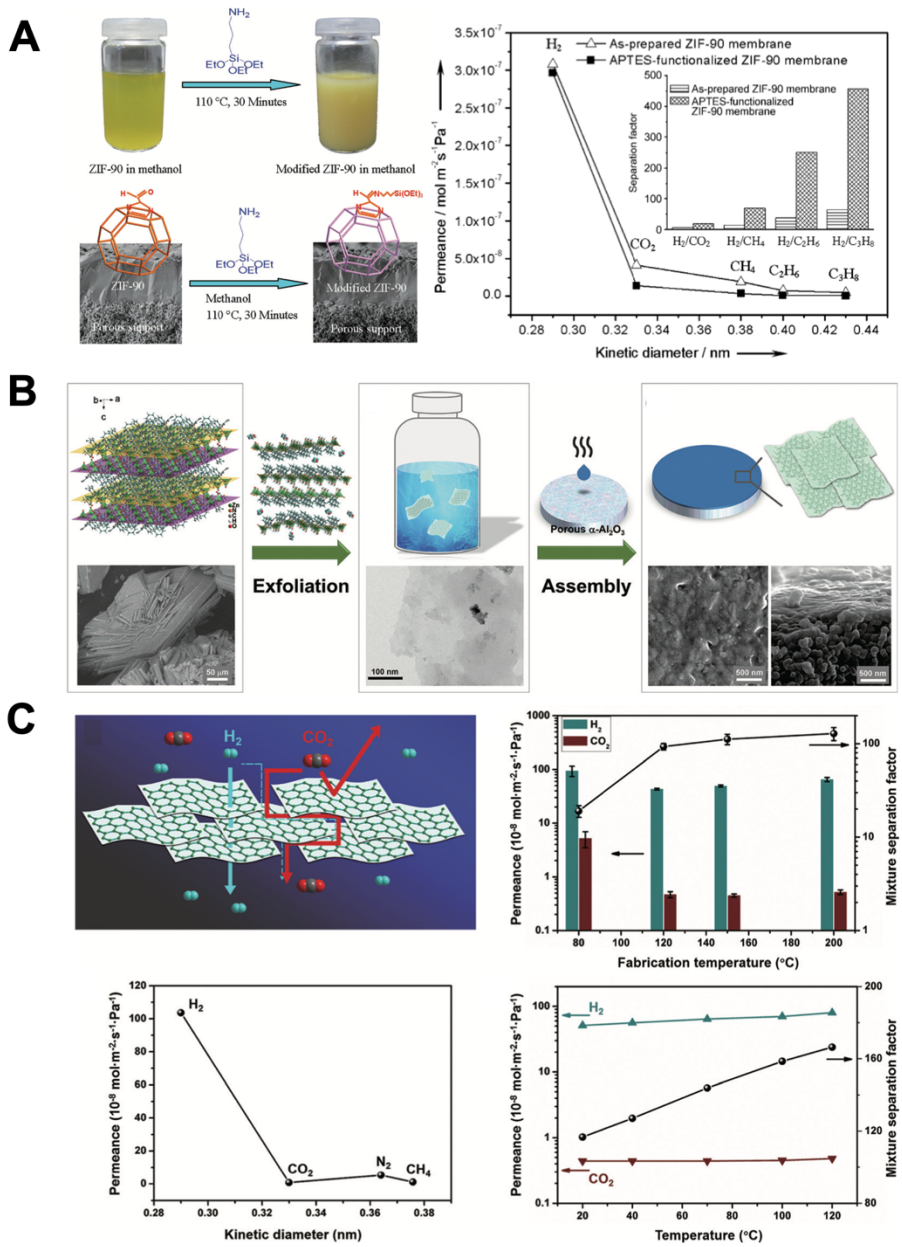

Figure 10. The Illustration of the ZIF-90 pore modification using organosilica and the impact of the modification process on the hydrogen separation performance (A). The illustration of the fabrication process of 2D $Zn_2(bim)_3$ MOF membrane through exfoliation and drop-casting on a hot substrate (B) and its hydrogen separation performance (C). Reproduced with permission from [302] (A) and [307] (B and C), Copyright 2012 (A) and 2017 (B and C) John Wiley and Sons, Inc.

As in the case of zeolite membrane, a MOF membrane for hydrogen separation can also be fabricated from two different MOFs constructed as double layer, as studied in in ZIF-90/ZIF-8 [290], ZIF-8/ZIF-9 [308] and ZIF-67/ZIF-9 [308]. In the case of ZIF-8/ZIF-9 and ZIF-67/ZIF-9, the main rationale to exploit the hydrogen molecular sieving property from ZIF-9 that has smaller pore size than ZIF-8 and ZIF-67 [308]. Meanwhile, both ZIF-8 and ZIF-67 contributes in reducing the CO_2 preferential adsorption. Using this strategy, the H_2 permeance of the ZIF-8/ZIF-9 and ZIF-67/ZIF-9 at 150°C is found to be around 83.9 x 10^{-9} mol m^{-2} s^{-1} Pa^{-1} and 53.3 x 10^{-9} mol m^{-2} s^{-1} Pa^{-1}, respectively, and its H_2/CO_2 selectivity is found to be around 9. In another investigation, a double layered MOF membrane of ZIF-8/ZIF-67 and ZIF-67/ZIF-8 have been studied for hydrogen separation [297].

Compared with the ZIF-67 membrane, the H_2 selectivity against CO_2, N_2 and CH_4 can be improved almost twice to be around 13, 10 and 11, respectively. This might be attributed to the increase of the surface smoothness when growing the second layer of the MOF resulting in a MOF membrane with less defect densities.

One of the strongest-performing MOFs for the hydrogen separation probably comes from the employment of nanosheet architecture. In this case, a study using 2D CuTCPP membrane which is grown in the *c*-orientation has shown a promising H_2 permeance and H_2/CH_4 selectivity around 2.4 x 10^{-7} mol m^{-2} s^{-1} Pa^{-1} and 55, respectively [309]. Even though the pore aperture of this MOF is quite large around 1 nm, by growing the MOF as a highly oriented membrane, the AB stacking of the MOF can be established resulting in a reduction of the pore aperture and thus imparting the hydrogen molecular sieving ability. A different situation is encountered, however, in the case of $Zn_2(bim)_4$ because its pore aperture is already very tight around 0.21 nm and thus can potentially only allow hydrogen to pass through while rejecting all other light gases [310]. It has been successfully fabricated as a 1 nm thickness membrane through drop casting method on a hot surface. The H_2 permeance of this membrane is reported to be as high as 2700 GPU with around 291 H_2/CO_2 selectivity. Using the same strategy others sub-10-nm 2D MOFs such as $Zn_2(bim)_3$ MOF membrane, as illustrated in the Figure 10 (B and C), with H_2 permeance and H_2/CO_2 selectivity around 65.1 x 10^{-8} mol m^{-2} s^{-1} Pa^{-1} and 128, respectively [307] and $[Cu_2Br(IN)_2]_n$ with H_2 permeance around 600 GPU and H_2/CO_2 and H_2/CH_4 selectivity around 190 and 290, respectively, can also be produced [311] and thus demonstrating the versatility of this approach to fabricate a 2D MOF membrane with excellent hydrogen separation performance. In another study, an ultra-thin ZIF-L nanosheet membrane with a membrane-interlocked-support (MIS) architecture has also been developed by confining the grow of the nanosheets inside the voids of the porous support [312]. As a result, a MOF membrane with high H_2 permeance around 4033 GPU and a very good H_2/CO_2 selectivity of around 321 can be obtained because the membrane intercrystalline structure is significantly reinforced. One of the most interesting features related to the 2D MOF membrane is the inverse relationship that could occur between membrane thickness and selectivity. In the case of $Zn_2(bim)_4$, stacking the nanosheets more than a few layers can reduce the H_2/CO_2 selectivity from 291 up to 53 [310]. Similarly, in the case of $Co_2(bim)_4$ 2D membrane which is fabricated using ligand-vapor phase transformation of a cobalt gel, increasing the membrane thickness from 57 nm to 750 nm results in the decrease of the H_2/CO_2 selectivity from 58.7 to around 10 [313]. This phenomenon then suggests the dependency of the gas selectivity on the nanosheet stacking behavior (i.e., misalignments or orderliness) which could lead to the generation of non-selective voids in the nanosheet stacking resulting in the reduction of gas selectivity.

Advancement in this field has also revealed the possibility to utilize the competing permeating gas to further enhance the gas selectivity. For instance, the performance of a CAU-10-PDC membrane has been observed to be significantly affected by the CH_4 molecule since it can induce the conformational change in the crystal lattice of the MOF [244]. During the initial period of separation, the H_2 permeance is found to be 3326 Barrer with H_2/CH_4 selectivity around 2 x 10^{-8} mol m^{-2} s^{-1} Pa^{-1}. After more than 1300 minutes equilibration time, the H_2 permeance drops almost one order of magnitude lower but the H_2/CH_4 selectivity increases to be around 101. This could be attributed to

the change of the pore limiting diameter of the MOF from 0.415 nm to 0.295 nm upon exposure to CH_4. Another case is also observed in the amino-modified $Zn_2(bim)_4$, which is synthesized through a mixed ligand strategy by mixing benzimidazole and 5-aminobenzimidazole [314]. The H_2 permeance of the resulting nanosheet membrane is around 1966 GPU with a very high H_2/CO_2 selectivity around 985, which coud be caused by the CO_2 molecules that are physisorbed at the interlayer of the nanosheets during permeation and thus contributing to regulate and stabilize the nanosheet stacking resulting in a significant improvement of the molecular sieving capability of the membrane.

In addition to the 2D MOF, another promising approach can also be seen in the direction of the employment of MOF-glass membrane. This has been investigated by using ZIF-62 because it has the glass-forming ability [315]. The MOF-glass membrane is obtained by melt-quenching process where it is subjected to the melting temperature before being cooled down to form the glass. The advantage of this approach is, during the melting process, the MOF is in the liquid phase and thus has the ability to penetrate the porous support and also heal its intercrystalline defects generated during the polycrystalline membrane fabrication. In addition, the resulting MOF glass can still maintain its microporous structure and thus able to separate hydrogen from the light gases. The H_2 permeability of this membrane has been reported to be around 4600 Barrer with selectivity against N_2 and CH_4 to be 53 and 60, respectively.

For some of the MOF membranes, increasing the operating temperature does seem to benefit the hydrogen separation performance. This is evidenced, for instance, in the case of ZIF-7 membranes where the H_2/CO_2 selectivity increases at higher operating temperature [263–265]. In one study, this value can improve remarkably to 13.6 from 5.4 as the operating temperature increases from 50°C to 220°C [264]. In the case of ZIF-95 membrane, the H_2/CO_2 separation factor also increases from around 19 to be around 42 as the temperature goes up from 50°C to 200°C [304]. The H_2/CO_2 selectivity of a 2D MOF membrane $Zn_2(bim)_3$ has also shown the same trend where it increases from around 120 to be 160 as the operating temperature increases from 20°C to 120°C [307]. In these cases, higher temperature will considerably enhance the H_2 diffusion compared to other gases, as can be indicated through the permeation activation energy. In addition, the adsorption of other gases might also be hindered as the temperature increases.

A contrasting trend, however, is also reported as in can be seen in the selectivity trend of a CuBTC [246], MIL-53(Al)-NH_2 [257], MOF-74(Mg) [258], amine-modified MOF-74(Mg) [258], ZIF-9 [295] and ZIF-100 [306]. For instance, the H_2/CO_2 selectivity of a ZIF-9 membrane reduces from around 22 at 25°C to be around 15 at 125°C. Such a decrease in the selectivity can also be more pronounced in a MOF membrane with high affinity towards CO_2. For instance, the amine-modified MOF-74(Mg) experiences a drop in H_2/CO_2 selectivity from 28 to around 10 as the operating temperature increases from 25°C to 100°C [258]. Meanwhile, its non-modified counterpart only exhibits a slight drop from 10.5 to be around 10. In these cases, the diffusion of the competitor gases is more affected by the change of the operating temperature, as can be indicated by their activation energy, and thus increasing the competitive diffusion process of hydrogen to go through the membrane. Another example can be seen in the case of ZIF-100 membrane, where the H_2/CO_2 separation is highly dependent on the retardation of the

CO_2 permeation because of the strong adsorption, increasing the operating temperature from 25°C to 150°C results in the reduction of H_2/CO_2 selectivity from 70 to around 20 [306]. This is because less CO_2 is adsorbed at higher temperature and therefore it can permeate more freely resulting in lower H_2/CO_2 selectivity.

Covalent organic frameworks (COF)

Differing from MOF, COF is completely built from organic materials and thus does not contain any inorganic parts. As in MOF, the architecture of COF can also be rationally tuned and thus rendering it for principally having endless possible structure. There are a number of studies using different type of COFs investigated for hydrogen separation process such as ACOF-1 [316], COF-300 [317,318], COF-320 [319], DMTA-TAM-COF [320], LZU-1 [316,321], N-COF [318], TFB-BD [321], TpEBr [322], TpPaMe [323] and TpPa-SO_3Na [322].

As in the case of MOF membrane fabrication, the porous substrate for the COF membrane fabrication can also be modified using different approach in order to improve the attachment of the COF membrane such as by using 3-aminopropyltriethoxysilane [316,319] and polyaniline [317,320]. Such a stronger attachment is possible since a covalent bond can be established between one of the COF monomers and the modifier. For example, by using 3-aminopropyltriethoxysilane, the amino group of this molecule can react with the aldehyde group through imine condensation [319]. In addition, the substrate can also be functionalized to control the orientation of the COF membrane as exemplified by the use of CoAl-LDH layer to vertically grow COF-LZU-1 and TFB-BD COF membranes [321]. However, it is also possible to fabricate a self-standing COF membrane in the absence of a porous substrate as exemplified in the case of N-COF and COF-300 [318]. This strategy relies on molding the mixture of the COF building blocks and transforming them into a crystalline structure in an autoclave with the assistance of the vapor from the solvents.

Despite these numerous attempts, not all of them have shown an excellent performance for hydrogen separation because of their relatively big pore aperture. For example, COF-320 membrane with pore aperture around 0.8 nm also shows H_2 selectivity against N_2 and CH_4 around 3.5 and 2.5, respectively [319]. A better performance has then been shown by LZU-1 COF membrane with around 1.8 nm pore aperture that has moderate H_2 selectivity against CO_2, N_2 and CH_4 around 6, 8 and 9, respectively [316]. However, it a rather sharp hydrogen molecular sieving cannot be seen in these cases.

There are, however, cases where a sharp hydrogen molecular sieving is observed in COF membranes. For example, in the case of N-COF and COF-300, the H_2/CO_2 separation factor is found to be around 13.8 and 11, respectively, while the H_2 permeance is around 4319 and 5160 GPU, respectively [318]. In both cases, although the pore aperture of the COF is relatively big, the CO_2 molecules do have a tendency to get adsorbed in the COF's pores while the H_2 can diffuse freely resulting in high H_2 permeance and selectivity. Numerous studies have also been attempted to improve the molecular sieving capability of the COF membranes.

One possible strategy to improve the hydrogen molecular sieving in a COF membrane is to fabricate it as a dual-layer membrane as in the case of zeolite and MOF. In this case, a dual-layer LZU-1 – ACOF-1 membrane has been successfully fabricated with H_2 permeability around 600 Barrer and has exhibited a high H_2 selectivity against CO_2, N_2

and CH_4 around 24, 84 and 100, respectively [316]. Such a high hydrogen selectivity can be obtained because of the interlacing of the pore network at the interface between the COF layers resulting in improved molecular sieving. Another strategy is to vertically-aligned the COF rather than conventionally aligning them horizontally. In this case, the separation process will take place through the interlayer spacing of the COF which is around 0.3-0.4 nm and thus can perform hydrogen molecular sieving [321]. Using this strategy, the LZU-1 COF membrane has shown H_2 permeance around 3500 GPU with H_2/CO_2 and H_2/CH_4 selectivity around 30.

Another strategy is to stack the COF membrane with other materials with opposing charge to reduce its pore aperture. In this case, a combination of cationic TpEBr COF nanosheet and anionic TpPa-SO_3Na COF nanosheet has been studied for showing a great promise for hydrogen separation [322]. As illustrated in the Figure 11, the rationale behind this strategy is to reduce the pore aperture of the COF's constituents by alternately stacking the cationic-anionic COFs on a porous alumina substrate using the Langmuir-Schaefer (LS) method. As a result, an ultrathin 41 nm COF composite membrane can be fabricated showing H_2 permeability around 108 Barrer and H_2 selectivity against CO_2, N_2 and CH_4 around 26, 40 and 74, respectively. This is in stark contrast to the H_2 selectivity of both COF constituents against CO_2, N_2 and CH_4 which is only found to be moderate in the range of 7, 10 and 12, respectively. Using the same strategy, the pore aperture of cationic TpPa-1 COF can also be reduced by stacking with non-porous anionic MXene $Ti_3C_2T_x$ by utilizing the opposite charge of the two materials [324]. Compared with the pure TpPa-1 COF membrane, the H_2 permeance of the composite decreases from 73.9 x 10^{-8} mol m^{-2} s^{-1} Pa^{-1} to 23.5 x 10^{-8} mol m^{-2} s^{-1} Pa^{-1} but the H_2/CO_2 selectivity can be significantly improved almost 6 times to be 64.

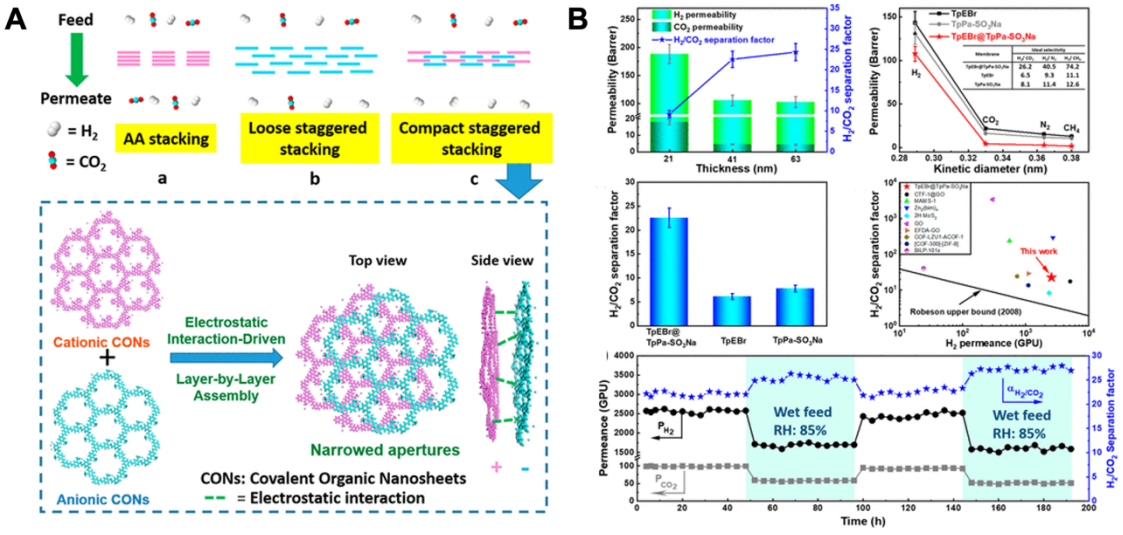

Figure 11. A schematic to improve the hydrogen molecular sieving in a COF membrane by alternately stacking cationic and anionic COF (A) and the hydrogen separation performance of the resulting COF membrane (B). Reproduced with permission from [322]. Copyright 2020 American Chemical Society

As observed in the MOF membranes, the hydrogen separation performance in COF membranes can also be affected by the operating temperature considering the activated diffusion process of the hydrogen. It has been reported that increasing the operating temperature can improve the hydrogen selectivity towards the light gases [322]. This can happen when the hydrogen permeation is more affected by the change of

temperature in comparison to other gases, which might also be effectively blocked because of the molecular sieving effect [322]. For some cases, the H_2 selectivity can also be unchanged or slightly drop [316,318]. In these cases, the activated diffusion process of the light gases is in a strong competition with the hydrogen and thus resulting in unchanged hydrogen selectivity or a slight reduction since the hydrogen permeation will be slightly blocked [318].

A membrane for hydrogen separation can also be constructed from a composite containing both MOF and COF. The first strategy is to fabricate them as a bilayer membrane. This has been investigated by a number of investigations involving COF-300 – $Zn_2(bdc)_2(dabco)$ [317], COF-300 – ZIF-8 [317] and H_2P-DHPh COF – UiO-66 [260]. As can be seen in the Figure 12 (A), the resulting COF-300 – $Zn_2(bdc)_2(dabco)$ and COF-300 – ZIF-8 composite membranes have shown an increase in H_2/CO_2 selectivity to be around 12.6 and 9, respectively, from 6 that is observed in the pure COF-300 membrane. A better performance is obtained in H_2P-DHPh COF – UiO-66 where H_2 permeability and H_2/CO_2 selectivity around 109000 Barrer and 33, respectively, can be obtained and is significantly better than the pure UiO-66 membrane [260]. In these cases, the performance improvement could be attributed to the synergistic interaction occurring at the interlayer such as by acting as an anchor for other materials or to heal the defective sites. Another strategy to combine MOF and COF is to grow the former within the pore of the latter as exemplified in the case of ZIF-67 grown in TpPa-1 and is also illustrated in the Figure 12 (B and C) [325]. Considering the relatively big pore size of the COF, such a space can actually be utilized to grow MOF which resulting in the establishment of a complex MOF-in-COF structure with improved hydrogen molecular sieving when compared with the pure COF membrane. The resulting composite membrane has then shown H_2 permeance around 3400 GPU with H_2/CO_2 and H_2/CH_4 in the range of 33-35. This strategy has also been successfully used to fabricate a free-standing ultrathin MOF-in-COF membrane utilizing ZIF-67 which is grown inside the PBD COF membrane [326]. Such a modification is highly effective to reduce the COF pore size from 2 nm to be around 0.3-0.6 nm and thus rendering the composite membrane to be suitable for hydrogen separation. The optimized synthesis condition can then result in a composite membrane with H_2 permeance around 73.9 x 10^{-8} mol m^{-2} s^{-1} Pa^{-1} and H_2/CH_4 selectivity around 34.

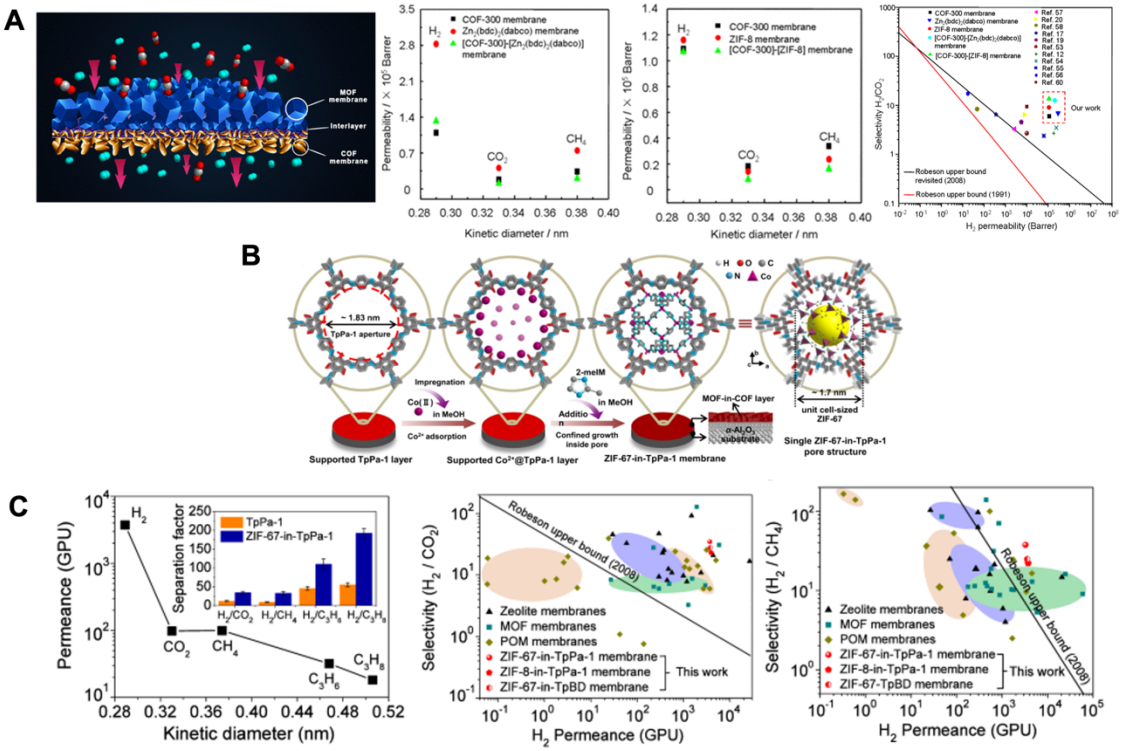

Figure 12. An illustration of a MOF-COF bilayer membrane fabricated using COF-300 - $Zn_2(bdc)_2(dabco)$ and COF-300 – ZIF-8 and their corresponding hydrogen gas separation performance (A). A schematic of the ZIF-67-in-TpPa1 MOF-in-COF membrane (B) and its hydrogen gas separation performance (C). Reproduced with permission from [317] (A), copyright 2016 American Chemical Society and [325] (B and C), copyright 2021 the authors and Springer Nature

3.5 Microporous polymeric membranes

While the already discussed materials can be considered as inorganic, except MOFs which can be considered hybrid, there is also recently a significant advancement in the field of polymeric materials with promising hydrogen separation performance, particularly in the field of microporous polymeric membranes. Differing from the conventional polymeric materials, these microporous polymers have intrinsic microporosity that can be rationally tuned during the synthesis process. There are then two types of microporous polymers that have been recently developed as an advanced membrane material: polymer of intrinsic microporosity (PIM) and thermally rearranged (TR) polymers. Despite its huge potential as a material for gas separation processes, most of the studies using both microporous polymers are usually directed for CO_2 separation considering their high selectivity because they usually exhibit high solubility towards CO_2. Despite this, because of the possibility to rationally tune their property, a number of researches have also been directed to use both for hydrogen separation.

Polymer of intrinsic microporosity (PIM)

Polymers of intrinsic microporosity (PIM) was firstly discovered by Budd and McKeown in 2004 [327,328]. Differing from the already discussed materials previously, PIM is solution processable and therefore improving its ease of processing when it is going to be fabricated as a membrane. The high porosity and surface area of PIM is caused by the inability of the PIM polymer to efficiently pack and rotate because of the presence of the bulky contortion sites in the polymer backbone. PIM can then be generally

classified into two main types: ladder PIMs and PIM-polyimide [329]. Ladder-PIM can be further grouped based on its site of contortion such as spiro-center, ethanoanthracene and Troger's base [329,330]. Similarly, the PIM-polyimide can also be further grouped based on its contortion site either it is based on dianhydride or diamine [329].

The first PIMs that are investigated for hydrogen separation is PIM-1 and PIM-7 which are cast as a film with thickness around 46 μm and 28 μm, respectively [331]. The H_2 permeability for PIM-1 and PIM-7 is found to be around 1300 Barrer and 860 Barrer, respectively. The H_2 selectivity against N_2 and CH_4 is reported to be around 14 and 10.4, respectively, for PIM-1 and 20.4 and 14, respectively, for PIM-7. Despite this satisfactory performance, the H_2/CO_2 selectivity of both PIMs is below 1 because of the high CO_2 solubility of the materials. Afterwards, attempts are made to improve its gas separation performance, particularly focusing in enhancing the rigidity of PIM's structure and increasing the inefficiency of its chain packing to yield a membrane with more microporous structure. In the case of PIM-1, for instance, the chain rigidity can be improved through intramolecular locking mechanism of the spiro carbon resulting in the increase of H_2 permeability from 4270 to 9870 Barrer and H_2 selectivity against N_2 and CH_4 from 8 to 10 and 4.3 to 7.5, respectively [332]. Meanwhile, for other cases, the most common employed strategy is by using monomers bearing different units such as hexaphenylbenzene (HPB) [333], spirobifluorene (SBF) [334–336], triptycene [337–340] and Tröger's base (TB) [341–344] to rationally tune PIM microporous structure and its rigidity as illustrated in the Figure 13.

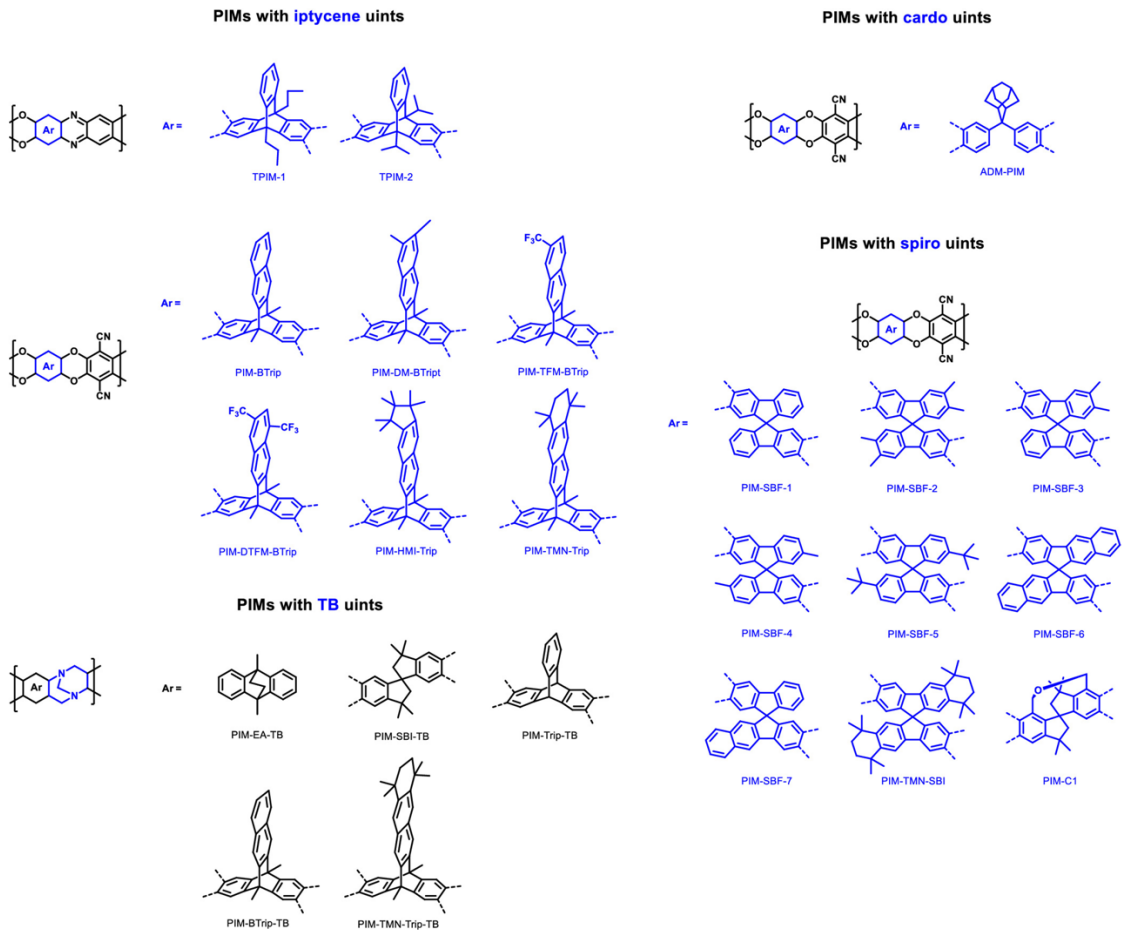

Figure 13. PIMs bearing different units to improve their microporosity and rigidity. Reproduced with permission from [330]. Copyright 2020 John Wiley and Sons, Inc.

Among this PIMs, there are several good candidates for hydrogen separation. TB-based PIMs such as PIM-EA-TB looks promising because it has an unusual gas transport property since H_2 permeates faster than CO_2 and thus indicating the preference for the permeation of smaller gas molecule [341]. As a result, PIM-EA-TB exhibits H_2/N_2 and H_2/CH_4 selectivity around 11, which is considerably higher than other PIMs and quite close to both PIM-1 and PIM-7, but with significantly higher H_2 permeability around 7700 Barrer, which is significantly higher than PIM-1 and PIM-7. A similar result is also obtained with PIM-MP-TB by using methanopentacene as the bridged bicyclic structural unit [342]. The H_2 permeability of this particular PIM is found to be around 4000 Barrer and its H_2 selectivity against N_2 and CH_4 is found to be around 20 and 15, respectively. Higher hydrogen separation performance can also be obtained using triptycene-based PIM such as PIM-Trip-TB that has comparable performance with PIM-EA-TB [340]. A better hydrogen separation performance, however, can be obtained using another triptycene-based PIM called TPIM 1 utilizing the rigid and paddlewheel-structure of the bridgehead-substituted triptycene moiety [338]. As a result, a PIM membrane with a more prominent ultramicroporous structure capable of enhanced hydrogen molecular sieving can be obtained as reflected by its H_2 permeability reaching 2666 Barrer and its H_2 selectivity against N_2 and CH_4 falling around 50.

PIM-PI is also another class of PIM that can be used for hydrogen purification. The first development of PIM-PI is initiated by the synthesis of the PIM-PI series 1-8 [345,346]

with the further addition of PIM-PI series 9-11 a few years later [347]. Compared with the ladder PIM, the H_2 selectivity of PIM-PI looks more promising. For example, the H_2/N_2 and H_2/CH_4 selectivity of PIM-PI-2 is found to be around 24 and its H_2 permeability is about 220 Barrer [345]. Similarly, PIM-PI-4 and PIM-PI-7 have shown H_2/N_2 and H_2/CH_4 selectivity around 18 and 14, respectively, with H_2 permeability in the range of 300-350 Barrer [345]. Later on, a series of KAUST-PI 1-7 were also developed [348]. Differing from the PIM-PI series, except for KAUST-PI-7, the trend of the gas transport property of the KAUST-PI is similar with the PIM-EA-TB where hydrogen is the fastest permeating gas. Therefore, most of them can combine good H_2 permeability and selectivity. In particular, KAUST-PI-1 has exhibited H_2 permeability almost 4000 Barrer, which is about one order of magnitude higher than the best-performing PIM-PI series, and is also accompanied with relatively high H_2/N_2 and H_2/CH_4 selectivity around 38 [348].

As in the case of ladder PIM, the dianhydride contortion site of the PIM-PI can also be constructed using spirobifluorene-based dianhydride resulting in a PIM-PI called SBFDA-DMN [349]. However, the resulting H_2/N_2 and H_2/CH_4 selectivity is only around 10 and therefore very moderate. A slightly better result is reported using triptycene-based dianhydride with diamine as the monomers to construct both TDA-DMN1 and TDA*i*3-DMN [350]. Both membranes show H_2 permeability in the range of 2200-3000 Barrer and H_2 selectivity against N_2 and CH_4 in the range of 14-18. As in the case of PIM, a quite promising result can also be obtained by using ethanoantracene (EA) as exemplified by the fabrication of PIM EA-DMN and EAD-DMN [351,352]. By fabricating the PIM EA-DMN as a 15 μm film, the resulting membrane has H_2 permeability and H_2/N_2 and H_2/CH_4 selectivity around 1844 Barrer and more than 40, respectively. Meanwhile, the H_2 permeability of a 23 μm EAD-DMN membrane is around 1289 Barrer with H_2 selectivity against N_2 and CH_4 to be around 30 and 23, respectively [351]. In addition, PIM-PI can also be constructed using a pseudo-TB-derived dianhydride and its dione-substituted resulting in PIM-PI called CTB1-DMN and CTB2-DMN, respectively [353]. The latter performs better than the former with H_2 permeability around 1150 Barrer and both H_2/N_2 and H_2/CH_4 selectivity around 28.

Another strategy to fabricate PIM-PI membranes is to have contortion site in the diamine part of the PI and this can be constructed using spirobifluorene [354]. Using 6FDA as the dianhydride, it has H_2/N_2 and H_2/CH_4 selectivity around 30 and 37, respectively, but low H_2 permeability around 200 Barrer. Another possibility is to use TB-based diamines. However, some of them have still shown a similar performance as in the previous case, as exemplified in the PI-TB-1 to PI-TB-5 [355,356]. In this case, the H_2 permeability of PI-TB-3 is found to be around 300 Barrer with H_2/N_2 and H_2/CH_4 selectivity around 31 and 44, respectively [355]. Also using two different TB-based diamine called TBDA1 and TBDA2, a series of PIM-PI with significantly higher H_2/N_2 and H_2/CH_4 selectivity around 54 and 72, respectively, can be achieved but still with relatively low H_2 permeability around 159 Barrer [357,358]. A PIM-PI membrane with H_2 permeability around 3300 Barrer is then reported with methyl-substituted TB diamine (4MTBDA) combined with 4 different dianhydrides [359]. However, this must also be compensated with relatively low H_2/N_2 and H_2/CH_4 selectivity around 11 and 9, respectively, in 4MTBDA-PMDA. A relatively good trade-off is reported in another TB-based PIM-PI-TB-1 and PIM-PI-TB-2 utilizing the *di-ortho*-substituted groups TB-based diamine with 6FDA as the dianhydride [360]. The H_2 permeability of PIM-PI-TB-2 is found

to be around 600 Barrer with H_2/N_2 and H_2/CH_4 selectivity around 17 and 19, respectively. Similarly, PIM-PIs using TB-based diamine with bio-dianhydride as the comonomer called Bio-TPBI-1, Bio-TPBI-2, Bio-PITB-1 and Bio-PITB-2 have also exhibited a good permeability-selectivity trade-off [361,362]. The H_2 permeability and H_2/N_2 and H_2/CH_4 selectivity for these membranes is in the range between 700-1000 Barrer of 20-30, respectively. Iptycene family can also be used to construct the contortion site of the diamine side of the PIM-PI as exemplified by using substituted 1,4-triptycene [363], 2,6-diaminotriptycene and its extended version (DAT-1 and 2) [364] and pentiptycene [365]. For triptycene-based PIM-PI, even though a significantly high H_2/N_2 and H_2/CH_4 selectivity up to around 90 and 161 is reported for 6FDA-1,4-trip_CH_3, all the membranes suffer from a relatively low H_2 permeability that is around 50 Barrer [363]. Meanwhile, for pentiptycene PIM-PI, the H_2 permeability is generally slightly higher in the range of 100-190 Barrer accompanied with H_2/N_2 and H_2/CH_4 selectivity in the range of 26 to 42 and 34 to 52, respectively [365]. A similarly better performance can also be seen in both 6FDA-DAT1 and 6FDA-DAT2 which have H_2 permeability around 200 Barrer and H_2 selectivity against N_2 and CH_4 around 42 and 62, respectively, for 6FDA-DAT1 and 31 and 45, respectively, for 6FDA-DAT2 [364]. In this case, the selectivity of the 6FDA-DAT1 is better than 6FDA-DAT2 since the latter is constructed using the extended version of the DAT-1 and thus enlarging its pore size which could then negatively impact its hydrogen molecular sieving ability.

Both ladder PIM and PIM-PI can also be functionalized with different functional groups to improve its hydrogen separation properties by introducing various functional groups such as amidoxime [366] carboxyl [367–369], hydroxyl [370] and thioamide [371]. For example, as high as around 50 in H_2/N_2 selectivity is reported in PIM containing high carboxylate functional groups, even though the H_2 permeability decreases to be around 90 Barrer, which is caused by the shortening of the interchain distances and thus increasing the diffusivity selectivity [368]. A rather high H_2 permeability around 900 Barrer can then be found in the case of amidoxime-functionalized PIM-1 (AO-PIM-1) with H_2/N_2 and H_2/CH_4 selectivity around 27, which is more than twice higher than the PIM-1, since this functional group enhances the rigidity of the PIM and shifts the PIM porosity to be in the ultramicroporous region resulting in a more enhanced molecular sieving [366]. A better performance for hydrogen separation is then exhibited by a combination of using carboxylate-containing PIM and cross-linking process as demonstrated in the C-CoPIM-TB-1 and C-CoPIM-TB-2 [369]. Both PIM membranes are obtained by crosslinking the carboxylate-containing triptycene-based copolymer named CoPIM-TB-1 and Co-PIM-TB-2 using glycidol. The H_2 permeability of both membranes falls around 5000 Barrer, which is just slightly lower than their non-cross-linked counterparts, but they exhibit a relatively high H_2/N_2 and H_2/CH_4 selectivity around 30, which is almost a twofold improvement compared with the non-cross-linked ones.

In addition to the functionalization, PIM membranes can also be modified through various treatments to improve their hydrogen separation performance. In general, the function of such treatments is to increase the diffusive selectivity through the generation of ultramicropore and creation of a denser membrane structure suitable for molecular sieving [372,373]. Therefore, the first consequence of such treatments is a significant drop in H_2 permeability. There are various techniques to accomplish this. For instance, by thermally treating AO-PIM-1 in argon atmosphere, the amidoxime group

can be converted into oxadiazole and triazine rings in the interchains to self-cross-link the AO-PIM-1, as illustrated in the Figure 14 [373]. Thermal treatment at 390°C for 2 days results in a membrane with H_2 permeability around 300 Barrer and H_2 selectivity against CO_2, N_2 and CH_4 around 16, 500 and 1000, respectively. Ozone can also be used to post-treat a PIM membrane. After 5-minutes ozone treatment, the H_2 permeability of the treated membrane drops to 683 Barrer but its selectivity against CO_2, N_2 and CH_4 can be significantly improved to be around 5, 142, 182, respectively [372].

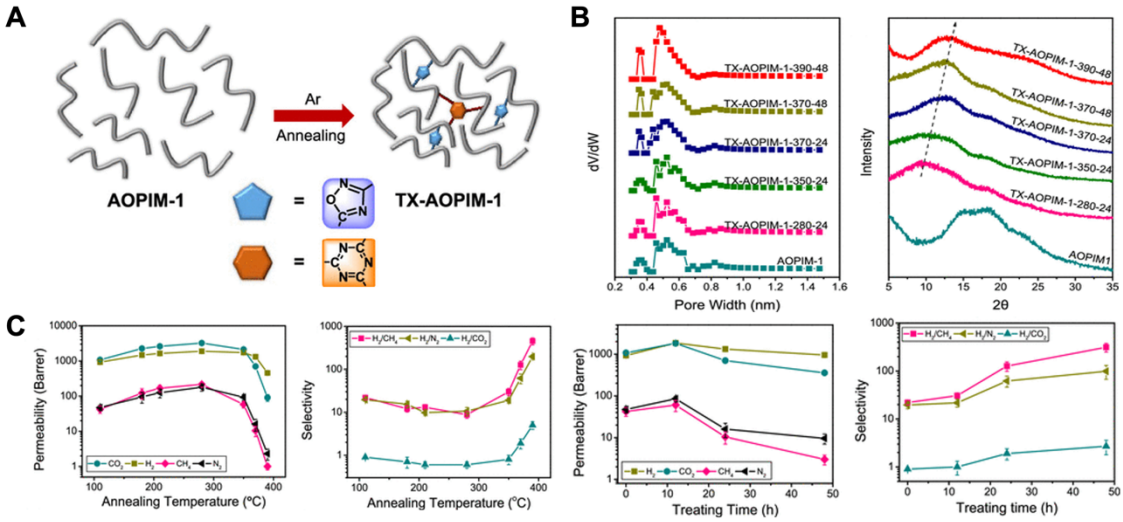

Figure 14. An illustration of the thermal treatment process to self-cross-link AO-PIM-1 (A), the pore structure evolution of the AO-PIM-1 after the thermal treatment (B) and the impact of various thermal treatment parameters on the hydrogen separation performance of thermally-treated AO-PIM-1. Reproduced with permission from [373]. Copyright 2021 American Chemical Society

For PIM-based membrane, increasing the operating temperature might negatively impact the separation performance. As has been studied in PIM-1, for instance, the H_2 permeation activation energy is -0.4 kJ mol^{-1} while the N_2 and CH_4 activation energy is 14.3 and 19.4 kJ mol^{-1}, respectively [374]. This means that with increasing temperature, the H_2 permeance also gets lower while the N_2 and CH_4 permeance increases resulting in a decrease in selectivity. Similarly, in the case of PIM-Btrip, increasing the operating temperature from 25°C to 55°C decreases both the H_2 permeability from 8929 to 8649 Barrer and H_2 selectivity against N_2 and CH_4 from 22.2 to 11.1 and from 22 to 9, respectively [339]. The PIM-TMN-Trip also faces similar condition in this condition since its H_2 permeability drops from 13828 to 12478 Barrer and its H_2 selectivity against N_2 and CH_4 drops from 9 to 7 and from 6 to 4, respectively. In both cases, the major cause is the negative activation energy of hydrogen resulting in a decrease of hydrogen permeability as the temperature increases.

One of the major drawbacks in the field of PIM membrane is the aging phenomenon experienced by PIM membranes. During the aging phase, the PIM polymeric chain undergoes rearrangement and as a result, the H_2 permeability usually goes down which is accompanied by the enhancement of the H_2 selectivity. Therefore, such a phenomenon could actually be exploited to improve the hydrogen separation performance as long as the permeability reduction is acceptable. For instance, a systematic study using PIM-SBF has shown that the H_2/N_2 selectivity of the PIM-SBF 2 increases from around 8 to 26 after around 3 years of aging [335]. However, the

permeability reduces from 9160 to 4240 Barrer. A more pronounced difference is also observed in PIM-MP-TB where after about one year of aging, the H_2 permeability decreases from 4000 Barrer to be around 800 Barrer but the H_2/N_2 and H_2/CH_4 selectivity can be significantly enhanced to be 61 and 55, respectively, from around 20 and 15, respectively [342].

This aging phenomenon might then be influenced by several factors. For instance, in a systematic study involving various PIMs, it has been observed that a very prominent aging phenomenon occurs in TPIM-1 and TPIM-2. In both cases, after around 720-780 days of aging, the H_2/N_2 selectivity increases almost 10-fold to be around 156 and 90 for TPIM-1 and TPIM-2, respectively [375]. However, this must also be paid by almost 70% decrease of H_2 permeability to be 1105 and 354 Barrer for TPIM-1 and TPIM-2, respectively. When compared with PIM-1, the aging for both TPIM-1 and TPIM-2 is significantly faster which might be attributed to two major reasons, namely their initially higher free volume and their ribbon-like 2D geometry that is more prone to efficient chain packing. The aging phenomenon also depends on the membrane thickness. Usually, thinner PIM membranes experience faster rate of physical aging while also becoming less permeable and more selective towards hydrogen. For instance, after 50 days, the H_2 permeability of a 23 μm EAD-DMN drops from 1289 to 830 Barrer (35% lower) with an increase about 35% in H_2/N_2 selectivity to be around 40. Meanwhile, it takes around 180 days for a 172 μm EAD-DMN to have a comparable drop in H_2 permeability to be around 3476 Barrer with 13.3 H_2/N_2 selectivity [351]. However, it also seems that post-treatment of a PIM-membrane might help to reduce the aging phenomenon. For instance, after 180 days, the thermally-cross-linked AO-PIM only shows a slight H_2 permeability reduction from 952 to 707 Barrer and thus increasing the H_2/CO_2 and H_2/CH_4 selectivity from 2.7 and 313 to 8.1 and 880, respectively [373]. Similarly, the cross-linked c-CoPIM-TB-1 and c-CoPIM-TB-2 shows a negligible reduction in performance after 40 days of aging and thus can maintain their H_2 permeability around 5000 Barrer and H_2 selectivity against N_2 and CH_4 to be in the range of 30-40. This could then be attributed to the effective impediment of the inter-chain mobility after the cross-linking process [369].

Thermally rearranged (TR) polymers

In the TR polymers, the microporous structure is obtained through the spatial rearrangement of the rigid polymeric chains after experiencing heat treatment. Usually, TR polymers are rod-like and contain heterocyclic rings such as benzimidazole, benzoxazole and benzothiazole which are obtained after thermally treating the precursors [330,376]. For hydrogen separation process, these TR polymers can then be obtained by using poly(*o*-hydroxylamide)s [377–379], hydroxyl-containing polyimide [380–383] or poly(ether *o*-hydroxyimide) [384] as the precursors which are thermally treated to improve their microporous structure. Some studies have investigated the use of TR polymers for hydrogen purification which can be synthesized from the precursors containing different units such as cardo [385], iptycene [386–390] and spiro [391–393] to result TR polymers bearing these units as can be seen in the Figure 15. The precursors can also be chosen from cross-linkable polyimides [394,395] or already-functionalized precursors such as in the case of PIM-6FDA-OH [202].

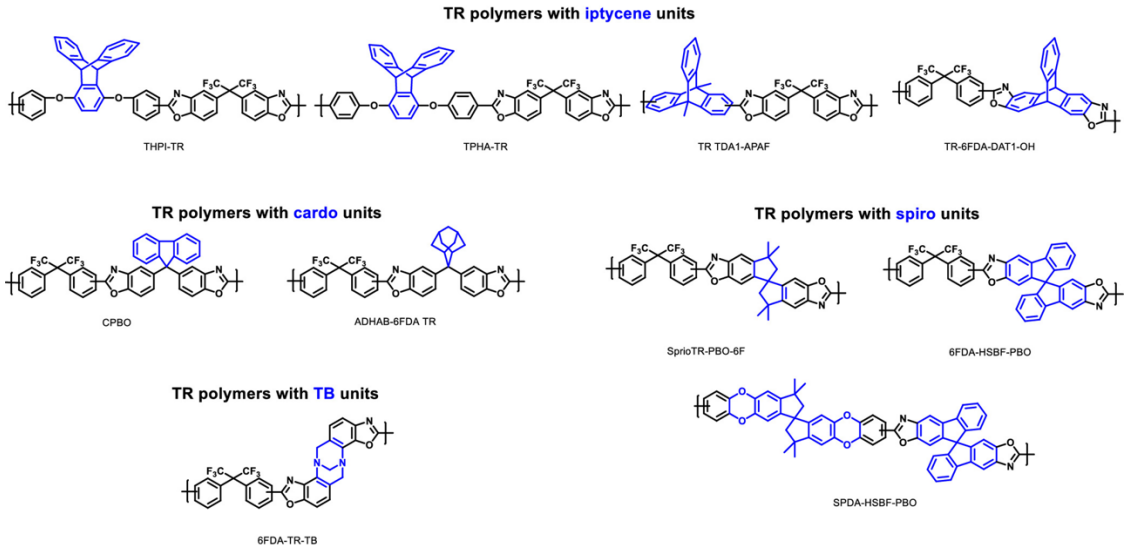

Figure 15. TR polymers containing different shape-persistent units. Reproduced with permission from [330]. Copyright 2020 John Wiley and Sons, Inc

In the TR polymers used for hydrogen separation, increasing the fractional free volume (FFV) in the TR polymer has to be optimized since this might negatively impact the hydrogen separation performance. For instance, in a study using poly(*o*-hydroxylamide)s as the precursor with three different diacid chlorides, *6f*PBO with the highest FFV of 0.28 shows the highest H_2 permeability and H_2/CH_4 selectivity around 255 Barrer and 40, respectively [379]. Meanwhile, the *m*PBO and *p*PBO with less FFV around 0.24 and 0.2, respectively, exhibits lower H_2 permeability but with higher H_2/CH_4 selectivity around 60 and 85 Barrer, respectively and 115 and 59, respectively. In another study using spiro-based TR, spiroTR-PBO-6F with FFV around 0.27 shows the highest H_2 permeability around 430 Barrer but only moderate H_2/N_2 and H_2/CH_4 selectivity around 13 [391]. For this membrane, CO_2 is also the fastest permeating gas because the gas sorption is the predominant gas transport mechanism in TR with large microcavities. Meanwhile, spiroTR-PBO-BP with FFV around 0.2 shows H_2 permeability around 143 Barrer but with higher H_2/N_2 and H_2/CH_4 selectivity around 27. For this membrane, H_2 is the fastest permeating gas diffusion is now more restricted and thus the transport is governed by the kinetic diameter of the gases.

To further improve the performance of the TR polymers, the rigidity of the stiff segments of the TR polymers can also be enhanced. For instance, the synthesis of *ortho*-hydroxyl diamine with four methyl groups and a fixed biphenyl center as a precursor for polyimide can improve the polymer rigidity which are suitable to improve the molecular sieving ability for hydrogen separation [396]. The performance of the TR polymers can also be enhanced by fabricating them from co-polymers [377,382,397,398]. For example, by combining non-TR-able part in the precursors that has bulky non-polar side groups such as 2,4,5-trimethyl-m-phenylene diamine (DAM) and 4,4'-methylene-bis-(3-chloro-2,6-diethylaniline) (MCDEA) the chain packing can be more efficiently disrupted to increase the fractional free volume resulting in high gas permeability and better hydrogen selectivity [382]. When compared with the TR polymer made from homo polymer, all the TR membranes show similar H_2 permeability around 44 Barrer but the ones with DAM and MCDEA show H_2/N_2 and H_2/CH_4 selectivity in the range of 70-80 and 106-120, respectively, while the normal TR polymer only exhibits around 36 and 26, respectively.

In another study involving DAM and 4,4'-oxidiamine (ODA) as the non-TR-able part, as can be seen in the Figure 16 (A and B), the H_2 permeability of the TR fabricated using this non-TR-able (TR-APAF-DAM and TR-APAF-ODA) part can be increased for the former up to 308.6 Barrer while the latter shows a decreasing trend up to 60.8 Barrer from 180 Barrer observed in the TR polymer without non-TR-able part [397]. However, this must also be accompanied with decreasing H_2/N_2 selectivity in the former up to 20.3 while the latter shows an improvement up to 45 from 34 observed in the TR polymer without non-TR-able part. This is because DAM can increase the chain rigidity and is therefore more effective in disrupting the chain packing resulting during the thermal rearrangement process resulting in higher gas permeability while ODA increases the polymer flexibility and thus lowering the overall fractional free volume after thermal rearrangement process and could contribute in improving the molecular sieving effect.

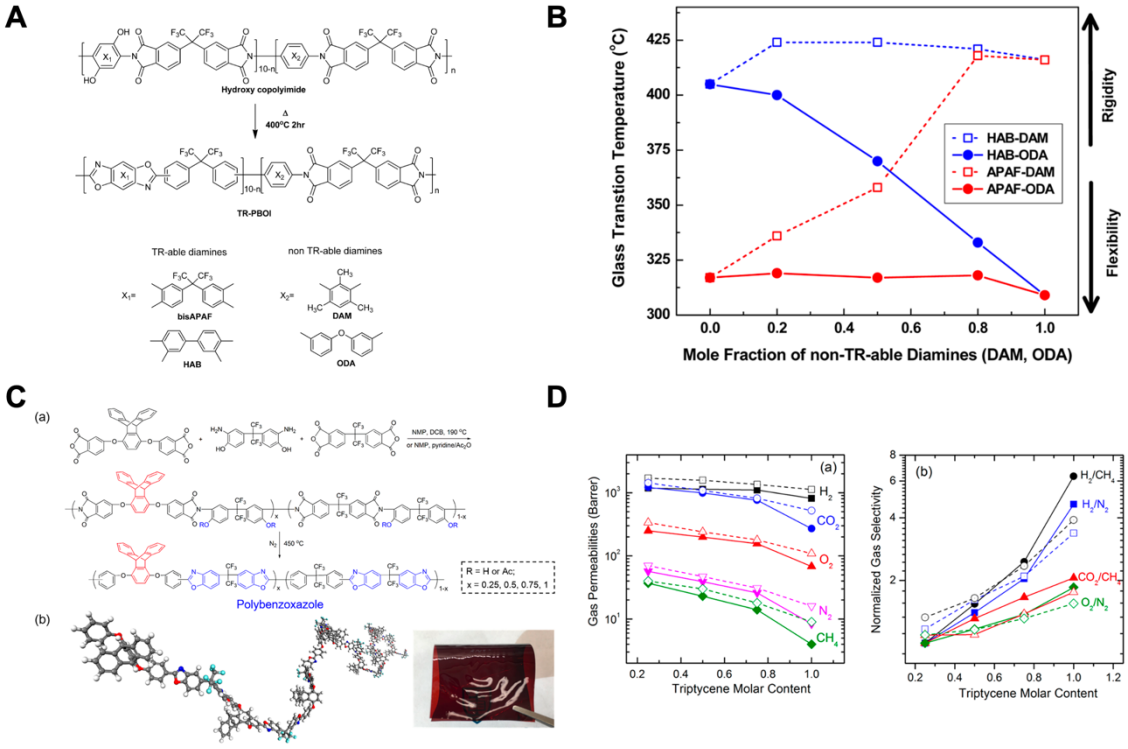

Figure 16. Scheme to fabricate a TR-polymer membrane with DAM and ODA as the non-TR-able parts (A) and its impact on the rigidity and flexibility of the resulting membranes (B). An illustration to fabricate a TR polymer membrane with triptycene unit (C) and the impact of the triptycene molar content on the gases permeability and selectivity (D). Reproduced with permission from [397] (A and B) and [387] (C and D). Copyright 2015 and 2018, respectively, American Chemical Society.

During the fabrication of a TR membrane, the temperature for the thermal treatment has to be optimized by observing the weight loss trend obtained through gravimetric method, which is compared with the expected theoretical weight loss [386,390]. Usually, treating the precursors at higher temperature than the theoretical or calculated temperature could be beneficial to constrain the chain relaxation and the collapse of the microcavities [390]. The optimization is required to balance the increase of H_2 permeability and the loss of H_2 selectivity -relative to the precursors- caused by the increase of the fractional free volume and the collapse of the microcavities that [380,384,392]. For instance, after thermally treating the polyetherimide at 450°C, the H_2 permeability increases from 29.1 Barrer to 439 Barrer but its selectivity against CH_4

decreases from 223.8 to 25.8 [384]. In another study using spiro-based polyimide, 6FDA-HSBF, the H_2 permeability increases from 162 Barrer to 985 Barrer after the thermal treatment but the H_2 selectivity against N_2 and CH_4 decreases from 42.5 and 67.5, respectively, to 17.9 and 17.6, respectively [392]. Such optimization needs also to consider the chemistry of the precursors. In a systematic study using four different polyimide as the precursors, for instance, namely 6F-TM-Ac, 6F-TM-OH, PM-TM-Ac and PM-TM-OH, the maximum H_2/CH_4 selectivity observed for the first three TRs is found to be 50, 63, 44, respectively, which is obtained by thermally treating the precursor at 425°C [396]. A further increase in the thermal treatment will only yield an increase in hydrogen permeability but a significant reduction in selectivity. Meanwhile, for the PM-TM-OH, the maximum selectivity of 77 is obtained by thermal treatment at 450°C.

In addition, the content of the units inside the TR polymers should also be controlled since they can also influence the H_2 gas separation performance. For example, as illustrated in the Figure 16 (C and D), in a study using triptycene-based poly(o-hydroxyimide) and triptycene-based poly(o-acetateimide) copolymer as precursors has shown that increasing the iptycene unit is beneficial to increase the number of microcavities in the resulting TR polymers so they can retain the permeability for small gases [387]. The highest H_2/N_2 and H_2/CH_4 selectivity of the TR membranes fabricated with the highest triptycene loading is found to be around 96 and 203, respectively, for TPBO-1.0 and 70 and 125, respectively, for TPBO-Ac-1.0. Meanwhile, the H_2 permeability of both TR membranes is also relatively high in the range of 800-1100 Barrer. However, in another study, it is also found that an optimization is required for the cardo-based TR membranes since incorporating too much cardo unit in the precursor does not linearly correlate with TR containing higher fractional free volume because of the repulsion effect [385]. In the study, 5% of the cardo unit gives the best H_2 separation performance showing permeability around 1189 Barrer and H_2/N_2 and H_2/CH_4 selectivity around 21 and 29, respectively.

The hydrogen separation performance of TR polymers can also be further enhanced by embedding various additives such as functionalized boron nitride (BN) [399]. Compared with the pure TR membrane with H_2 permeability around 219 Barrer, the 1 wt% BN TR polymer shows a decrease in H_2 permeability to be around 97 Barrer but its H_2/CH_4 selectivity can be significantly increased from 24.6 to 322.3 because since the BN adds a more tortuous pathway for larger gas molecules to pass through [399].

As in the case with the PIM, TR polymers also suffer from the aging phenomenon. It has been observed that after 197 days, the H_2 permeability of PIM-PBO-3 decreases significantly from 768 to 277 Barrer. Meanwhile, the H_2 selectivity against N_2 and CH_4 selectivity increases from around 20 to be around 38 [393].

3.6 Composites and other microporous materials

In addition to the above materials, there are also other attempts to synthesize novel advanced microporous materials with a great promise for hydrogen purification. One of the common strategies to achieve this objective is by fabricating a composite of the above microporous materials.

In this case, a number of composite consisting of GO or rGO with MOFs such as HKUST-1 [227,400], MIL-100 [400], UiO-66-NH_2 [401], ZIF-7 [400], ZIF-8 [222,400,402] and $Zn_2(bim)_4$ [403] and zeolite [404] have been investigated to produce a membrane with

excellent hydrogen separation performance. The improvement of the separation performance can result from the defects healing mechanism from one of the constituents. This is observed in the case where the GO acts a sealant to heal the intercrystalline defect of the MOF membranes and also to restrict the framework flexibility as owned by ZIF-8 and thus, when compared to the ZIF-8 membrane, resulting in about 4 times increase of H_2/CH_4 selectivity to be around 139 [402]. In another study, layering the GO after a porous substrate is coated with ZnO nanoparticles is not only helpful to heal the defects of the resulting $Zn_2(bim)_4$ – GO composite membrane but also beneficial to guide the crystal orientation during the $Zn_2(bim)_4$ crystal growth [403]. Through this bottom-up approach, the resulting shows H_2 permeance around 1.5 x 10^{-7} mol m^{-2} s^{-1} Pa^{-1} and H_2 selectivity against CO_2, N_2 and CH_4 around 106, 126 and 256, respectively. Retrospectively, MOF can also contribute to cover the defective sites of a GO membrane and thus resulting in an increase of H_2/CO_2 selectivity from around 6 in a GO membrane to be around 400 in the ZIF-8 – GO composite membrane [222].

Another synergistic effect can also be observed where the resulting new composites can combine the properties of its constituents and not just healing the defects. For instance, the use of HKUST-1 in a HKUST-1 – GO composite can improve the CO_2 affinity of the resulting membrane [227]. During the separation H_2/CO_2 process, this will then result in an improvement of H_2/CO_2 to be around 73 from 9 observed in GO membrane. This might be associated with the hindered CO_2 permeation as it now interacts more strongly with the composite. In another study using zeolite, it has also been observed that both the GO and the zeolite can work synergistically by contributing to ensure high hydrogen permeance up to 4900 GPU and high H_2/CO_2 selectivity up to 56, respectively, in the presence of steam [404]. In another study, the MOF can also be used as a mean to control the interlayer spacing of the rGO membrane, which is not permeable to gases, as studied using different 4 different MOFs, namely CuBTC, MIL-100, ZIF-7 and ZIF-8 [400]. As a result, the H_2 permeability for the CuBTC – rGO, MIL-100 – rGO, ZIF-7 – rGO and ZIF-8 – rGO composite membrane is found to be around 21112, 311, 73 and 151 Barrer, respectively, with H_2/CO_2 selectivity around 10, 12, 25 and 20, respectively.

Another case of composite can also be seen in the form of a composite membrane combining microporous nanoparticles with PIM or TR polymers. The first simple strategy is to form a mixed matrix membrane (MMM) where microporous nanoparticles act as a discrete phase. Various MOFs such as MIL-53 [405], Mg-MOF-74 [405], UiO-66-$(OH)_2$ [406], TIFSIX3 [405], ZIF-8 [380] and $Zn_2(bim)_4$ [405] and silica nanoparticle [381] have been incorporated in these microporous polymers as the nanofillers. One of the most important criteria to be fulfilled is to use MOF with suitable pore opening and to ensure the absence of interfacial defect in order to simultaneously enhance the H_2 permeability and selectivity. TIFSIX3/PIM-1 has shown an improvement both in the hydrogen permeability from 670 to 1010 Barrer and H_2/N_2 and H_2/CH_4 selectivity to be around 19 and 14, respectively, which are almost double the selectivity observed in the PIM-1 [405]. In another study using silica nanoparticle, the H_2 permeability and H2/CH4 selectivity of the TR polymers can be improved around 335 Barrer and 79, respectively, from 292 Barrer and 53, respectively, observed in the non-composite TR [381]. In addition to MOF selection, establishing a good polymer-particle interaction is also paramount to obtain a good MMM. This can then be realized by modifying the nanoparticles such as by fabricating them as a gel [407] or porous liquid [408]. For

example, by loading the AO-PIM with 5% of SOD zeolite type 1 porous liquid the H_2 permeability the H_2/N_2 selectivity can be improved from 400 to 1390 Barrer and from 15 to 34, respectively [408].

Another strategy to construct a composite membrane based on the microporous polymers and MOF is to construct a bilayer composite membrane. This is shown by growing ZIF-8 on AO-PIM-1 where the latter acts as a nucleation site for the former [409]. After the ZIF-8 formation, AO-PIM-1 chain rigidification could occur and thus resulting in a composite membrane with H_2 permeability around 5700 Barrer and H_2/CO_2 selectivity around 12. This strategy can also be enhanced by firstly chelating the PIM with the metal ion corresponding to the MOF as exemplified in the case of ZIF-67 using Co^{2+}-chelated PIM-1 as the interlayer for heterogeneous nucleation sites [410]. The resulting defect-free composite membrane shows H_2 permeance around 6.2 x 10^{-7} mol m^{-2} s^{-1} Pa^{-1} with selectivity against CO_2 and CH_4 around 15 and 52, respectively.

Recently, there is also a new research direction in fabricating a microporous polymeric membrane that is derived from surface mounted MOF (SURMOF) called SURGEL for hydrogen separation as illustrated in the Figure 17 (A and B) [411]. The process is initiated by fabricating a MOF membrane followed by crosslinking and the removal of the metal as the final step. Using this strategy, compared with commercial polymeric membranes, the SURGEL membrane exhibits a relatively higher H_2 permeance around 12.8 x 10^{-7} mol m^{-2} s^{-1} Pa^{-1} (around 8000 Barrer) with satisfactory H_2/CO_2 separation performance around 3.9, which is close to the Knudsen selectivity value. In this case, the relatively high H_2 permeance and Knudsen selectivity is inherited from the microporous structure of the SURMOF which is further constricted during the cross-linking process to improve the hydrogen selectivity.

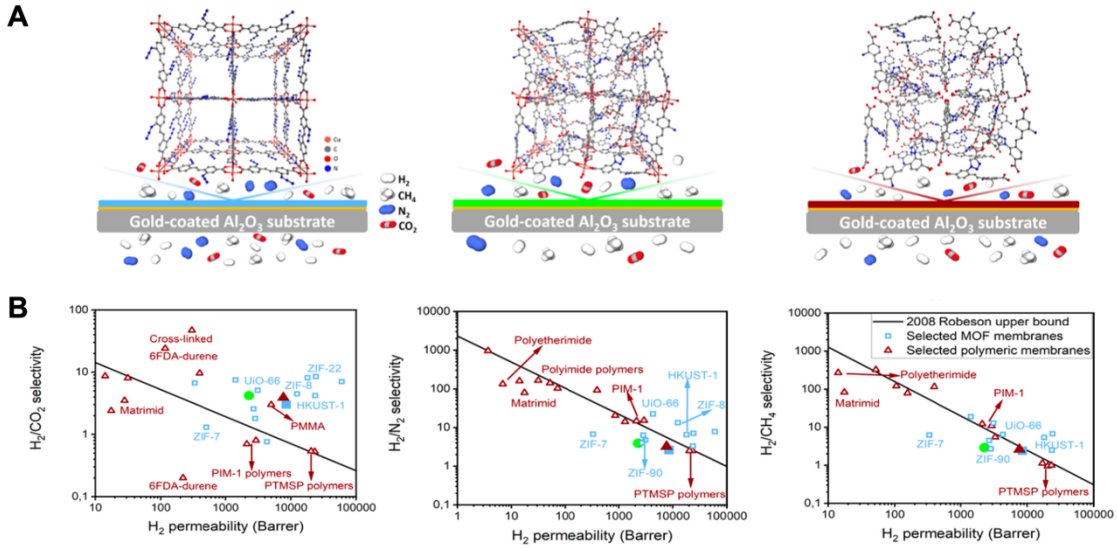

Figure 17. An illustration of the transformation from SURMOF (A, left) to cross-linked SURMOF (A, middle) to SURGEL (A, right) and the hydrogen separation performance of the SURMOF (blue square), cross-linked SURMOF (green circle) and SURGEL (brown triangle) (B). Reproduced with permission from [411]. Copyright 2023 Royal Society of Chemistry

4. Summary and outlooks

Having extensively discussed the performance of various promising microporous materials, their hydrogen separation performance can then be summarized as shown in the Figure 18.

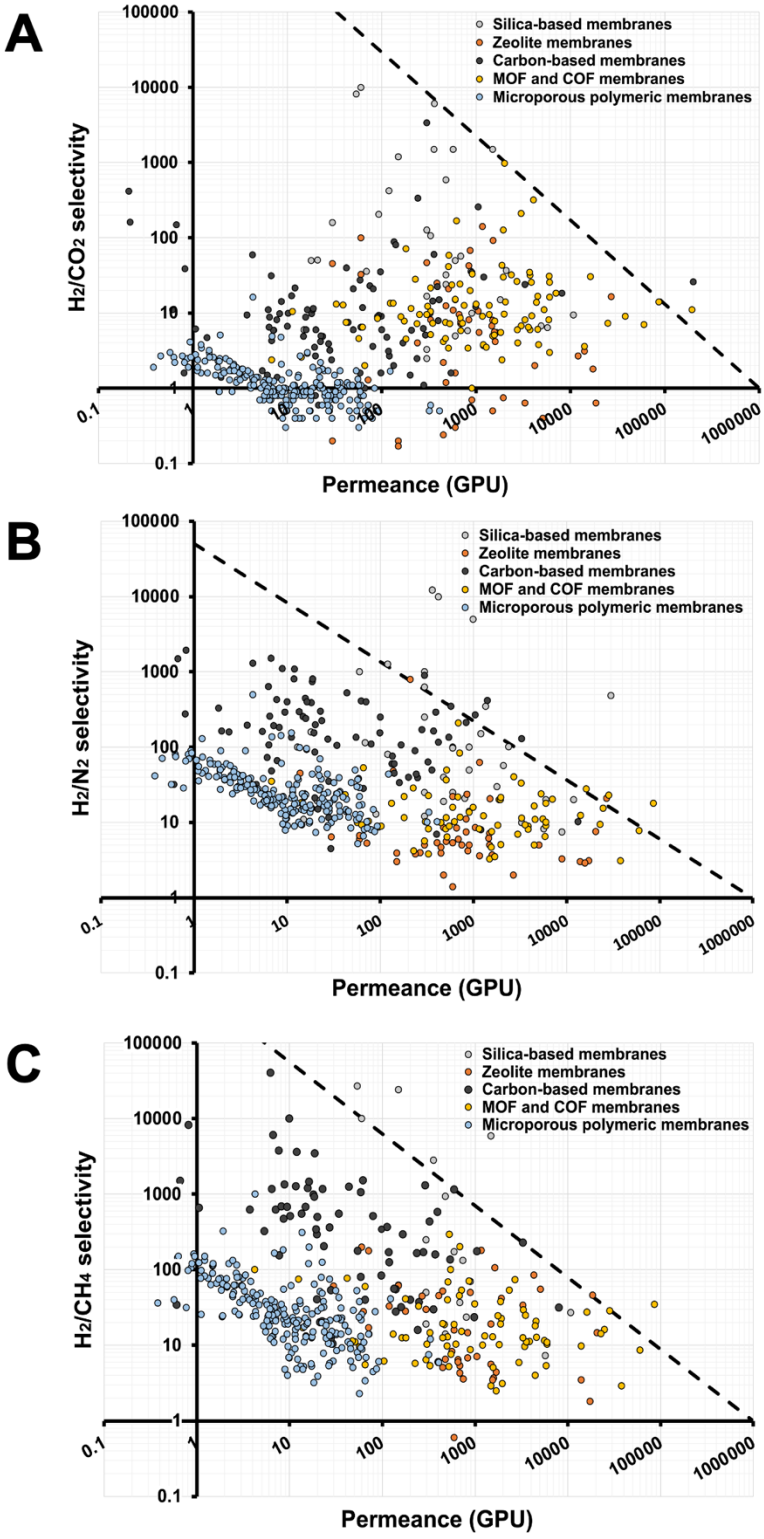

Figure 18. Hydrogen separation performance of the membranes fabricated from various microporous materials

First, as can be seen in the Figure 18 (A), in the field of H_2/CO_2 separation, there are three main clusters exhibiting relatively high permeance (more than 1000 GPU) with satisfactory selectivity (between 10-100): silica-based membranes, zeolite membranes and MOF-COF membranes. Meanwhile, as can also be seen, the microporous polymeric membranes suffer both from relatively low gas permeance and selectivity. This might then be caused by two phenomena: thick film fabrication and high CO_2 solubility. Since most of studies involving microporous polymeric membranes are fabricated as thick films, they usually exhibit low gas permeance. In addition, as has been discussed, they are usually used to separate CO_2 from other gases and thus have high CO_2 solubility which hinders them to effectively molecularly sieve the H_2 from CO_2.

In contrast, such a situation is not encountered when one looks on both the Figure 18 (B) and (C) for H_2/N_2 and H_2/CH_4 separation, respectively. In this case, even though microporous polymeric membranes still suffer from relatively low H_2 permeance, their selectivity is within the range of 10-100. Since the solubility of both gases is low in microporous polymeric materials, the material can now become more selective towards for hydrogen separation. However, the performance of the microporous polymeric materials is still lower in comparison to the other 4 microporous materials in terms of gas permeance. Regarding this, it can be seen that there are two main clusters formed between carbon-based/silica-based membranes and zeolite/MOF-COF membranes. The former shows relatively lower hydrogen permeance than the latter but it has higher selectivity. One of the main reasons of this phenomenon could be associated with tighter pore structures that can be formed by the former. For example, tighter pore structure can be formed by increasing the pyrolysis temperature of the carbon membrane and thus resulting in improved molecular sieving. Meanwhile, in the case of zeolite and MOF-COF membranes, the presence of both intra- and inter-crystalline defects might result in lower gas selectivity than the predicated values and increased gas permeance. In addition, in the case of ZIF-8 MOF for example, the structural flexibility cannot be completely eliminated which might also contribute in reduced gas selectivity.

Having looking closely on the performance of the microporous materials for hydrogen separation, some recommendations can then be proposed for future research. First, the research direction can be directed towards fabrication of a thin film membrane to increase gas permeance. This is not only true for microporous polymeric materials but also to other microporous materials in order to increase its applicability. In this case, the involvement of machine learning during the fabrication process could be considered to optimize the membrane performance to avoid trial-error approach. Moreover, the machine learning approach can also be extended, for example, to fabricate tailorable material such as MOF or COF-based membranes. In this case, the promising materials can be firstly screened which is then followed by fabrication process. This is also true when one intends to combine the microporous materials in the form of composites such as MMM. Lastly, the research should also be directed towards the investigation of hydrogen separation that mimics the real conditions. When these approaches are combined together, the research in the field of microporous material can be more advanced to further support and advance the hydrogen economy in the future.

5. Conclusions

As the energy source continues to transition from fossil-based fuels into a more sustainable ones, it cannot be doubted that hydrogen as an energy carrier will play a major role in this field. However, in order to use it effectively, it has to be separated from other light gases. In this regard, membrane technology will also play a significant role since it holds a great promise to effectively purify hydrogen without huge energy consumption. Differing from polymeric materials, microporous materials could be a better alternative since it can combine high hydrogen permeance and precise molecular sieving and thus surpassing the permeance-selectivity trade-off. In this article, we have then thoroughly reviewed the state of the arts of various promising microporous materials that can be used for hydrogen separation against light gases. As one of the earliest investigated materials, silica-based microporous membranes have actually held a good promise in this field as reflected by their high hydrogen selectivity. However, recent advances in the microporous materials have also shown the possibility to use other porous materials including zeolite, carbon-based porous materials, metal organic frameworks, covalent organic frameworks and microporous polymers to push further the performance boundaries. Some of these materials also offer a number of advantages including the possibility to rationally tailor their architecture to further improve the hydrogen separation performance. It could be then expected that future research should be directed on such porous materials, particularly to test their separation performance in the real conditions, which will contribute to significantly accelerate the employment of these porous materials to fully support the transition from the fossil fuel-based to hydrogen-based green economy.

6. Acknowledgments

N. P acknowledges the funding from the Alexander von Humboldt Postdoctoral Fellowship (Ref 3.3 – GBR – 1219268 – HFST-P).

7. References

[1] G. Bernardo, T. Araújo, T. da Silva Lopes, J. Sousa, A. Mendes, Recent advances in membrane technologies for hydrogen purification, International Journal of Hydrogen Energy 45 (2020) 7313–7338.

[2] H. Nazir, C. Louis, S. Jose, J. Prakash, N. Muthuswamy, M.E. Buan, C. Flox, S. Chavan, X. Shi, P. Kauranen, Is the H2 economy realizable in the foreseeable future? Part I: H2 production methods, International Journal of Hydrogen Energy 45 (2020) 13777–13788.

[3] N. Prasetya, Z. Wu, A.G. Gil, K. Li, Compact hollow fibre reactors for efficient methane conversion, Journal of the European Ceramic Society 37 (2017) 5281–5287.

[4] N. Prasetya, N.F. Himma, P.D. Sutrisna, I.G. Wenten, B.P. Ladewig, A review on emerging organic-containing microporous material membranes for carbon capture and separation, Chemical Engineering Journal 391 (2020) 123575.

[5] C.A. Scholes, K.H. Smith, S.E. Kentish, G.W. Stevens, CO2 capture from pre-combustion processes—Strategies for membrane gas separation, International Journal of Greenhouse Gas Control 4 (2010) 739–755.

[6] M. Maarefian, S. Bandehali, S. Azami, H. Sanaeepur, A. Moghadassi, Hydrogen recovery from ammonia purge gas by a membrane separator: A simulation study, International Journal of Energy Research 43 (2019) 8217–8229.

[7] S. Sircar, T. Golden, Purification of hydrogen by pressure swing adsorption, Separation Science and Technology 35 (2000) 667–687.

[8] G. Moral, R. Ortiz-Imedio, A. Ortiz, D. Gorri, I. Ortiz, Hydrogen recovery from coke oven gas. Comparative analysis of technical alternatives, Industrial & Engineering Chemistry Research 61 (2022) 6106–6124.
[9] O.A. Ojelade, S.F. Zaman, B.-J. Ni, Green ammonia production technologies: A review of practical progress, Journal of Environmental Management 342 (2023) 118348.
[10] D.R. MacFarlane, P.V. Cherepanov, J. Choi, B.H. Suryanto, R.Y. Hodgetts, J.M. Bakker, F.M.F. Vallana, A.N. Simonov, A roadmap to the ammonia economy, Joule 4 (2020) 1186–1205.
[11] M. Yáñez, F. Relvas, A. Ortiz, D. Gorri, A. Mendes, I. Ortiz, PSA purification of waste hydrogen from ammonia plants to fuel cell grade, Separation and Purification Technology 240 (2020) 116334.
[12] O.C. David, D. Gorri, K. Nijmeijer, I. Ortiz, A. Urtiaga, Hydrogen separation from multicomponent gas mixtures containing CO, N2 and CO2 using Matrimid® asymmetric hollow fiber membranes, Journal of Membrane Science 419 (2012) 49–56.
[13] W. Liemberger, D. Halmschlager, M. Miltner, M. Harasek, Efficient extraction of hydrogen transported as co-stream in the natural gas grid–The importance of process design, Applied Energy 233 (2019) 747–763.
[14] M. Nordio, S.A. Wassie, M.V.S. Annaland, D.A.P. Tanaka, J.L.V. Sole, F. Gallucci, Techno-economic evaluation on a hybrid technology for low hydrogen concentration separation and purification from natural gas grid, International Journal of Hydrogen Energy 46 (2021) 23417–23435.
[15] L. Hu, S. Pal, H. Nguyen, V. Bui, H. Lin, Molecularly engineering polymeric membranes for H2/CO2 separation at 100–300° C, Journal of Polymer Science 58 (2020) 2467–2481.
[16] D. Nikolic, A. Giovanoglou, M.C. Georgiadis, E.S. Kikkinides, Hydrogen purification by pressure swing adsorption, in: 2007.
[17] M. Amin, A.S. Butt, J. Ahmad, C. Lee, S.U. Azam, H.A. Mannan, A.B. Naveed, Z.U.R. Farooqi, E. Chung, A. Iqbal, Issues and challenges in hydrogen separation technologies, Energy Reports 9 (2023) 894–911.
[18] L.M. Robeson, The upper bound revisited, Journal of Membrane Science 320 (2008) 390–400.
[19] T. Graham, XVIII. On the absorption and dialytic separation of gases by colloid septa, Philosophical Transactions of the Royal Society of London (1866) 399–439.
[20] E. Harrison, L. Hobbis, Nickel Diffusion Leak for Hydrogen, Review of Scientific Instruments 26 (1955) 305–306.
[21] D. Juenker, M. Van Swaay, C. Birchenall, On the use of palladium diffusion membranes for the purification of hydrogen, Review of Scientific Instruments 26 (1955) 888–888.
[22] K. Landecker, A. Gray, Diffusion of Gases through Nickel and Design of a Convenient Leak for Hydrogen and Deuterium, Review of Scientific Instruments 25 (1954) 1151–1153.
[23] M.A. Habib, A. Harale, S. Paglieri, F.S. Alrashed, A. Al-Sayoud, M.V. Rao, M.A. Nemitallah, S. Hossain, M. Hussien, A. Ali, Palladium-alloy membrane reactors for fuel reforming and hydrogen production: A review, Energy & Fuels 35 (2021) 5558–5593.
[24] S. Yun, S.T. Oyama, Correlations in palladium membranes for hydrogen separation: A review, Journal of Membrane Science 375 (2011) 28–45.

[25] M.L. Bosko, A. Dalla Fontana, A. Tarditi, L. Cornaglia, Advances in hydrogen selective membranes based on palladium ternary alloys, International Journal of Hydrogen Energy 46 (2021) 15572–15594.
[26] A.W. Thornton, J.M. Hill, A.J. Hill, Modelling gas separation in porous membranes, Membrane Gas Separation (2010) 85–109.
[27] C. Li, S.M. Meckler, Z.P. Smith, J.E. Bachman, L. Maserati, J.R. Long, B.A. Helms, Engineered transport in microporous materials and membranes for clean energy technologies, Advanced Materials 30 (2018) 1704953.
[28] T. Okubo, H. Inoue, Single gas permeation through porous glass modified with tetraethoxysilane, AIChE Journal 35 (1989) 845–848.
[29] B. Ballinger, J. Motuzas, S. Smart, J.C.D. da Costa, Palladium cobalt binary doping of molecular sieving silica membranes, Journal of Membrane Science 451 (2014) 185–191.
[30] S. Smart, J. Vente, J.D. Da Costa, High temperature H2/CO2 separation using cobalt oxide silica membranes, International Journal of Hydrogen Energy 37 (2012) 12700–12707.
[31] R. Igi, T. Yoshioka, Y.H. Ikuhara, Y. Iwamoto, T. Tsuru, Characterization of Co-doped silica for improved hydrothermal stability and application to hydrogen separation membranes at high temperatures, Journal of the American Ceramic Society 91 (2008) 2975–2981.
[32] M. Kanezashi, M. Asaeda, Stability of H2-permeselective Ni-doped silica membranes in steam at high temperature, Journal of Chemical Engineering of Japan 38 (2005) 908–912.
[33] Y.-S. Kim, K. Kusakabe, S. Morooka, S.-M. Yang, Preparation of microporous silica membranes for gas separation, Korean Journal of Chemical Engineering 18 (2001) 106–112.
[34] Y. Yoshino, T. Suzuki, B.N. Nair, H. Taguchi, N. Itoh, Development of tubular substrates, silica based membranes and membrane modules for hydrogen separation at high temperature, Journal of Membrane Science 267 (2005) 8–17.
[35] D.-W. Lee, B. Sea, K.-Y. Lee, K.-H. Lee, Preparation and characterizaton of SiO2 composite membranes for purification of hydrogen for PEMFC, Industrial & Engineering Chemistry Research 41 (2002) 3594–3600.
[36] K. Kusakabe, F. Shibao, G. Zhao, K.-I. Sotowa, K. Watanabe, T. Saito, Surface modification of silica membranes in a tubular-type module, Journal of Membrane Science 215 (2003) 321–326.
[37] M. Kanezashi, M. Asaeda, Hydrogen permeation characteristics and stability of Ni-doped silica membranes in steam at high temperature, Journal of Membrane Science 271 (2006) 86–93.
[38] S. Battersby, S. Smart, B. Ladewig, S. Liu, M.C. Duke, V. Rudolph, J.C.D. da Costa, Hydrothermal stability of cobalt silica membranes in a water gas shift membrane reactor, Separation and Purification Technology 66 (2009) 299–305.
[39] D.-W. Lee, C.-Y. Yu, K.-H. Lee, Synthesis of Pd particle-deposited microporous silica membranes via a vacuum-impregnation method and their gas permeation behavior, Journal of Colloid and Interface Science 325 (2008) 447–452.
[40] K. Yoshida, Y. Hirano, H. Fujii, T. Tsuru, M. Asaeda, Hydrothermal stability and performance of silica-zirconia membranes for hydrogen separation in hydrothermal conditions, Journal of Chemical Engineering of Japan 34 (2001) 523–530.

[41] E.J. Kappert, A. Nijmeijer, N.E. Benes, Expeditious calcination of inorganic membranes by an instant temperature increment, Microporous and Mesoporous Materials 151 (2012) 211–215.
[42] D.K. Wang, J.C.D. da Costa, S. Smart, Development of rapid thermal processing of tubular cobalt oxide silica membranes for gas separations, Journal of Membrane Science 456 (2014) 192–201.
[43] Q. Wei, F. Wang, Z.-R. Nie, C.-L. Song, Y.-L. Wang, Q.-Y. Li, Highly hydrothermally stable microporous silica membranes for hydrogen separation, The Journal of Physical Chemistry B 112 (2008) 9354–9359.
[44] H.R. Lee, M. Kanezashi, T. Yoshioka, T. Tsuru, Preparation of hydrogen separation membranes using disiloxane compounds, Desalination and Water Treatment 17 (2010) 120–126.
[45] H.R. Lee, M. Kanezashi, Y. Shimomura, T. Yoshioka, T. Tsuru, Evaluation and fabrication of pore-size-tuned silica membranes with tetraethoxydimethyl disiloxane for gas separation, AIChE Journal 57 (2011) 2755–2765.
[46] H.R. Lee, T. Shibata, M. Kanezashi, T. Mizumo, J. Ohshita, T. Tsuru, Pore-size-controlled silica membranes with disiloxane alkoxides for gas separation, Journal of Membrane Science 383 (2011) 152–158.
[47] H. Qi, H. Chen, L. Li, G. Zhu, N. Xu, Effect of Nb content on hydrothermal stability of a novel ethylene-bridged silsesquioxane molecular sieving membrane for H2/CO2 separation, Journal of Membrane Science 421 (2012) 190–200.
[48] H.F. Qureshi, A. Nijmeijer, L. Winnubst, Influence of sol–gel process parameters on the micro-structure and performance of hybrid silica membranes, Journal of Membrane Science 446 (2013) 19–25.
[49] H. Zhang, Y. Wei, H. Qi, Palladium-niobium bimetallic doped organosilica membranes for H2/CO2 separation, Microporous and Mesoporous Materials 305 (2020) 110279.
[50] Y. Wei, H. Zhang, J. Lei, H. Song, H. Qi, Controlling pore structures of Pd-doped organosilica membranes by calcination atmosphere for gas separation, Chinese Journal of Chemical Engineering 27 (2019) 3036–3042.
[51] H. Song, Y. Wei, C. Wang, S. Zhao, H. Qi, Tuning sol size to optimize organosilica membranes for gas separation, Chinese Journal of Chemical Engineering 26 (2018) 53–59.
[52] H.H. Han, S.H. Ryu, S. Nakao, Y.T. Lee, Gas permeation properties and preparation of porous ceramic membrane by CVD method using siloxane compounds, Journal of Membrane Science 431 (2013) 72–78.
[53] D. Lee, L. Zhang, S. Oyama, S. Niu, R. Saraf, Synthesis, characterization, and gas permeation properties of a hydrogen permeable silica membrane supported on porous alumina, Journal of Membrane Science 231 (2004) 117–126.
[54] D. Lee, S.T. Oyama, Gas permeation characteristics of a hydrogen selective supported silica membrane, Journal of Membrane Science 210 (2002) 291–306.
[55] Y. Gu, P. Hacarlioglu, S.T. Oyama, Hydrothermally stable silica–alumina composite membranes for hydrogen separation, Journal of Membrane Science 310 (2008) 28–37.
[56] S. Nakao, T. Suzuki, T. Sugawara, T. Tsuru, S. Kimura, Preparation of microporous membranes by TEOS/O3 CVD in the opposing reactants geometry, Microporous and Mesoporous Materials 37 (2000) 145–152.

[57] A.K. Prabhu, S.T. Oyama, Highly hydrogen selective ceramic membranes: application to the transformation of greenhouse gases, Journal of Membrane Science 176 (2000) 233–248.
[58] K. Kuraoka, T. Kakitani, T. Suetsugu, T. Yazawa, Methanol vapor separation through the silica membrane prepared by the CVD method with the aid of evacuation, Separation and Purification Technology 25 (2001) 161–166.
[59] R. Levy, E. Ramos, L. Krasnoperov, A. Datta, J. Grow, Microporous SiO2/Vycor membranes for gas separation, Journal of Materials Research 11 (1996) 3164–3173.
[60] S.-W. Nam, H.-Y. Ha, S.-P. Yoon, J. Han, T.-H. Lim, I.-H. Oh, S.-A. Hong, Hydrogen-Permselective TiO $ _2 $2/SiO $ _2 $2 Membranes Formed by Chemical Vapor Deposition, Korean Membrane Journal 3 (2001) 69–74.
[61] H.Y. Ha, J.S. Lee, S.W. Nam, I.W. Kim, S.-A. Hong, Alumina composite membranes prepared by MOCVD, Journal of Materials Science Letters 16 (1997) 1023–1026.
[62] H.Y. Ha, S.W. Nam, W.K. Lee, Chemical vapor deposition of hydrogen-permselective silica films on porous glass supports from tetraethylorthosilicate, Journal of Membrane Science 85 (1993) 279–290.
[63] C.E. Megiris, J.H. Glezer, Synthesis of hydrogen-permselective membranes by modified chemical vapor deposition. Microstructure and permselectivity of silica/carbon/Vycor membranes, Industrial & Engineering Chemistry Research 31 (1992) 1293–1299.
[64] S. Jiang, Y. Yan, G. Gavalas, Temporary carbon barriers in the preparation of H2-permselective silica membranes, Journal of Membrane Science 103 (1995) 211–218.
[65] S. Kim, G.R. Gavalas, Preparation of H2 permselective silica membranes by alternating reactant vapor deposition, Industrial & Engineering Chemistry Research 34 (1995) 168–176.
[66] M. Tsapatsis, G. Gavalas, Structure and aging characteristics of H2-permselective SiO2-Vycor membranes, Journal of Membrane Science 87 (1994) 281–296.
[67] S. Yan, H. Maeda, K. Kusakabe, S. Morooka, Y. Akiyama, Hydrogen-permselective SiO2 membrane formed in pores of alumina support tube by chemical vapor deposition with tetraethylorthosilicate, Industrial & Engineering Chemistry Research 33 (1994) 2096–2101.
[68] S. Morooka, S. Yan, K. Kusakabe, Y. Akiyama, Formation of hydrogen-permselective SiO2 membrane in macropores of α-alumina support tube by thermal decomposition of TEOS, Journal of Membrane Science 101 (1995) 89–98.
[69] Y. Gu, S.T. Oyama, Ultrathin, hydrogen-selective silica membranes deposited on alumina-graded structures prepared from size-controlled boehmite sols, Journal of Membrane Science 306 (2007) 216–227.
[70] Y. Gu, S.T. Oyama, Permeation properties and hydrothermal stability of silica–titania membranes supported on porous alumina substrates, Journal of Membrane Science 345 (2009) 267–275.
[71] S. Gopalakrishnan, J.C.D. da Costa, Hydrogen gas mixture separation by CVD silica membrane, Journal of Membrane Science 323 (2008) 144–147.
[72] B.-K. Sea, M. Watanabe, K. Kusakabe, S. Morooka, S.-S. Kim, Formation of hydrogen permselective silica membrane for elevated temperature hydrogen recovery from a mixture containing steam, Gas Separation & Purification 10 (1996) 187–195.

[73] S.-S. Kin, B.-K. Sea, Gas permeation characteristics of silica/alumina composite membrane prepared by chemical vapor deposition, Korean Journal of Chemical Engineering 18 (2001) 322–329.
[74] B. Sea, K.-H. Lee, Modification of mesoporous γ-alumina with silica and application for hydrogen separation at elevated temperature, Journal of Industrial and Engineering Chemistry 7 (2001) 417–423.
[75] B.G. Sea, G.H. Lee, Molecular sieve silica membrane synthesized in mesoporous γ-alumina layer, Bulletin of the Korean Chemical Society 22 (2001) 1400–1402.
[76] A. Nijmeijer, B. Bladergroen, H. Verweij, Low-temperature CVI modification of γ-alumina membranes, Microporous and Mesoporous Materials 25 (1998) 179–184.
[77] G.-J. Hwang, K. Onuki, S. Shimizu, H. Ohya, Hydrogen separation in H2–H2O–HI gaseous mixture using the silica membrane prepared by chemical vapor deposition, Journal of Membrane Science 162 (1999) 83–90.
[78] M. Nomura, K. Ono, S. Gopalakrishnan, T. Sugawara, S.-I. Nakao, Preparation of a stable silica membrane by a counter diffusion chemical vapor deposition method, Journal of Membrane Science 251 (2005) 151–158.
[79] Y. Gu, B. Vaezian, S.J. Khatib, S.T. Oyama, Z. Wang, L. Achenie, Hybrid H2-selective silica membranes prepared by chemical vapor deposition, Separation Science and Technology 47 (2012) 1698–1708.
[80] K. Akamatsu, M. Nakane, T. Sugawara, T. Hattori, S. Nakao, Development of a membrane reactor for decomposing hydrogen sulfide into hydrogen using a high-performance amorphous silica membrane, Journal of Membrane Science 325 (2008) 16–19.
[81] S. Araki, N. Mohri, Y. Yoshimitsu, Y. Miyake, Synthesis, characterization and gas permeation properties of a silica membrane prepared by high-pressure chemical vapor deposition, Journal of Membrane Science 290 (2007) 138–145.
[82] T. Nagano, S. Fujisaki, K. Sato, K. Hataya, Y. Iwamoto, M. Nomura, S. Nakao, Relationship between the mesoporous intermediate layer structure and the gas permeation property of an amorphous silica membrane synthesized by counter diffusion chemical vapor deposition, Journal of the American Ceramic Society 91 (2008) 71–76.
[83] A. Comite, Chapter 1 - Preparation of Silica Membranes by Sol-Gel Method, in: A. Basile, K. Ghasemzadeh (Eds.), Current Trends and Future Developments on (Bio-) Membranes, Elsevier, 2017: pp. 3–23. https://doi.org/10.1016/B978-0-444-63866-3.00001-7.
[84] N.W. Ockwig, T.M. Nenoff, Membranes for hydrogen separation, Chemical Reviews 107 (2007) 4078–4110.
[85] C. Barboiu, B. Sala, S. Bec, S. Pavan, E. Petit, Ph. Colomban, J. Sanchez, S. de Perthuis, D. Hittner, Structural and mechanical characterizations of microporous silica–boron membranes for gas separation, Journal of Membrane Science 326 (2009) 514–525. https://doi.org/10.1016/j.memsci.2008.10.052.
[86] J. Motuzas, A. Darmawan, M. Elma, D.K. Wang, Microporous Silica Membrane: Structure, Preparation, Characterization, and Applications, in: Current Trends and Future Developments on (Bio-) Membranes, Elsevier, 2019: pp. 77–99.
[87] S.J. Khatib, S.T. Oyama, Silica membranes for hydrogen separation prepared by chemical vapor deposition (CVD), Separation and Purification Technology 111 (2013) 20–42.

[88] B. Wang, N. Hu, H. Wang, Y. Zheng, R. Zhou, Improved AlPO-18 membranes for light gas separation, Journal of Materials Chemistry A 3 (2015) 12205–12212.
[89] L. Yu, M.S. Nobandegani, A. Holmgren, J. Hedlund, Highly permeable and selective tubular zeolite CHA membranes, Journal of Membrane Science 588 (2019) 117224.
[90] A. Bose, M. Sen, J.K. Das, N. Das, Sonication mediated hydrothermal process–an efficient method for the rapid synthesis of DDR zeolite membranes, Rsc Advances 4 (2014) 19043–19052.
[91] S. Himeno, T. Tomita, K. Suzuki, K. Nakayama, K. Yajima, S. Yoshida, Synthesis and permeation properties of a DDR-type zeolite membrane for separation of CO2/CH4 gaseous mixtures, Industrial & Engineering Chemistry Research 46 (2007) 6989–6997.
[92] M. Kanezashi, J. O'Brien-Abraham, Y. Lin, K. Suzuki, Gas permeation through DDR-type zeolite membranes at high temperatures, AIChE Journal 54 (2008) 1478–1486.
[93] Z. Zheng, A.S. Hall, V.V. Guliants, Synthesis, characterization and modification of DDR membranes grown on α-alumina supports, Journal of Materials Science 43 (2008) 2499–2502.
[94] T. Tomita, K. Nakayama, H. Sakai, Gas separation characteristics of DDR type zeolite membrane, Microporous and Mesoporous Materials 68 (2004) 71–75.
[95] L. Wang, C. Zhang, X. Gao, L. Peng, J. Jiang, X. Gu, Preparation of defect-free DDR zeolite membranes by eliminating template with ozone at low temperature, Journal of Membrane Science 539 (2017) 152–160.
[96] S. Yang, Z. Cao, A. Arvanitis, X. Sun, Z. Xu, J. Dong, DDR-type zeolite membrane synthesis, modification and gas permeation studies, Journal of Membrane Science 505 (2016) 194–204.
[97] P. Du, J. Song, X. Wang, Y. Zhang, J. Xie, G. Liu, Y. Liu, Z. Wang, Z. Hong, X. Gu, Efficient scale-up synthesis and hydrogen separation of hollow fiber DD3R zeolite membranes, Journal of Membrane Science 636 (2021) 119546.
[98] L. Sandström, M. Palomino, J. Hedlund, High flux zeolite X membranes, Journal of Membrane Science 354 (2010) 171–177.
[99] G. Zhu, Y. Li, H. Zhou, J. Liu, W. Yang, FAU-type zeolite membranes synthesized by microwave assisted in situ crystallization, Materials Letters 62 (2008) 4357–4359.
[100] A. Huang, N. Wang, J. Caro, Seeding-free synthesis of dense zeolite FAU membranes on 3-aminopropyltriethoxysilane-functionalized alumina supports, Journal of Membrane Science 389 (2012) 272–279.
[101] C. Zhou, C. Yuan, Y. Zhu, J. Caro, A. Huang, Facile synthesis of zeolite FAU molecular sieve membranes on bio-adhesive polydopamine modified Al2O3 tubes, Journal of Membrane Science 494 (2015) 174–181.
[102] A. Huang, Q. Liu, N. Wang, X. Tong, B. Huang, M. Wang, J. Caro, Covalent synthesis of dense zeolite LTA membranes on various 3-chloropropyltrimethoxysilane functionalized supports, Journal of Membrane Science 437 (2013) 57–64.
[103] C. Yuan, Q. Liu, H. Chen, A. Huang, Mussel-inspired polydopamine modification of supports for the facile synthesis of zeolite LTA molecular sieve membranes, RSC Advances 4 (2014) 41982–41988.
[104] A. Huang, F. Liang, F. Steinbach, J. Caro, Preparation and separation properties of LTA membranes by using 3-aminopropyltriethoxysilane as covalent linker, Journal of Membrane Science 350 (2010) 5–9.

[105] A. Huang, N. Wang, J. Caro, Synthesis of multi-layer zeolite LTA membranes with enhanced gas separation performance by using 3-aminopropyltriethoxysilane as interlayer, Microporous and Mesoporous Materials 164 (2012) 294–301.
[106] A. Huang, J. Caro, Facile synthesis of LTA molecular sieve membranes on covalently functionalized supports by using diisocyanates as molecular linkers, Journal of Materials Chemistry 21 (2011) 11424–11429.
[107] Y. Li, H. Chen, J. Liu, W. Yang, Microwave synthesis of LTA zeolite membranes without seeding, Journal of Membrane Science 277 (2006) 230–239.
[108] X. Li, K. Li, S. Tao, H. Ma, R. Xu, B. Wang, P. Wang, Z. Tian, Ionothermal synthesis of LTA-type aluminophosphate molecular sieve membranes with gas separation performance, Microporous and Mesoporous Materials 228 (2016) 45–53.
[109] A. Huang, F. Liang, F. Steinbach, T.M. Gesing, J. Caro, Neutral and cation-free LTA-type aluminophosphate (AlPO4) molecular sieve membrane with high hydrogen permselectivity, Journal of the American Chemical Society 132 (2010) 2140–2141.
[110] A. Huang, J. Caro, Steam-stable hydrophobic ITQ-29 molecular sieve membrane with H 2 selectivity prepared by secondary growth using Kryptofix 222 as SDA, Chemical Communications 46 (2010) 7748–7750.
[111] A. Huang, J. Caro, Highly oriented, neutral and cation-free AlPO 4 LTA: from a seed crystal monolayer to a molecular sieve membrane, Chemical Communications 47 (2011) 4201–4203.
[112] T. Wu, C. Shu, S. Liu, B. Xu, S. Zhong, R. Zhou, Separation performance of Si-CHA zeolite membrane for a binary H2/CH4 mixture and ternary and quaternary mixtures containing impurities, Energy & Fuels 34 (2020) 11650–11659.
[113] K. Kida, Y. Maeta, K. Yogo, Preparation and gas permeation properties on pure silica CHA-type zeolite membranes, Journal of Membrane Science 522 (2017) 363–370.
[114] C. Algieri, P. Bernardo, G. Golemme, G. Barbieri, E. Drioli, Permeation properties of a thin silicalite-1 (MFI) membrane, Journal of Membrane Science 222 (2003) 181–190.
[115] W. Xiao, Z. Chen, L. Zhou, J. Yang, J. Lu, J. Wang, A simple seeding method for MFI zeolite membrane synthesis on macroporous support by microwave heating, Microporous and Mesoporous Materials 142 (2011) 154–160.
[116] N. Kosinov, E.J. Hensen, Synthesis and separation properties of an α-alumina-supported high-silica MEL membrane, Journal of Membrane Science 447 (2013) 12–18.
[117] X. Zhu, H. Wang, Y. Lin, Effect of the membrane quality on gas permeation and chemical vapor deposition modification of MFI-type zeolite membranes, Industrial & Engineering Chemistry Research 49 (2010) 10026–10033.
[118] Y. Zhang, Z. Wu, Z. Hong, X. Gu, N. Xu, Hydrogen-selective zeolite membrane reactor for low temperature water gas shift reaction, Chemical Engineering Journal 197 (2012) 314–321.
[119] Z. Tang, S.-J. Kim, G.K. Reddy, J. Dong, P. Smirniotis, Modified zeolite membrane reactor for high temperature water gas shift reaction, Journal of Membrane Science 354 (2010) 114–122.
[120] Z. Hong, F. Sun, D. Chen, C. Zhang, X. Gu, N. Xu, Improvement of hydrogen-separating performance by on-stream catalytic cracking of silane over hollow fiber MFI zeolite membrane, International Journal of Hydrogen Energy 38 (2013) 8409–8414.
[121] Z. Hong, Z. Wu, Y. Zhang, X. Gu, Catalytic cracking deposition of methyldiethoxysilane for modification of zeolitic pores in MFI/α-Al2O3 zeolite membrane with H+ ion

exchange pretreatment, Industrial & Engineering Chemistry Research 52 (2013) 13113–13119.
[122] Z. Tang, J. Dong, T.M. Nenoff, Internal surface modification of MFI-type zeolite membranes for high selectivity and high flux for hydrogen, Langmuir 25 (2009) 4848–4852.
[123] T. Masuda, N. Fukumoto, M. Kitamura, S.R. Mukai, K. Hashimoto, T. Tanaka, T. Funabiki, Modification of pore size of MFI-type zeolite by catalytic cracking of silane and application to preparation of H2-separating zeolite membrane, Microporous and Mesoporous Materials 48 (2001) 239–245.
[124] X. Xu, W. Yang, J. Liu, L. Lin, Synthesis of NaA zeolite membranes from clear solution, Microporous and Mesoporous Materials 43 (2001) 299–311.
[125] X. Xu, Y. Bao, C. Song, W. Yang, J. Liu, L. Lin, Synthesis, characterization and single gas permeation properties of NaA zeolite membrane, Journal of Membrane Science 249 (2005) 51–64.
[126] K.P. Dey, D. Kundu, M. Chatterjee, M.K. Naskar, Preparation of NaA zeolite membranes using poly (ethyleneimine) as buffer layer, and study of their permeation behavior, Journal of the American Ceramic Society 96 (2013) 68–72.
[127] Y.M. Galeano, L. Cornaglia, A.M. Tarditi, NaA zeolite membranes synthesized on top of APTES-modified porous stainless steel substrates, Journal of Membrane Science 512 (2016) 93–103.
[128] S. Zhong, N. Bu, R. Zhou, W. Jin, M. Yu, S. Li, Aluminophosphate-17 and silicoaluminophosphate-17 membranes for CO2 separations, Journal of Membrane Science 520 (2016) 507–514.
[129] M. Hong, J.L. Falconer, R.D. Noble, Modification of zeolite membranes for H2 separation by catalytic cracking of methyldiethoxysilane, Industrial & Engineering Chemistry Research 44 (2005) 4035–4041.
[130] J.K. Das, N. Das, S. Bandyopadhyay, Highly oriented improved SAPO 34 membrane on low cost support for hydrogen gas separation, Journal of Materials Chemistry A 1 (2013) 4966–4973.
[131] J.K. Das, N. Das, S.N. Roy, S. Bandyopadhyay, The growth of SAPO 34 membrane layer on support surface for gas permeation application, Ceramics International 38 (2012) 333–340.
[132] J.C. Poshusta, V.A. Tuan, J.L. Falconer, R.D. Noble, Synthesis and permeation properties of SAPO-34 tubular membranes, Industrial & Engineering Chemistry Research 37 (1998) 3924–3929.
[133] J.C. Poshusta, V.A. Tuan, E.A. Pape, R.D. Noble, J.L. Falconer, Separation of light gas mixtures using SAPO-34 membranes, AIChE Journal 46 (2000) 779–789.
[134] Z. Jabbari, S. Fatemi, M. Davoodpour, Comparative study of seeding methods; dip-coating, rubbing and EPD, in SAPO-34 thin film fabrication, Advanced Powder Technology 25 (2014) 321–330.
[135] M. Yu, H.H. Funke, R.D. Noble, J.L. Falconer, H2 separation using defect-free, inorganic composite membranes, Journal of the American Chemical Society 133 (2011) 1748–1750.
[136] L. Zhou, J. Yang, G. Li, J. Wang, Y. Zhang, J. Lu, D. Yin, Highly H2 permeable SAPO-34 membranes by steam-assisted conversion seeding, International Journal of Hydrogen Energy 39 (2014) 14949–14954.

[137] W. Mei, Y. Du, T. Wu, F. Gao, B. Wang, J. Duan, J. Zhou, R. Zhou, High-flux CHA zeolite membranes for H2 separations, Journal of Membrane Science 565 (2018) 358–369.
[138] M. Hong, S. Li, J.L. Falconer, R.D. Noble, Hydrogen purification using a SAPO-34 membrane, Journal of Membrane Science 307 (2008) 277–283.
[139] H. Kalipcilar, T.C. Bowen, R.D. Noble, J.L. Falconer, Synthesis and separation performance of SSZ-13 zeolite membranes on tubular supports, Chemistry of Materials 14 (2002) 3458–3464.
[140] N. Kosinov, C. Auffret, V.G. Sripathi, C. Gücüyener, J. Gascon, F. Kapteijn, E.J. Hensen, Influence of support morphology on the detemplation and permeation of ZSM-5 and SSZ-13 zeolite membranes, Microporous and Mesoporous Materials 197 (2014) 268–277.
[141] N. Kosinov, C. Auffret, C. Gücüyener, B.M. Szyja, J. Gascon, F. Kapteijn, E.J. Hensen, High flux high-silica SSZ-13 membrane for CO 2 separation, Journal of Materials Chemistry A 2 (2014) 13083–13092.
[142] R. Zhou, H. Wang, B. Wang, X. Chen, S. Li, M. Yu, Defect-patching of zeolite membranes by surface modification using siloxane polymers for CO2 separation, Industrial & Engineering Chemistry Research 54 (2015) 7516–7523.
[143] Y. Zheng, N. Hu, H. Wang, N. Bu, F. Zhang, R. Zhou, Preparation of steam-stable high-silica CHA (SSZ-13) membranes for CO2/CH4 and C2H4/C2H6 separation, Journal of Membrane Science 475 (2015) 303–310.
[144] H. Tang, L. Bai, M. Wang, Y. Zhang, M. Li, M. Wang, L. Kong, N. Xu, Y. Zhang, P. Rao, Fast synthesis of thin high silica SSZ-13 zeolite membrane using oil-bath heating, International Journal of Hydrogen Energy 44 (2019) 23107–23119.
[145] B. Wang, Y. Zheng, J. Zhang, W. Zhang, F. Zhang, W. Xing, R. Zhou, Separation of light gas mixtures using zeolite SSZ-13 membranes, Microporous and Mesoporous Materials 275 (2019) 191–199.
[146] T. Zhou, M. Shi, L. Chen, C. Gong, P. Zhang, J. Xie, X. Wang, X. Gu, Fluorine-free synthesis of all-silica STT zeolite membranes for H2/CH4 separation, Chemical Engineering Journal 433 (2022) 133567.
[147] T. Zhou, M. Zhu, Y. Dai, L. Chen, J. Xie, Y. Zhang, X. Wang, X. Gu, Static state synthesis of STT zeolite membranes for high-pressure H2/CH4 separation, Journal of Membrane Science 700 (2024) 122699. https://doi.org/10.1016/j.memsci.2024.122699.
[148] X. Li, C. Zhou, Z. Lin, J. Rocha, P.F. Lito, A.S. Santiago, C.M. Silva, Titanosilicate AM-3 membrane: A new potential candidate for H2 separation, Microporous and Mesoporous Materials 137 (2011) 43–48.
[149] P.F. Lito, C.F. Zhou, A.S. Santiago, A.E. Rodrigues, J. Rocha, Z. Lin, C.M. Silva, Modelling gas permeation through new microporous titanosilicate AM-3 membranes, Chemical Engineering Journal 165 (2010) 395–404.
[150] V. Sebastián, Z. Lin, J. Rocha, C. Téllez, J. Santamaría, J. Coronas, Improved Ti-silicate umbite membranes for the separation of H2, Journal of Membrane Science 323 (2008) 207–212.
[151] V. Sebastián, Z. Lin, J. Rocha, C. Téllez, J. Santamaría, J. Coronas, A new titanosilicate umbite membrane for the separation of H 2, Chemical Communications (2005) 3036–3037.
[152] H. Wang, X. Dong, Y. Lin, Highly stable bilayer MFI zeolite membranes for high temperature hydrogen separation, Journal of Membrane Science 450 (2014) 425–432.

[153] H. Kalipcilar, S.K. Gade, R.D. Noble, J.L. Falconer, Synthesis and separation properties of B-ZSM-5 zeolite membranes on monolith supports, Journal of Membrane Science 210 (2002) 113–127.
[154] F. Bonhomme, M.E. Welk, T.M. Nenoff, CO2 selectivity and lifetimes of high silica ZSM-5 membranes, Microporous and Mesoporous Materials 66 (2003) 181–188.
[155] Y. Li, J. Wang, J. Shi, X. Zhang, J. Lu, Z. Bao, D. Yan, Synthesis of ZSM-5 zeolite membranes with large area on porous, tubular α-Al2O3 supports, Separation and Purification Technology 32 (2003) 397–401.
[156] Y. Cheng, J.-S. Li, L.-J. Wang, X.-Y. Sun, X.-D. Liu, Synthesis and characterization of Ce-ZSM-5 zeolite membranes, Separation and Purification Technology 51 (2006) 210–218.
[157] A. Huang, N. Wang, J. Caro, Stepwise synthesis of sandwich-structured composite zeolite membranes with enhanced separation selectivity, Chemical Communications 48 (2012) 3542–3544.
[158] H. Wu, X. Liu, Y. Guo, Preparation of a zeolite-palladium composite membrane for hydrogen separation: Influence of zeolite film on membrane stability, Chinese Journal of Chemical Engineering 72 (2024) 44–52. https://doi.org/10.1016/j.cjche.2024.01.011.
[159] L. Lei, A. Lindbråthen, M. Hillestad, X. He, Carbon molecular sieve membranes for hydrogen purification from a steam methane reforming process, Journal of Membrane Science 627 (2021) 119241.
[160] L. Lei, F. Pan, A. Lindbråthen, X. Zhang, M. Hillestad, Y. Nie, L. Bai, X. He, M.D. Guiver, Carbon hollow fiber membranes for a molecular sieve with precise-cutoff ultramicropores for superior hydrogen separation, Nature Communications 12 (2021) 268.
[161] D. Grainger, M.-B. Hägg, Evaluation of cellulose-derived carbon molecular sieve membranes for hydrogen separation from light hydrocarbons, Journal of Membrane Science 306 (2007) 307–317.
[162] T. Araújo, G. Bernardo, A. Mendes, High-performance hydrogen separation using cellulose-based carbon molecular sieve membranes, Journal of Membrane Science 693 (2024) 122337.
[163] J.A. Lie, M.-B. Hägg, Carbon membranes from cellulose: Synthesis, performance and regeneration, Journal of Membrane Science 284 (2006) 79–86.
[164] M. Campo, F.D. Magalhães, Ajj. Mendes, Carbon molecular sieve membranes from cellophane paper, Journal of Membrane Science 350 (2010) 180–188.
[165] H. Richter, H. Voss, N. Kaltenborn, S. Kämnitz, A. Wollbrink, A. Feldhoff, J. Caro, S. Roitsch, I. Voigt, High-flux carbon molecular sieve membranes for gas separation, Angewandte Chemie International Edition 56 (2017) 7760–7763.
[166] H. Hatori, H. Takagi, Y. Yamada, Gas separation properties of molecular sieving carbon membranes with nanopore channels, Carbon 42 (2004) 1169–1173.
[167] I. Kumakiri, K. Tamura, Y. Sasaki, K. Tanaka, H. Kita, Influence of iron additive on the hydrogen separation properties of carbon molecular sieve membranes, Industrial & Engineering Chemistry Research 57 (2018) 5370–5377.
[168] H. Kita, K. Nanbu, T. Hamano, M. Yoshino, K. Okamoto, M. Funaoka, Carbon molecular sieving membranes derived from lignin-based materials, Journal of Polymers and the Environment 10 (2002) 69–75.
[169] T. Koga, H. Kita, T. Suzuki, K. Uemura, K. Tanaka, I. Kawafune, M. Funaoka, Carbon membranes from wood materials and their separation properties, Transactions of the Materials Research Society of Japan 33 (2008) 825–828.

[170] K. Briceño, D. Montané, R. Garcia-Valls, A. Iulianelli, A. Basile, Fabrication variables affecting the structure and properties of supported carbon molecular sieve membranes for hydrogen separation, Journal of Membrane Science 415 (2012) 288–297.
[171] C. Zhang, W.J. Koros, Ultraselective carbon molecular sieve membranes with tailored synergistic sorption selective properties, Advanced Materials 29 (2017) 1701631.
[172] M.A.L. Tanco, J.A. Medrano, V. Cechetto, F. Gallucci, D.A.P. Tanaka, Hydrogen permeation studies of composite supported alumina-carbon molecular sieves membranes: Separation of diluted hydrogen from mixtures with methane, International Journal of Hydrogen Energy 46 (2021) 19758–19767.
[173] M. Nordio, J. Melendez, M. van Sint Annaland, D.A.P. Tanaka, M.L. Tanco, F. Gallucci, Comparison between carbon molecular sieve and Pd-Ag membranes in H2-CH4 separation at high pressure, International Journal of Hydrogen Energy 45 (2020) 28876–28892.
[174] A. Rahimalimamaghani, D.P. Tanaka, M.L. Tanco, F.N. D'Angelo, F. Gallucci, Effect of aluminium acetyl acetonate on the hydrogen and nitrogen permeation of carbon molecular sieves membranes, International Journal of Hydrogen Energy 47 (2022) 14570–14579.
[175] M.A.L. Tanco, D.A.P. Tanaka, S.C. Rodrigues, M. Texeira, A. Mendes, Composite-alumina-carbon molecular sieve membranes prepared from novolac resin and boehmite. Part I: Preparation, characterization and gas permeation studies, International Journal of Hydrogen Energy 40 (2015) 5653–5663.
[176] W. Wei, G. Qin, H. Hu, L. You, G. Chen, Preparation of supported carbon molecular sieve membrane from novolac phenol–formaldehyde resin, Journal of Membrane Science 303 (2007) 80–85.
[177] R. Xu, L. He, L. Li, M. Hou, Y. Wang, B. Zhang, C. Liang, T. Wang, Ultraselective carbon molecular sieve membrane for hydrogen purification, Journal of Energy Chemistry 50 (2020) 16–24.
[178] G.M. Iyer, C. Zhang, Precise hydrogen sieving by carbon molecular sieve membranes derived from solution-processable aromatic polyamides, ACS Materials Letters 5 (2022) 243–248.
[179] Y. Jiao, Q. Wu, W. Xu, W. Lai, L. Xiao, X. Mei, H. Zhang, S. Luo, Coordination enhancement of hydrogen and helium recovery in polybenzimidazole-based carbon molecular sieve membranes, Separation and Purification Technology 315 (2023) 123691.
[180] V. Pirouzfar, S.S. Hosseini, M.R. Omidkhah, A.Z. Moghaddam, Modeling and optimization of gas transport characteristics of carbon molecular sieve membranes through statistical analysis, Polymer Engineering & Science 54 (2014) 147–157.
[181] R. Wu, W. Yue, Y. Li, A. Huang, Ultra-thin and high hydrogen permeable carbon molecular sieve membrane prepared by using polydopamine as carbon precursor, Materials Letters 295 (2021) 129863.
[182] M. Hou, L. Li, Z. He, R. Xu, Y. Lu, T. Wang, High hydrogen permselective carbon molecular sieve membrane and its structural formation mechanism, Carbon 205 (2023) 194–206.
[183] Y.-T. Lin, J.-Y. Li, H.-H. Tseng, M.-Y. Wey, Insights into the role of polymer conformation on the cutoff size of carbon molecular sieving membranes for hydrogen separation and its novel pore size detection technology, ACS Applied Materials & Interfaces 13 (2021) 5165–5175.

[184] H.-H. Tseng, A.K. Itta, Modification of carbon molecular sieve membrane structure by self-assisted deposition carbon segment for gas separation, Journal of Membrane Science 389 (2012) 223–233.
[185] H. Wang, L. Zhang, G.R. Gavalas, Preparation of supported carbon membranes from furfuryl alcohol by vapor deposition polymerization, Journal of Membrane Science 177 (2000) 25–31.
[186] M.B. Shiflett, H.C. Foley, On the preparation of supported nanoporous carbon membranes, Journal of Membrane Science 179 (2000) 275–282.
[187] M.B. Shiflett, H.C. Foley, Ultrasonic deposition of high-selectivity nanoporous carbon membranes, Science 285 (1999) 1902–1905.
[188] C. Song, T. Wang, X. Wang, J. Qiu, Y. Cao, Preparation and gas separation properties of poly (furfuryl alcohol)-based C/CMS composite membranes, Separation and Purification Technology 58 (2008) 412–418.
[189] C. Song, T. Wang, J. Qiu, Preparation of C/CMS composite membranes derived from Poly (furfuryl alcohol) polymerized by iodine catalyst, Desalination 249 (2009) 486–489.
[190] S.O. Lawal, K. Watanabe, R. Uchino, N. Moriyama, H. Nagasawa, T. Tsuru, M. Kanezashi, Gas-Permeable Carbon Molecular Sieve Membranes Fabricated from a Norbornene-Functionalized Polyimide–Polyhedral Oligomeric Silsesquioxane Composite, Industrial & Engineering Chemistry Research 63 (2024) 1554–1565.
[191] B. Zhang, T. Wang, S. Zhang, J. Qiu, X. Jian, Preparation and characterization of carbon membranes made from poly (phthalazinone ether sulfone ketone), Carbon 44 (2006) 2764–2769.
[192] P.T. Ngamou, M. Ivanova, O. Guillon, W.A. Meulenberg, High-performance carbon molecular sieve membranes for hydrogen purification and pervaporation dehydration of organic solvents, Journal of Materials Chemistry A 7 (2019) 7082–7091.
[193] M. Hou, L. Li, J. Song, R. Xu, Z. He, Y. Lu, Z. Pan, C. Song, T. Wang, Polyimide-derived carbon molecular sieve membranes for high-efficient hydrogen purification: The development of a novel phthalide-containing polyimide precursor, Separation and Purification Technology 301 (2022) 121982.
[194] Y.M. Lee, Y.K. Kim, J.M. Lee, H.B. Park, Hydrogen separation of carbon molecular sieve membranes derived from polyimides having decomposable side groups, Membrane Journal 14 (2004) 99–107.
[195] J. Petersen, M. Matsuda, K. Haraya, Capillary carbon molecular sieve membranes derived from Kapton for high temperature gas separation, Journal of Membrane Science 131 (1997) 85–94. https://doi.org/10.1016/S0376-7388(97)00041-0.
[196] J. Liang, Z. Wang, M. Huang, S. Wu, Y. Shi, Y. Zhang, J. Jin, Effects on carbon molecular sieve membrane properties for a precursor polyimide with simultaneous flatness and contortion in the repeat unit, ChemSusChem 13 (2020) 5531–5538.
[197] Q. Wang, F. Huang, C.J. Cornelius, Y. Fan, Carbon molecular sieve membranes derived from crosslinkable polyimides for CO2/CH4 and C2H4/C2H6 separations, Journal of Membrane Science 621 (2021) 118785.
[198] M. Hou, W. Qi, L. Li, R. Xu, J. Xue, Y. Zhang, C. Song, T. Wang, Carbon molecular sieve membrane with tunable microstructure for CO2 separation: Effect of multiscale structures of polyimide precursors, Journal of Membrane Science 635 (2021) 119541.
[199] Y. Wu, F. Wang, B. Zhang, D. Zhao, T. Wang, J. Qiu, A simple one-step drop-coating approach on fabrication of supported carbon molecular sieve membranes with high gas separation performance, Asia-Pacific Journal of Chemical Engineering 13 (2018) e2251.

[200] L. Shao, T.-S. Chung, K. Pramoda, The evolution of physicochemical and transport properties of 6FDA-durene toward carbon membranes; from polymer, intermediate to carbon, Microporous and Mesoporous Materials 84 (2005) 59–68.
[201] B.T. Low, T.S. Chung, Carbon molecular sieve membranes derived from pseudo-interpenetrating polymer networks for gas separation and carbon capture, Carbon 49 (2011) 2104–2112.
[202] X. Ma, R. Swaidan, B. Teng, H. Tan, O. Salinas, E. Litwiller, Y. Han, I. Pinnau, Carbon molecular sieve gas separation membranes based on an intrinsically microporous polyimide precursor, Carbon 62 (2013) 88–96.
[203] K. Okamoto, M. Yoshino, K. Noborio, H. Maeda, K. Tanaka, H. Kita, Preparation of carbon molecular sieve membranes and their gas separation properties, in: ACS Publications, 2000.
[204] H. Li, Q. Zhang, Z. Xie, B. Zhao, Y. Yu, Y. Liu, Simultaneously enhanced gas permeability, selectivity and aging stability of carbon molecular sieve membranes by the molecule doping of silicon, Carbon 203 (2023) 47–58.
[205] Z. Dai, H. Guo, J. Deng, L. Deng, J. Yan, R.J. Spontak, Carbon molecular-sieve membranes developed from a Tröger's base polymer and possessing superior gas-separation performance, Journal of Membrane Science 680 (2023) 121731.
[206] H. Guo, J. Wei, Y. Ma, Z. Qin, X. Ma, R. Selyanchyn, B. Wang, X. He, B. Tang, L. Yang, Carbon molecular sieve membranes fabricated at low carbonization temperatures with novel polymeric acid porogen for light gas separation, Separation and Purification Technology 317 (2023) 123883.
[207] K. Hazazi, Y. Wang, N.S. Bettahalli, X. Ma, Y. Xia, I. Pinnau, Catalytic arene-norbornene annulation (CANAL) ladder polymer derived carbon membranes with unparalleled hydrogen/carbon dioxide size-sieving capability, Journal of Membrane Science 654 (2022) 120548.
[208] J. Nie, F. Okada, H. Kita, K. Tanaka, T. Mihara, D. Kondo, Y. Yamashita, N. Yahagi, Fabrication of carbon molecular sieve membranes supported on a novel porous carbon fiber, Energy & Fuels 36 (2022) 7147–7157.
[209] A.K. Itta, H.-H. Tseng, M.-Y. Wey, Fabrication and characterization of PPO/PVP blend carbon molecular sieve membranes for H2/N2 and H2/CH4 separation, Journal of Membrane Science 372 (2011) 387–395.
[210] Y.K. Kim, H.B. Park, Y.M. Lee, Gas separation properties of carbon molecular sieve membranes derived from polyimide/polyvinylpyrrolidone blends: effect of the molecular weight of polyvinylpyrrolidone, Journal of Membrane Science 251 (2005) 159–167.
[211] S.S. Hosseini, T.S. Chung, Carbon membranes from blends of PBI and polyimides for N2/CH4 and CO2/CH4 separation and hydrogen purification, Journal of Membrane Science 328 (2009) 174–185.
[212] N. Sazali, W.N.W. Salleh, A.F. Ismail, Y. Iwamoto, Incorporation of thermally labile additives in polyimide carbon membrane for hydrogen separation, International Journal of Hydrogen Energy 46 (2021) 24855–24863.
[213] M. Cai, H. Liu, J. Chen, J. Wu, Z. Han, Z. Chen, S. Zhang, Y. Min, Excellent gas separation performance of hybrid carbon molecular sieve membrane derived from polyimide/10X zeolite for hydrogen purification, Microporous and Mesoporous Materials 365 (2024) 112889.
[214] N. Widiastuti, A.R. Widyanto, I.S. Caralin, T. Gunawan, R. Wijiyanti, W.N. Wan Salleh, A.F. Ismail, M. Nomura, K. Suzuki, Development of a P84/ZCC composite carbon

membrane for gas separation of H2/CO2 and H2/CH4, ACS Omega 6 (2021) 15637–15650.
[215] Y. Zhang, M. Sun, L. Li, R. Xu, Y. Pan, T. Wang, Carbon molecular sieve/ZSM-5 mixed matrix membranes with enhanced gas separation performance and the performance recovery of the aging membranes, Journal of Membrane Science 660 (2022) 120869.
[216] K. Shimizu, T. Ohba, Extremely permeable porous graphene with high H 2/CO 2 separation ability achieved by graphene surface rejection, Physical Chemistry Chemical Physics 19 (2017) 18201–18207.
[217] K. Celebi, J. Buchheim, R.M. Wyss, A. Droudian, P. Gasser, I. Shorubalko, J.-I. Kye, C. Lee, H.G. Park, Ultimate permeation across atomically thin porous graphene, Science 344 (2014) 289–292.
[218] S. Huang, M. Dakhchoune, W. Luo, E. Oveisi, G. He, M. Rezaei, J. Zhao, D.T. Alexander, A. Züttel, M.S. Strano, Single-layer graphene membranes by crack-free transfer for gas mixture separation, Nature Communications 9 (2018) 2632.
[219] T. Ashirov, A. Coskun, Ultrahigh permeance metal coated porous graphene membranes with tunable gas selectivities, Chem 7 (2021) 2385–2394.
[220] H.W. Kim, H.W. Yoon, S.-M. Yoon, B.M. Yoo, B.K. Ahn, Y.H. Cho, H.J. Shin, H. Yang, U. Paik, S. Kwon, Selective gas transport through few-layered graphene and graphene oxide membranes, Science 342 (2013) 91–95.
[221] H. Li, Z. Song, X. Zhang, Y. Huang, S. Li, Y. Mao, H.J. Ploehn, Y. Bao, M. Yu, Ultrathin, molecular-sieving graphene oxide membranes for selective hydrogen separation, Science 342 (2013) 95–98.
[222] X. Wang, C. Chi, J. Tao, Y. Peng, S. Ying, Y. Qian, J. Dong, Z. Hu, Y. Gu, D. Zhao, Improving the hydrogen selectivity of graphene oxide membranes by reducing non-selective pores with intergrown ZIF-8 crystals, Chemical Communications 52 (2016) 8087–8090.
[223] J. Zhu, X. Meng, J. Zhao, Y. Jin, N. Yang, S. Zhang, J. Sunarso, S. Liu, Facile hydrogen/nitrogen separation through graphene oxide membranes supported on YSZ ceramic hollow fibers, Journal of Membrane Science 535 (2017) 143–150.
[224] C. Chi, X. Wang, Y. Peng, Y. Qian, Z. Hu, J. Dong, D. Zhao, Facile preparation of graphene oxide membranes for gas separation, Chemistry of Materials 28 (2016) 2921–2927.
[225] H. Lin, R. Liu, S. Dangwal, S.-J. Kim, N. Mehra, Y. Li, J. Zhu, Permselective H2/CO2 separation and desalination of hybrid GO/rGO membranes with controlled pre-cross-linking, ACS Applied Materials & Interfaces 10 (2018) 28166–28175.
[226] A. Ibrahim, Y. Lin, Gas permeation and separation properties of large-sheet stacked graphene oxide membranes, Journal of Membrane Science 550 (2018) 238–245.
[227] Z. Kang, S. Wang, L. Fan, M. Zhang, W. Kang, J. Pang, X. Du, H. Guo, R. Wang, D. Sun, In situ generation of intercalated membranes for efficient gas separation, Communications Chemistry 1 (2018) 3.
[228] S. Ma, Z. Tang, Y. Fan, J. Zhao, X. Meng, N. Yang, S. Zhuo, S. Liu, Surfactant-modified graphene oxide membranes with tunable structure for gas separation, Carbon 152 (2019) 144–150.
[229] A.F. Ibrahim, F. Banihashemi, Y. Lin, Graphene oxide membranes with narrow inter-sheet galleries for enhanced hydrogen separation, Chemical Communications 55 (2019) 3077–3080.

[230] K. Huang, J. Yuan, G. Shen, G. Liu, W. Jin, Graphene oxide membranes supported on the ceramic hollow fibre for efficient H2 recovery, Chinese Journal of Chemical Engineering 25 (2017) 752–759.
[231] L. Cheng, K. Guan, G. Liu, W. Jin, Cysteamine-crosslinked graphene oxide membrane with enhanced hydrogen separation property, Journal of Membrane Science 595 (2020) 117568.
[232] C.Y. Chuah, L. Nie, J.-M. Lee, T.-H. Bae, The influence of cations intercalated in graphene oxide membranes in tuning H2/CO2 separation performance, Separation and Purification Technology 246 (2020) 116933.
[233] R. Zeynali, K. Ghasemzadeh, A.B. Sarand, F. Kheiri, A. Basile, Performance evaluation of graphene oxide (GO) nanocomposite membrane for hydrogen separation: Effect of dip coating sol concentration, Separation and Purification Technology 200 (2018) 169–176.
[234] X. Meng, Y. Fan, J. Zhu, Y. Jin, C. Li, N. Yang, J. Zhao, J. Sunarso, S. Liu, Improving hydrogen permeation and interface property of ceramic-supported graphene oxide membrane via embedding of silicalite-1 zeolite into Al2O3 hollow fiber, Separation and Purification Technology 227 (2019) 115712.
[235] J. Shen, G. Liu, K. Huang, Z. Chu, W. Jin, N. Xu, Subnanometer two-dimensional graphene oxide channels for ultrafast gas sieving, ACS Nano 10 (2016) 3398–3409.
[236] K. Guan, J. Shen, G. Liu, J. Zhao, H. Zhou, W. Jin, Spray-evaporation assembled graphene oxide membranes for selective hydrogen transport, Separation and Purification Technology 174 (2017) 126–135.
[237] G. Romanos, L. Pastrana-Martínez, T. Tsoufis, C. Athanasekou, E. Galata, F. Katsaros, E. Favvas, K. Beltsios, E. Siranidi, P. Falaras, A facile approach for the development of fine-tuned self-standing graphene oxide membranes and their gas and vapor separation performance, Journal of Membrane Science 493 (2015) 734–747.
[238] R. Nair, H. Wu, P.N. Jayaram, I.V. Grigorieva, A. Geim, Unimpeded permeation of water through helium-leak–tight graphene-based membranes, Science 335 (2012) 442–444.
[239] N. Prasetya, I.G. Wenten, M. Franzreb, C. Wöll, Metal-organic frameworks for the adsorptive removal of pharmaceutically active compounds (PhACs): comparison to activated carbon, Coordination Chemistry Reviews 475 (2023) 214877.
[240] L.E. Kreno, K. Leong, O.K. Farha, M. Allendorf, R.P. Van Duyne, J.T. Hupp, Metal–organic framework materials as chemical sensors, Chemical Reviews 112 (2012) 1105–1125.
[241] Q. Qian, P.A. Asinger, M.J. Lee, G. Han, K. Mizrahi Rodriguez, S. Lin, F.M. Benedetti, A.X. Wu, W.S. Chi, Z.P. Smith, MOF-based membranes for gas separations, Chemical Reviews 120 (2020) 8161–8266.
[242] S. Zhou, X. Zou, F. Sun, H. Ren, J. Liu, F. Zhang, N. Zhao, G. Zhu, Development of hydrogen-selective CAU-1 MOF membranes for hydrogen purification by 'dual-metal-source'approach, International Journal of Hydrogen Energy 38 (2013) 5338–5347.
[243] H. Jin, A. Wollbrink, R. Yao, Y. Li, J. Caro, W. Yang, A novel CAU-10-H MOF membrane for hydrogen separation under hydrothermal conditions, Journal of Membrane Science 513 (2016) 40–46.
[244] C.-K. Chang, H.J. Yu, H. Jang, T.-H. Hung, J. Kim, J.S. Lee, D.-Y. Kang, Conformational-change-induced selectivity enhancement of CAU-10-PDC membrane for H2/CH4 and CO2/CH4 separation, Journal of Membrane Science Letters 1 (2021) 100005.

[245] M.N. Shah, M.A. Gonzalez, M.C. McCarthy, H.-K. Jeong, An unconventional rapid synthesis of high performance metal–organic framework membranes, Langmuir 29 (2013) 7896–7902.
[246] W. Li, Z. Yang, G. Zhang, Z. Fan, Q. Meng, C. Shen, C. Gao, Stiff metal–organic framework–polyacrylonitrile hollow fiber composite membranes with high gas permeability, Journal of Materials Chemistry A 2 (2014) 2110–2118.
[247] Y. Mao, J. Li, W. Cao, Y. Ying, L. Sun, X. Peng, Pressure-assisted synthesis of HKUST-1 thin film on polymer hollow fiber at room temperature toward gas separation, ACS Applied Materials & Interfaces 6 (2014) 4473–4479.
[248] W. Li, Q. Meng, C. Zhang, G. Zhang, Metal–organic framework/PVDF composite membranes with high H2 permselectivity synthesized by ammoniation, Chemistry–A European Journal 21 (2015) 7224–7230.
[249] S. Zhou, X. Zou, F. Sun, F. Zhang, S. Fan, H. Zhao, T. Schiestel, G. Zhu, Challenging fabrication of hollow ceramic fiber supported Cu 3 (BTC) 2 membrane for hydrogen separation, Journal of Materials Chemistry 22 (2012) 10322–10328.
[250] T. Ben, C. Lu, C. Pei, S. Xu, S. Qiu, Polymer-Supported and Free-Standing Metal–Organic Framework Membrane, Chemistry–A European Journal 18 (2012) 10250–10253.
[251] S. Hurrle, S. Friebe, J. Wohlgemuth, C. Wöll, J. Caro, L. Heinke, Sprayable, large-area metal–organic framework films and membranes of varying thickness, Chemistry–A European Journal 23 (2017) 2294–2298.
[252] H. Guo, G. Zhu, I.J. Hewitt, S. Qiu, "Twin copper source" growth of metal− organic framework membrane: Cu3 (BTC) 2 with high permeability and selectivity for recycling H2, Journal of the American Chemical Society 131 (2009) 1646–1647.
[253] D. Nagaraju, D.G. Bhagat, R. Banerjee, U.K. Kharul, In situ growth of metal-organic frameworks on a porous ultrafiltration membrane for gas separation, Journal of Materials Chemistry A 1 (2013) 8828–8835.
[254] Y. Mao, H. Huang, W. Cao, J. Li, L. Sun, X. Jin, X. Peng, Room temperature synthesis of free-standing HKUST-1 membranes from copper hydroxide nanostrands for gas separation, Chemical Communications 49 (2013) 5666–5668.
[255] Y. Hu, X. Dong, J. Nan, W. Jin, X. Ren, N. Xu, Y.M. Lee, Metal–organic framework membranes fabricated via reactive seeding, Chemical Communications 47 (2011) 737–739.
[256] F. Zhang, X. Zou, X. Gao, S. Fan, F. Sun, H. Ren, G. Zhu, Hydrogen selective NH2-MIL-53 (Al) MOF membranes with high permeability, Advanced Functional Materials 22 (2012) 3583–3590.
[257] W. Li, P. Su, G. Zhang, C. Shen, Q. Meng, Preparation of continuous NH2–MIL-53 membrane on ammoniated polyvinylidene fluoride hollow fiber for efficient H2 purification, Journal of Membrane Science 495 (2015) 384–391.
[258] N. Wang, A. Mundstock, Y. Liu, A. Huang, J. Caro, Amine-modified Mg-MOF-74/CPO-27-Mg membrane with enhanced H2/CO2 separation, Chemical Engineering Science 124 (2015) 27–36.
[259] D.-J. Lee, Q. Li, H. Kim, K. Lee, Preparation of Ni-MOF-74 membrane for CO2 separation by layer-by-layer seeding technique, Microporous and Mesoporous Materials 163 (2012) 169–177.
[260] S. Das, T. Ben, S. Qiu, V. Valtchev, Two-dimensional COF–three-dimensional MOF dual-layer membranes with unprecedentedly high H2/CO2 selectivity and ultrahigh gas permeabilities, ACS Applied Materials & Interfaces 12 (2020) 52899–52907.

[261] S. Friebe, B. Geppert, F. Steinbach, J. Caro, Metal–organic framework UiO-66 layer: a highly oriented membrane with good selectivity and hydrogen permeance, ACS Applied Materials & Interfaces 9 (2017) 12878–12885.
[262] H. Guo, J. Liu, Y. Li, J. Caro, A. Huang, Post-synthetic modification of highly stable UiO-66-NH2 membranes on porous ceramic tubes with enhanced H2 separation, Microporous and Mesoporous Materials 313 (2021) 110823.
[263] F. Cacho-Bailo, S. Catalan-Aguirre, M. Etxeberria-Benavides, O. Karvan, V. Sebastian, C. Tellez, J. Coronas, Metal-organic framework membranes on the inner-side of a polymeric hollow fiber by microfluidic synthesis, Journal of Membrane Science 476 (2015) 277–285.
[264] Y. Li, F. Liang, H. Bux, W. Yang, J. Caro, Zeolitic imidazolate framework ZIF-7 based molecular sieve membrane for hydrogen separation, Journal of Membrane Science 354 (2010) 48–54.
[265] V.M.A. Melgar, H.T. Kwon, J. Kim, Direct spraying approach for synthesis of ZIF-7 membranes by electrospray deposition, Journal of Membrane Science 459 (2014) 190–196.
[266] W. Li, Q. Meng, X. Li, C. Zhang, Z. Fan, G. Zhang, Non-activation ZnO array as a buffering layer to fabricate strongly adhesive metal–organic framework/PVDF hollow fiber membranes, Chemical Communications 50 (2014) 9711–9713.
[267] S. Zhang, Z. Wang, H. Ren, F. Zhang, J. Jin, Nanoporous film-mediated growth of ultrathin and continuous metal–organic framework membranes for high-performance hydrogen separation, Journal of Materials Chemistry A 5 (2017) 1962–1966.
[268] M.C. McCarthy, V. Varela-Guerrero, G.V. Barnett, H.-K. Jeong, Synthesis of zeolitic imidazolate framework films and membranes with controlled microstructures, Langmuir 26 (2010) 14636–14641.
[269] O. Shekhah, R. Swaidan, Y. Belmabkhout, M. Du Plessis, T. Jacobs, L.J. Barbour, I. Pinnau, M. Eddaoudi, The liquid phase epitaxy approach for the successful construction of ultra-thin and defect-free ZIF-8 membranes: pure and mixed gas transport study, Chemical Communications 50 (2014) 2089–2092.
[270] X. Zhang, Y. Liu, L. Kong, H. Liu, J. Qiu, W. Han, L.-T. Weng, K.L. Yeung, W. Zhu, A simple and scalable method for preparing low-defect ZIF-8 tubular membranes, Journal of Materials Chemistry A 1 (2013) 10635–10638.
[271] V. Chernikova, O. Shekhah, M. Eddaoudi, Advanced fabrication method for the preparation of MOF thin films: Liquid-phase epitaxy approach meets spin coating method, ACS Applied Materials & Interfaces 8 (2016) 20459–20464.
[272] Y. Liu, Y. Peng, N. Wang, Y. Li, J.H. Pan, W. Yang, J. Caro, Significantly enhanced separation using ZIF-8 membranes by partial conversion of calcined layered double hydroxide precursors, ChemSusChem 8 (2015) 3582–3586.
[273] G. He, M. Dakhchoune, J. Zhao, S. Huang, K.V. Agrawal, Electrophoretic nuclei assembly for crystallization of high-performance membranes on unmodified supports, Advanced Functional Materials 28 (2018) 1707427.
[274] H. Yin, J. Shang, J. Choi, A.C. Yip, Generation and extraction of hydrogen from low-temperature water-gas-shift reaction by a ZIF-8-based membrane reactor, Microporous and Mesoporous Materials 280 (2019) 347–356.
[275] P. Hu, Y. Yang, Y. Mao, J. Li, W. Cao, Y. Ying, Y. Liu, J. Lei, X. Peng, Room temperature synthesis of ZIF-8 membranes from seeds anchored in gelatin films for gas separation, CrystEngComm 17 (2015) 1576–1582.

[276] M. Drobek, M. Bechelany, C. Vallicari, A. Abou Chaaya, C. Charmette, C. Salvador-Levehang, P. Miele, A. Julbe, An innovative approach for the preparation of confined ZIF-8 membranes by conversion of ZnO ALD layers, Journal of Membrane Science 475 (2015) 39–46.
[277] Y. Liu, N. Wang, J.H. Pan, F. Steinbach, J. Caro, In situ synthesis of MOF membranes on ZnAl-CO3 LDH buffer layer-modified substrates, Journal of the American Chemical Society 136 (2014) 14353–14356.
[278] X. Zhang, Y. Liu, S. Li, L. Kong, H. Liu, Y. Li, W. Han, K.L. Yeung, W. Zhu, W. Yang, New membrane architecture with high performance: ZIF-8 membrane supported on vertically aligned ZnO nanorods for gas permeation and separation, Chemistry of Materials 26 (2014) 1975–1981.
[279] J. Li, W. Cao, Y. Mao, Y. Ying, L. Sun, X. Peng, Zinc hydroxide nanostrands: unique precursors for synthesis of ZIF-8 thin membranes exhibiting high size-sieving ability for gas separation, CrystEngComm 16 (2014) 9788–9791.
[280] H. Chen, X. Wang, Y. Liu, T. Yang, N. Yang, B. Meng, X. Tan, S. Liu, A dual-layer ZnO–Al2O3 hollow fiber for directly inducing the formation of ZIF membrane, Journal of Membrane Science 640 (2021) 119851.
[281] Y. Pan, B. Wang, Z. Lai, Synthesis of ceramic hollow fiber supported zeolitic imidazolate framework-8 (ZIF-8) membranes with high hydrogen permeability, Journal of Membrane Science 421 (2012) 292–298.
[282] K. Huang, Z. Dong, Q. Li, W. Jin, Growth of a ZIF-8 membrane on the inner-surface of a ceramic hollow fiber via cycling precursors, Chemical Communications 49 (2013) 10326–10328.
[283] X. Wang, M. Sun, B. Meng, X. Tan, J. Liu, S. Wang, S. Liu, Formation of continuous and highly permeable ZIF-8 membranes on porous alumina and zinc oxide hollow fibers, Chemical Communications 52 (2016) 13448–13451.
[284] E. Shamsaei, X. Lin, Z.-X. Low, Z. Abbasi, Y. Hu, J.Z. Liu, H. Wang, Aqueous phase synthesis of ZIF-8 membrane with controllable location on an asymmetrically porous polymer substrate, ACS Applied Materials & Interfaces 8 (2016) 6236–6244.
[285] J. Hou, P.D. Sutrisna, Y. Zhang, V. Chen, Formation of ultrathin, continuous metal–organic framework membranes on flexible polymer substrates, Angewandte Chemie International Edition 55 (2016) 3947–3951.
[286] E. Shamsaei, X. Lin, L. Wan, Y. Tong, H. Wang, A one-dimensional material as a nano-scaffold and a pseudo-seed for facilitated growth of ultrathin, mechanically reinforced molecular sieving membranes, Chemical Communications 52 (2016) 13764–13767.
[287] P. Su, W. Li, C. Zhang, Q. Meng, C. Shen, G. Zhang, Metal based gels as versatile precursors to synthesize stiff and integrated MOF/polymer composite membranes, Journal of Materials Chemistry A 3 (2015) 20345–20351.
[288] G. Zhang, K. Tang, X. Zhang, L. Xu, C. Shen, Q. Meng, Self-assembly of defect-free polymer-based zeolite imidazolate framework composite membranes with metal-phenolic networks for high efficient H2/CH4 separation, Journal of Membrane Science 617 (2021) 118612.
[289] Y. Li, C. Ma, P. Nian, H. Liu, X. Zhang, Green synthesis of ZIF-8 tubular membranes from a recyclable 2-methylimidazole water-solvent solution by ZnO nanorods self-converted strategy for gas separation, Journal of Membrane Science 581 (2019) 344–354.

[290] J. Hao, D.J. Babu, Q. Liu, H.-Y. Chi, C. Lu, Y. Liu, K.V. Agrawal, Synthesis of high-performance polycrystalline metal–organic framework membranes at room temperature in a few minutes, Journal of Materials Chemistry A 8 (2020) 7633–7640.
[291] L. Kong, X. Zhang, H. Liu, J. Qiu, Synthesis of a highly stable ZIF-8 membrane on a macroporous ceramic tube by manual-rubbing ZnO deposition as a multifunctional layer, Journal of Membrane Science 490 (2015) 354–363.
[292] H. Bux, F. Liang, Y. Li, J. Cravillon, M. Wiebcke, J. Caro, Zeolitic imidazolate framework membrane with molecular sieving properties by microwave-assisted solvothermal synthesis, Journal of the American Chemical Society 131 (2009) 16000–16001.
[293] W. Li, P. Su, Z. Li, Z. Xu, F. Wang, H. Ou, J. Zhang, G. Zhang, E. Zeng, Ultrathin metal–organic framework membrane production by gel–vapour deposition, Nature Communications 8 (2017) 406.
[294] D.J. Babu, G. He, J. Hao, M.T. Vahdat, P.A. Schouwink, M. Mensi, K.V. Agrawal, Restricting lattice flexibility in polycrystalline metal–organic framework membranes for carbon capture, Advanced Materials 31 (2019) 1900855.
[295] J. Liu, C. Liu, A. Huang, Co-based zeolitic imidazolate framework ZIF-9 membranes prepared on α-Al2O3 tubes through covalent modification for hydrogen separation, International Journal of Hydrogen Energy 45 (2020) 703–711.
[296] P. Nian, Y. Li, X. Zhang, Y. Cao, H. Liu, X. Zhang, ZnO nanorod-induced heteroepitaxial growth of SOD type Co-based zeolitic imidazolate framework membranes for H2 separation, ACS Applied Materials & Interfaces 10 (2018) 4151–4160.
[297] A. Knebel, P. Wulfert-Holzmann, S. Friebe, J. Pavel, I. Strauß, A. Mundstock, F. Steinbach, J. Caro, Hierarchical Nanostructures of Metal-Organic Frameworks Applied in Gas Separating ZIF-8-on-ZIF-67 Membranes, Chemistry–A European Journal 24 (2018) 5728–5733.
[298] Z. Zhou, C. Wu, B. Zhang, ZIF-67 membranes synthesized on α-Al2O3-plate-supported cobalt nanosheets with amine modification for enhanced H2/CO2 permselectivity, Industrial & Engineering Chemistry Research 59 (2020) 3182–3188.
[299] X. Dong, K. Huang, S. Liu, R. Ren, W. Jin, Y. Lin, Synthesis of zeolitic imidazolate framework-78 molecular-sieve membrane: defect formation and elimination, Journal of Materials Chemistry 22 (2012) 19222–19227.
[300] A. Huang, W. Dou, J. Caro, Steam-stable zeolitic imidazolate framework ZIF-90 membrane with hydrogen selectivity through covalent functionalization, Journal of the American Chemical Society 132 (2010) 15562–15564.
[301] A. Huang, J. Caro, Covalent post-functionalization of zeolitic imidazolate framework ZIF-90 membrane for enhanced hydrogen selectivity, Angewandte Chemie International Edition 21 (2011) 4979–4982.
[302] A. Huang, N. Wang, C. Kong, J. Caro, Organosilica-functionalized zeolitic imidazolate framework ZIF-90 membrane with high gas-separation performance., Angewandte Chemie (International Ed. in English) 51 (2012) 10551–10555.
[303] A. Huang, Y. Chen, N. Wang, Z. Hu, J. Jiang, J. Caro, A highly permeable and selective zeolitic imidazolate framework ZIF-95 membrane for H 2/CO 2 separation, Chemical Communications 48 (2012) 10981–10983.
[304] X. Ma, Y. Li, A. Huang, Synthesis of nano-sheets seeds for secondary growth of highly hydrogen permselective ZIF-95 membranes, Journal of Membrane Science 597 (2020) 117629.

[305] X. Ma, Z. Wan, Y. Li, X. He, J. Caro, A. Huang, Anisotropic gas separation in oriented ZIF-95 membranes prepared by vapor-assisted in-plane epitaxial growth, Angewandte Chemie 132 (2020) 21044–21048.
[306] N. Wang, Y. Liu, Z. Qiao, L. Diestel, J. Zhou, A. Huang, J. Caro, Polydopamine-based synthesis of a zeolite imidazolate framework ZIF-100 membrane with high H 2/CO 2 selectivity, Journal of Materials Chemistry A 3 (2015) 4722–4728.
[307] Y. Peng, Y. Li, Y. Ban, W. Yang, Two-dimensional metal–organic framework nanosheets for membrane-based gas separation, Angewandte Chemie 129 (2017) 9889–9893.
[308] F. Cacho-Bailo, I. Matito-Martos, J. Perez-Carbajo, M. Etxeberría-Benavides, O. Karvan, V. Sebastián, S. Calero, C. Téllez, J. Coronas, On the molecular mechanisms for the H 2/CO 2 separation performance of zeolite imidazolate framework two-layered membranes, Chemical Science 8 (2017) 325–333.
[309] Y. Song, Y. Sun, D. Du, M. Zhang, Y. Liu, L. Liu, T. Ji, G. He, Fabrication of c-oriented ultrathin TCPP-derived 2D MOF membrane for precise molecular sieving, Journal of Membrane Science 634 (2021) 119393.
[310] Y. Peng, Y. Li, Y. Ban, H. Jin, W. Jiao, X. Liu, W. Yang, Metal-organic framework nanosheets as building blocks for molecular sieving membranes, Science 346 (2014) 1356–1359.
[311] S. Song, W. Wang, Y. Zhao, W. Wu, Y. Wei, H. Wang, Tuning the Stacking Modes of Ultrathin Two-Dimensional Metal–Organic Framework Nanosheet Membranes for Highly Efficient Hydrogen Separation, Angewandte Chemie International Edition 62 (2023) e202312995.
[312] K. Yang, S. Hu, Y. Ban, Y. Zhou, N. Cao, M. Zhao, Y. Xiao, W. Li, W. Yang, ZIF-L membrane with a membrane-interlocked-support composite architecture for H2/CO2 separation, Science Bulletin 66 (2021) 1869–1876.
[313] P. Nian, H. Liu, X. Zhang, Bottom-up fabrication of two-dimensional Co-based zeolitic imidazolate framework tubular membranes consisting of nanosheets by vapor phase transformation of Co-based gel for H2/CO2 separation, Journal of Membrane Science 573 (2019) 200–209.
[314] H. Song, Y. Peng, C. Wang, L. Shu, C. Zhu, Y. Wang, H. He, W. Yang, Structure regulation of MOF nanosheet membrane for accurate H2/CO2 separation, Angewandte Chemie International Edition 62 (2023) e202218472.
[315] Y. Wang, H. Jin, Q. Ma, K. Mo, H. Mao, A. Feldhoff, X. Cao, Y. Li, F. Pan, Z. Jiang, A MOF glass membrane for gas separation, Angewandte Chemie 132 (2020) 4395–4399.
[316] H. Fan, A. Mundstock, A. Feldhoff, A. Knebel, J. Gu, H. Meng, J. Caro, Covalent organic framework–covalent organic framework bilayer membranes for highly selective gas separation, Journal of the American Chemical Society 140 (2018) 10094–10098.
[317] J. Fu, S. Das, G. Xing, T. Ben, V. Valtchev, S. Qiu, Fabrication of COF-MOF composite membranes and their highly selective separation of H2/CO2, Journal of the American Chemical Society 138 (2016) 7673–7680.
[318] B. Li, Z. Wang, Z. Gao, J. Suo, M. Xue, Y. Yan, V. Valtchev, S. Qiu, Q. Fang, Self-Standing Covalent Organic Framework Membranes for H2/CO2 Separation, Advanced Functional Materials 33 (2023) 2300219.
[319] H. Lu, C. Wang, J. Chen, R. Ge, W. Leng, B. Dong, J. Huang, Y. Gao, A novel 3D covalent organic framework membrane grown on a porous α-Al 2 O 3 substrate under solvothermal conditions, Chemical Communications 51 (2015) 15562–15565.

[320] J. Fu, T. Ben, Fabrication of a Novel Covalent Organic Framework Membrane and Its Gas Separation Performance, Acta Chimica Sinica 78 (2020) 805.
[321] H. Fan, M. Peng, I. Strauss, A. Mundstock, H. Meng, J. Caro, High-flux vertically aligned 2D covalent organic framework membrane with enhanced hydrogen separation, Journal of the American Chemical Society 142 (2020) 6872–6877.
[322] Y. Ying, M. Tong, S. Ning, S.K. Ravi, S.B. Peh, S.C. Tan, S.J. Pennycook, D. Zhao, Ultrathin two-dimensional membranes assembled by ionic covalent organic nanosheets with reduced apertures for gas separation, Journal of the American Chemical Society 142 (2020) 4472–4480.
[323] W. Zheng, J. Hou, C. Liu, P. Liu, L. Li, L. Chen, Z. Tang, Melamine-Doped Covalent Organic Framework Membranes for Enhanced Hydrogen Purification, Chemistry–An Asian Journal 16 (2021) 3624–3629.
[324] D. Xu, Y. Jin, C. Li, Y. Fan, S. Kawi, X. Meng, J. Song, N. Yang, COF/MXene composite membranes compact assembled by electrostatic interactions: A strategy for H2/CO2 separation, Journal of Membrane Science 700 (2024) 122678.
[325] H. Fan, M. Peng, I. Strauss, A. Mundstock, H. Meng, J. Caro, MOF-in-COF molecular sieving membrane for selective hydrogen separation, Nature Communications 12 (2021) 38.
[326] K. Qi, J. Yu, Y. Gao, L. Shi, Q. Yi, X. Li, J. Zeng, L. Gao, L. Gao, Ultrathin and Self-Supporting MOF/COF-Based Composite Membranes for Hydrogen Separation and Purification from Coke Oven Gas, Langmuir (2024).
[327] P.M. Budd, B.S. Ghanem, S. Makhseed, N.B. McKeown, K.J. Msayib, C.E. Tattershall, Polymers of intrinsic microporosity (PIMs): robust, solution-processable, organic nanoporous materials, Chemical Communications (2004) 230–231.
[328] P.M. Budd, E.S. Elabas, B.S. Ghanem, S. Makhseed, N.B. McKeown, K.J. Msayib, C.E. Tattershall, D. Wang, Solution-processed, organophilic membrane derived from a polymer of intrinsic microporosity, Advanced Materials 16 (2004) 456–459.
[329] Y. Wang, X. Ma, B. Ghanem, F. Alghunaimi, I. Pinnau, Y. Han, Polymers of intrinsic microporosity for energy-intensive membrane-based gas separations, Materials Today Nano 3 (2018) 69–95.
[330] W.H. Lee, J.G. Seong, X. Hu, Y.M. Lee, Recent progress in microporous polymers from thermally rearranged polymers and polymers of intrinsic microporosity for membrane gas separation: pushing performance limits and revisiting trade-off lines, Journal of Polymer Science 58 (2020) 2450–2466.
[331] P.M. Budd, K.J. Msayib, C.E. Tattershall, B.S. Ghanem, K.J. Reynolds, N.B. McKeown, D. Fritsch, Gas separation membranes from polymers of intrinsic microporosity, Journal of Membrane Science 251 (2005) 263–269.
[332] J. Zhang, H. Kang, J. Martin, S. Zhang, S. Thomas, T.C. Merkel, J. Jin, The enhancement of chain rigidity and gas transport performance of polymers of intrinsic microporosity via intramolecular locking of the spiro-carbon, Chemical Communications 52 (2016) 6553–6556.
[333] M. Carta, P. Bernardo, G. Clarizia, J.C. Jansen, N.B. McKeown, Gas permeability of hexaphenylbenzene based polymers of intrinsic microporosity, Macromolecules 47 (2014) 8320–8327.
[334] C.G. Bezzu, M. Carta, A. Tonkins, J.C. Jansen, P. Bernardo, F. Bazzarelli, N.B. McKeown, A spirobifluorene-based polymer of intrinsic microporosity with improved performance for gas separation, Advanced Materials 24 (2012) 5930.

[335] C.G. Bezzu, M. Carta, M.-C. Ferrari, J.C. Jansen, M. Monteleone, E. Esposito, A. Fuoco, K. Hart, T. Liyana-Arachchi, C.M. Colina, The synthesis, chain-packing simulation and long-term gas permeability of highly selective spirobifluorene-based polymers of intrinsic microporosity, Journal of Materials Chemistry A 6 (2018) 10507–10514.
[336] B.S. Ghanem, N.B. McKeown, P.M. Budd, D. Fritsch, Polymers of intrinsic microporosity derived from bis (phenazyl) monomers, Macromolecules 41 (2008) 1640–1646.
[337] I. Rose, C.G. Bezzu, M. Carta, B. Comesaña-Gándara, E. Lasseuguette, M.C. Ferrari, P. Bernardo, G. Clarizia, A. Fuoco, J.C. Jansen, Polymer ultrapermeability from the inefficient packing of 2D chains, Nature Materials 16 (2017) 932–937.
[338] B.S. Ghanem, R. Swaidan, X. Ma, E. Litwiller, I. Pinnau, Energy-efficient hydrogen separation by AB-type ladder-polymer molecular sieves, Advanced Materials 26 (2014) 6696–6700.
[339] A. Fuoco, B. Comesaña-Gándara, M. Longo, E. Esposito, M. Monteleone, I. Rose, C.G. Bezzu, M. Carta, N.B. McKeown, J.C. Jansen, Temperature dependence of gas permeation and diffusion in triptycene-based ultrapermeable polymers of intrinsic microporosity, ACS Applied Materials & Interfaces 10 (2018) 36475–36482.
[340] M. Carta, M. Croad, R. Malpass-Evans, J.C. Jansen, P. Bernardo, G. Clarizia, K. Friess, M. Lanč, N.B. McKeown, Triptycene induced enhancement of membrane gas selectivity for microporous Tröger's base polymers, Advanced Materials (Deerfield Beach, Fla.) 26 (2014) 3526.
[341] M. Carta, R. Malpass-Evans, M. Croad, Y. Rogan, J.C. Jansen, P. Bernardo, F. Bazzarelli, N.B. McKeown, An efficient polymer molecular sieve for membrane gas separations, Science 339 (2013) 303–307.
[342] R. Williams, L.A. Burt, E. Esposito, J.C. Jansen, E. Tocci, C. Rizzuto, M. Lanč, M. Carta, N.B. McKeown, A highly rigid and gas selective methanopentacene-based polymer of intrinsic microporosity derived from Tröger's base polymerization, Journal of Materials Chemistry A 6 (2018) 5661–5667.
[343] M. Carta, M. Croad, J.C. Jansen, P. Bernardo, G. Clarizia, N.B. McKeown, Synthesis of cardo-polymers using Tröger's base formation, Polymer Chemistry 5 (2014) 5255–5261.
[344] I. Rose, M. Carta, R. Malpass-Evans, M.-C. Ferrari, P. Bernardo, G. Clarizia, J.C. Jansen, N.B. McKeown, Highly permeable benzotriptycene-based polymer of intrinsic microporosity, ACS Macro Letters 4 (2015) 912–915.
[345] B.S. Ghanem, N.B. McKeown, P.M. Budd, N.M. Al-Harbi, D. Fritsch, K. Heinrich, L. Starannikova, A. Tokarev, Y. Yampolskii, Synthesis, characterization, and gas permeation properties of a novel group of polymers with intrinsic microporosity: PIM-polyimides, Macromolecules 42 (2009) 7881–7888.
[346] B.S. Ghanem, N.B. McKeown, P.M. Budd, J.D. Selbie, D. Fritsch, High-performance membranes from polyimides with intrinsic microporosity., Advanced Materials (Deerfield Beach, Fla.) 20 (2008) 2766–2771.
[347] Y. Rogan, L. Starannikova, V. Ryzhikh, Y. Yampolskii, P. Bernardo, F. Bazzarelli, J.C. Jansen, N.B. McKeown, Synthesis and gas permeation properties of novel spirobisindane-based polyimides of intrinsic microporosity, Polymer Chemistry 4 (2013) 3813–3820.
[348] R. Swaidan, M. Al-Saeedi, B. Ghanem, E. Litwiller, I. Pinnau, Rational design of intrinsically ultramicroporous polyimides containing bridgehead-substituted triptycene

for highly selective and permeable gas separation membranes, Macromolecules 47 (2014) 5104–5114.
[349] X. Ma, B. Ghanem, O. Salines, E. Litwiller, I. Pinnau, Synthesis and effect of physical aging on gas transport properties of a microporous polyimide derived from a novel spirobifluorene-based dianhydride, ACS Macro Letters 4 (2015) 231–235.
[350] B. Ghanem, F. Alghunaimi, X. Ma, N. Alaslai, I. Pinnau, Synthesis and characterization of novel triptycene dianhydrides and polyimides of intrinsic microporosity based on 3, 3'-dimethylnaphthidine, Polymer 101 (2016) 225–232.
[351] X. Ma, I. Pinnau, Effect of film thickness and physical aging on "intrinsic" gas permeation properties of microporous ethanoanthracene-based polyimides, Macromolecules 51 (2018) 1069–1076.
[352] Y. Rogan, R. Malpass-Evans, M. Carta, M. Lee, J.C. Jansen, P. Bernardo, G. Clarizia, E. Tocci, K. Friess, M. Lanč, A highly permeable polyimide with enhanced selectivity for membrane gas separations, Journal of Materials Chemistry A 2 (2014) 4874–4877.
[353] X. Ma, M.A. Abdulhamid, I. Pinnau, Design and synthesis of polyimides based on carbocyclic pseudo-Troger's base-derived dianhydrides for membrane gas separation applications, Macromolecules 50 (2017) 5850–5857.
[354] X. Ma, O. Salinas, E. Litwiller, I. Pinnau, Novel spirobifluorene-and dibromospirobifluorene-based polyimides of intrinsic microporosity for gas separation applications, Macromolecules 46 (2013) 9618–9624.
[355] Y. Zhuang, J.G. Seong, Y.S. Do, W.H. Lee, M.J. Lee, M.D. Guiver, Y.M. Lee, High-strength, soluble polyimide membranes incorporating Tröger's Base for gas separation, Journal of Membrane Science 504 (2016) 55–65.
[356] Y. Zhuang, J.G. Seong, Y.S. Do, H.J. Jo, Z. Cui, J. Lee, Y.M. Lee, M.D. Guiver, Intrinsically microporous soluble polyimides incorporating Tröger's base for membrane gas separation, Macromolecules 47 (2014) 3254–3262.
[357] Z. Wang, D. Wang, F. Zhang, J. Jin, Troger's base-based microporous polyimide membranes for high-performance gas separation, ACS Macro Letters 3 (2014) 597–601.
[358] Z. Wang, D. Wang, J. Jin, Microporous polyimides with rationally designed chain structure achieving high performance for gas separation, Macromolecules 47 (2014) 7477–7483.
[359] M. Lee, C.G. Bezzu, M. Carta, P. Bernardo, G. Clarizia, J.C. Jansen, N.B. McKeown, Enhancing the gas permeability of Troger's base derived polyimides of intrinsic microporosity, Macromolecules 49 (2016) 4147–4154.
[360] B. Ghanem, N. Alaslai, X. Miao, I. Pinnau, Novel 6FDA-based polyimides derived from sterically hindered Tröger's base diamines: Synthesis and gas permeation properties, Polymer 96 (2016) 13–19.
[361] X. Hu, W.H. Lee, J. Zhao, J.Y. Bae, J.S. Kim, Z. Wang, J. Yan, Y. Zhuang, Y.M. Lee, Tröger's Base (TB)-containing polyimide membranes derived from bio-based dianhydrides for gas separations, Journal of Membrane Science 610 (2020) 118255.
[362] X. Hu, W.H. Lee, J.Y. Bae, J. Zhao, J.S. Kim, Z. Wang, J. Yan, Y.M. Lee, Highly permeable polyimides incorporating Tröger's base (TB) units for gas separation membranes, Journal of Membrane Science 615 (2020) 118533.
[363] J.R. Wiegand, Z.P. Smith, Q. Liu, C.T. Patterson, B.D. Freeman, R. Guo, Synthesis and characterization of triptycene-based polyimides with tunable high fractional free volume for gas separation membranes, Journal of Materials Chemistry A 2 (2014) 13309–13320.

[364] F. Alghunaimi, B. Ghanem, N. Alaslai, R. Swaidan, E. Litwiller, I. Pinnau, Gas permeation and physical aging properties of iptycene diamine-based microporous polyimides, Journal of Membrane Science 490 (2015) 321–327.
[365] S. Luo, Q. Liu, B. Zhang, J.R. Wiegand, B.D. Freeman, R. Guo, Pentiptycene-based polyimides with hierarchically controlled molecular cavity architecture for efficient membrane gas separation, Journal of Membrane Science 480 (2015) 20–30.
[366] R. Swaidan, B.S. Ghanem, E. Litwiller, I. Pinnau, Pure-and mixed-gas CO2/CH4 separation properties of PIM-1 and an amidoxime-functionalized PIM-1, Journal of Membrane Science 457 (2014) 95–102.
[367] N. Du, G.P. Robertson, J. Song, I. Pinnau, M.D. Guiver, High-performance carboxylated polymers of intrinsic microporosity (PIMs) with tunable gas transport properties, Macromolecules 42 (2009) 6038–6043.
[368] J.W. Jeon, D.-G. Kim, E. Sohn, Y. Yoo, Y.S. Kim, B.G. Kim, J.-C. Lee, Highly carboxylate-functionalized polymers of intrinsic microporosity for CO2-selective polymer membranes, Macromolecules 50 (2017) 8019–8027.
[369] C. Zhang, L. Fu, Z. Tian, B. Cao, P. Li, Post-crosslinking of triptycene-based Tröger's base polymers with enhanced natural gas separation performance, Journal of Membrane Science 556 (2018) 277–284.
[370] X. Ma, R. Swaidan, Y. Belmabkhout, Y. Zhu, E. Litwiller, M. Jouiad, I. Pinnau, Y. Han, Synthesis and gas transport properties of hydroxyl-functionalized polyimides with intrinsic microporosity, Macromolecules 45 (2012) 3841–3849.
[371] C.R. Mason, L. Maynard-Atem, N.M. Al-Harbi, P.M. Budd, P. Bernardo, F. Bazzarelli, G. Clarizia, J.C. Jansen, Polymer of intrinsic microporosity incorporating thioamide functionality: preparation and gas transport properties, Macromolecules 44 (2011) 6471–6479.
[372] W. Ji, H. Geng, Z. Chen, H. Dong, H. Matsuyama, H. Wang, H. Wang, J. Li, W. Shi, X. Ma, Facile tailoring molecular sieving effect of PIM-1 by in-situ O3 treatment for high performance hydrogen separation, Journal of Membrane Science 662 (2022) 120971.
[373] M. Huang, K. Lu, Z. Wang, X. Bi, Y. Zhang, J. Jin, Thermally cross-linked amidoxime-functionalized polymers of intrinsic microporosity membranes for highly selective hydrogen separation, ACS Sustainable Chemistry & Engineering 9 (2021) 9426–9435.
[374] S. Thomas, I. Pinnau, N. Du, M.D. Guiver, Pure-and mixed-gas permeation properties of a microporous spirobisindane-based ladder polymer (PIM-1), Journal of Membrane Science 333 (2009) 125–131.
[375] R. Swaidan, B. Ghanem, E. Litwiller, I. Pinnau, Physical aging, plasticization and their effects on gas permeation in "rigid" polymers of intrinsic microporosity, Macromolecules 48 (2015) 6553–6561.
[376] S. Bandehali, A.E. Amooghin, H. Sanaeepur, R. Ahmadi, A. Fuoco, J.C. Jansen, S. Shirazian, Polymers of intrinsic microporosity and thermally rearranged polymer membranes for highly efficient gas separation, Separation and Purification Technology 278 (2021) 119513.
[377] Y.S. Do, J.G. Seong, S. Kim, J.G. Lee, Y.M. Lee, Thermally rearranged (TR) poly (benzoxazole-co-amide) membranes for hydrogen separation derived from 3, 3'-dihydroxy-4, 4'-diamino-biphenyl (HAB), 4, 4'-oxydianiline (ODA) and isophthaloyl chloride (IPCl), Journal of Membrane Science 446 (2013) 294–302.

[378] S. Kim, J.G. Seong, Y.S. Do, Y.M. Lee, Gas sorption and transport in thermally rearranged polybenzoxazole membranes derived from polyhydroxylamides, Journal of Membrane Science 474 (2015) 122–131.
[379] S.H. Han, H.J. Kwon, K.Y. Kim, J.G. Seong, C.H. Park, S. Kim, C.M. Doherty, A.W. Thornton, A.J. Hill, Á.E. Lozano, Tuning microcavities in thermally rearranged polymer membranes for CO 2 capture, Physical Chemistry Chemical Physics 14 (2012) 4365–4373.
[380] J.S. Kim, S.J. Moon, H.H. Wang, S. Kim, Y.M. Lee, Mixed matrix membranes with a thermally rearranged polymer and ZIF-8 for hydrogen separation, Journal of Membrane Science 582 (2019) 381–390.
[381] H.D. Patel, N.K. Acharya, Synthesis and characteristics of HAB-6FDA thermally rearranged polyimide nanocomposite membranes, Polymer Engineering & Science 61 (2021) 2782–2791.
[382] C.Y. Soo, H.J. Jo, Y.M. Lee, J.R. Quay, M.K. Murphy, Effect of the chemical structure of various diamines on the gas separation of thermally rearranged poly (benzoxazole-co-imide)(TR-PBO-co-I) membranes, Journal of Membrane Science 444 (2013) 365–377.
[383] S.H. Han, N. Misdan, S. Kim, C.M. Doherty, A.J. Hill, Y.M. Lee, Thermally rearranged (TR) polybenzoxazole: effects of diverse imidization routes on physical properties and gas transport behaviors, Macromolecules 43 (2010) 7657–7667.
[384] M. Calle, Y.M. Lee, Thermally rearranged (TR) poly (ether− benzoxazole) membranes for gas separation, Macromolecules 44 (2011) 1156–1165.
[385] Y.F. Yeong, H. Wang, K.P. Pramoda, T.-S. Chung, Thermal induced structural rearrangement of cardo-copolybenzoxazole membranes for enhanced gas transport properties, Journal of Membrane Science 397 (2012) 51–65.
[386] A. Yerzhankyzy, B.S. Ghanem, Y. Wang, N. Alaslai, I. Pinnau, Gas separation performance and mechanical properties of thermally-rearranged polybenzoxazoles derived from an intrinsically microporous dihydroxyl-functionalized triptycene diamine-based polyimide, Journal of Membrane Science 595 (2020) 117512.
[387] S. Luo, Q. Zhang, L. Zhu, H. Lin, B.A. Kazanowska, C.M. Doherty, A.J. Hill, P. Gao, R. Guo, Highly selective and permeable microporous polymer membranes for hydrogen purification and CO2 removal from natural gas, Chemistry of Materials 30 (2018) 5322–5332.
[388] S. Luo, Q. Zhang, T.K. Bear, T.E. Curtis, R.K. Roeder, C.M. Doherty, A.J. Hill, R. Guo, Triptycene-containing poly (benzoxazole-co-imide) membranes with enhanced mechanical strength for high-performance gas separation, Journal of Membrane Science 551 (2018) 305–314.
[389] F. Alghunaimi, B. Ghanem, Y. Wang, O. Salinas, N. Alaslai, I. Pinnau, Synthesis and gas permeation properties of a novel thermally-rearranged polybenzoxazole made from an intrinsically microporous hydroxyl-functionalized triptycene-based polyimide precursor, Polymer 121 (2017) 9–16.
[390] S. Luo, J. Liu, H. Lin, B.A. Kazanowska, M.D. Hunckler, R.K. Roeder, R. Guo, Preparation and gas transport properties of triptycene-containing polybenzoxazole (PBO)-based polymers derived from thermal rearrangement (TR) and thermal cyclodehydration (TC) processes, Journal of Materials Chemistry A 4 (2016) 17050–17062.
[391] S. Li, H.J. Jo, S.H. Han, C.H. Park, S. Kim, P.M. Budd, Y.M. Lee, Mechanically robust thermally rearranged (TR) polymer membranes with spirobisindane for gas separation, Journal of Membrane Science 434 (2013) 137–147.

[392] X. Ma, O. Salinas, E. Litwiller, I. Pinnau, Pristine and thermally-rearranged gas separation membranes from novel o-hydroxyl-functionalized spirobifluorene-based polyimides, Polymer Chemistry 5 (2014) 6914–6922.
[393] H. Shamsipur, B.A. Dawood, P.M. Budd, P. Bernardo, G. Clarizia, J.C. Jansen, Thermally rearrangeable PIM-polyimides for gas separation membranes, Macromolecules 47 (2014) 5595–5606.
[394] M. Calle, H.J. Jo, C.M. Doherty, A.J. Hill, Y.M. Lee, Cross-linked thermally rearranged poly (benzoxazole-co-imide) membranes prepared from ortho-hydroxycopolyimides containing pendant carboxyl groups and gas separation properties, Macromolecules 48 (2015) 2603–2613.
[395] M. Calle, C.M. Doherty, A.J. Hill, Y.M. Lee, Cross-linked thermally rearranged poly (benzoxazole-co-imide) membranes for gas separation, Macromolecules 46 (2013) 8179–8189.
[396] X. Hu, W.H. Lee, J. Zhao, J.S. Kim, Z. Wang, J. Yan, Y. Zhuang, Y.M. Lee, Thermally rearranged polymer membranes containing highly rigid biphenyl ortho-hydroxyl diamine for hydrogen separation, Journal of Membrane Science 604 (2020) 118053.
[397] H.J. Jo, C.Y. Soo, G. Dong, Y.S. Do, H.H. Wang, M.J. Lee, J.R. Quay, M.K. Murphy, Y.M. Lee, Thermally rearranged poly (benzoxazole-co-imide) membranes with superior mechanical strength for gas separation obtained by tuning chain rigidity, Macromolecules 48 (2015) 2194–2202.
[398] Y. Zhuang, J.G. Seong, W.H. Lee, Y.S. Do, M.J. Lee, G. Wang, M.D. Guiver, Y.M. Lee, Mechanically tough, thermally rearranged (TR) random/block poly (benzoxazole-co-imide) gas separation membranes, Macromolecules 48 (2015) 5286–5299.
[399] Y. Wang, Z. Low, S. Kim, H. Zhang, X. Chen, J. Hou, J.G. Seong, Y.M. Lee, G.P. Simon, C.H. Davies, Functionalized boron nitride nanosheets: a thermally rearranged polymer nanocomposite membrane for hydrogen separation, Angewandte Chemie 130 (2018) 16288–16293.
[400] W. Li, Y. Zhang, P. Su, Z. Xu, G. Zhang, C. Shen, Q. Meng, Metal–organic framework channelled graphene composite membranes for H 2/CO 2 separation, Journal of Materials Chemistry A 4 (2016) 18747–18752.
[401] M. Jia, Y. Feng, S. Liu, J. Qiu, J. Yao, Graphene oxide gas separation membranes intercalated by UiO-66-NH2 with enhanced hydrogen separation performance, Journal of Membrane Science 539 (2017) 172–177.
[402] A. Huang, Q. Liu, N. Wang, Y. Zhu, J. Caro, Bicontinuous zeolitic imidazolate framework ZIF-8@ GO membrane with enhanced hydrogen selectivity, Journal of the American Chemical Society 136 (2014) 14686–14689.
[403] Y. Li, H. Liu, H. Wang, J. Qiu, X. Zhang, GO-guided direct growth of highly oriented metal–organic framework nanosheet membranes for H 2/CO 2 separation, Chemical Science 9 (2018) 4132–4141.
[404] H. Guo, G. Kong, G. Yang, J. Pang, Z. Kang, S. Feng, L. Zhao, L. Fan, L. Zhu, A. Vicente, Cross-Linking between Sodalite Nanoparticles and Graphene Oxide in Composite Membranes to Trigger High Gas Permeance, Selectivity, and Stability in Hydrogen Separation, Angewandte Chemie 132 (2020) 6343–6347.
[405] E. Aliyev, J. Warfsmann, B. Tokay, S. Shishatskiy, Y.-J. Lee, J. Lillepaerg, N.R. Champness, V. Filiz, Gas transport properties of the metal–organic framework (MOF)-assisted polymer of intrinsic microporosity (PIM-1) thin-film composite membranes, ACS Sustainable Chemistry & Engineering 9 (2020) 684–694.

[406] Y. Sun, F. Fan, L. Bai, T. Li, J. Guan, F. Sun, Y. Liu, W. Xiao, G. He, C. Ma, Hydrogen-bonded hybrid membranes based on hydroxylated metal-organic frameworks and PIM-1 for ultrafast hydrogen separation, Results in Engineering 20 (2023) 101398.
[407] K. Zhang, X. Luo, S. Li, X. Tian, Q. Wang, C. Liu, Y. Tang, X. Feng, R. Zhang, S. Yin, ZIF-8 Gel/PIM-1 mixed matrix membranes for enhanced H2/CH4 separations, Chemical Engineering Journal (2024) 149489.
[408] S. Han, Z. Wang, J. Yu, F. Wang, X. Li, Conversion of SOD zeolite into type I porous liquid and preparation of mixed matrix membrane with AO-PIM for efficient gas separation, Journal of Cleaner Production 448 (2024) 141737.
[409] S. Xiong, C. Pan, G. Dai, C. Liu, Z. Tan, C. Chen, S. Yang, X. Ruan, J. Tang, G. Yu, Interfacial co-weaving of AO-PIM-1 and ZIF-8 in composite membranes for enhanced H2 purification, Journal of Membrane Science 645 (2022) 120217.
[410] R. Wu, Y. Li, A. Huang, Synthesis of high-performance Co-based ZIF-67 membrane for H2 separation by using cobalt ions chelated PIM-1 as interface layer, Journal of Membrane Science 620 (2021) 118841.
[411] L. Pilz, C. Natzeck, J. Wohlgemuth, N. Scheuermann, S. Spiegel, S. Oßwald, A. Knebel, S. Braese, C. Wöll, M. Tsotsalas, Utilizing Machine Learning to Optimize Metal-Organic Framework-Derived Polymer Membranes for Gas Separation, Journal of Materials Chemistry A (2023).